Validation and Improvement of Property and Process Modeling for Oleochemicals

Forero-Hernandez, Hector Alexander

Publication date:
2019

Document Version
Peer reviewed version

Ph.D. Thesis
Doctor of Philosophy

DTU Chemical Engineering
Department of Chemical and Biochemical Engineering

Validation and Improvement of Property and Process Modeling for Oleochemicals

Héctor Alexánder Forero-Hernández
(s163136)

Kongens Lyngby 2019

DTU Chemical Engineering

Department Of Chemical And Biochemical Engineering

Technical University of Denmark

Søltofts Plads

Building 229

2800 Kongens Lyngby, Denmark

Phone +45 4525 2800

kt@kt.dtu.dk

www.kt.dtu.dk

Summary

Fatty acids have been produced through reactions with water and vegetable oil on an industrial scale for more than 130 years. These reactions also produce several important industrial chemicals including monoglycerides, diglycerides and glycerol which can be further processed to high value market products. Given their importance in the chemical industry and with a fast-growing market for bio-based products, there is every reason to expect this demand to grow around the world, since oleochemicals are renewable and cheap.

Nevertheless, when one is reviewing the technical development of the manufacture of oleochemicals, one finds that some basic facts and properties have only been partially recognized due to the harsh physical conditions at which oleochemicals are exposed to during their processing. Hence, it has become more imperative for the industry to better respond to consumer needs by studying the chemical transformations involved in the processing of oils and fats. It is due to the fact that a good understanding of process phenomena leads to an effective design.

The aim of this study is to collect, validate, and improve properties and models of selected oleochemical processes, so as to get a better understanding of them to ensure high process efficiency. In particular, the batch hydrolysis of rapeseed oil at subcritical conditions was studied. The challenges presented by the absence of accurate models for this reaction and process were overcome by collecting data through experiments, rigorous mathematical modeling, uncertainty and sensitivity quantification, thermodynamic analysis of reactions and mixtures, simulation of technologies and scenarios, and analysis of fluid flow behavior in industrial settings. By applying these methodologies, it was possible to represent accurately the studied system. In this way, the production of fatty acids was analyzed in terms of its phenomena, design variables and process parameters. Furthermore, the results were used to validate and improve property and process modeling.

Since the lack of reliable data is a crucial issue in the processing of vegetable oils, a combined experimental and Process Systems Engineering approach proved to be of substantial value to provide necessary information for

detailed modeling and characterization of the production of fatty acids. The results are important and valuable in order to improve the understanding of design and operating variables which increase the feasibility of vegetable oil utilization. They are important and valuable because they provide one with information which can be used in the simulation, design, and optimization of the reactions, and recovery of oleochemicals.

Resumé

Fedtsyrer er blevet produceret igennem reaktioner med vand og vegetabilsk olie på industriel skala i mere end 130 år. Disse reaktioner producerer flere vigtige industrielle kemikalier, herunder monoglycerider, diglycerider og glycerol, som yderligere kan forarbejdes til produkter af høj værdi. I betragtning af deres betydning i kemi industrien og med et hurtigt voksende marked for biobaserede produkter, er der al mulig grund til at forvente, at denne efterspørgsel kommer til at vokse over hele verden, især da oleokemikalierne er vedvarende og billige.

Alligevel finder man, når man undersøger den tekniske udvikling af fremstillingen af oleokemikalier, at nogle grundlæggende fakta og egenskaber kun er blevet delvist anerkendt på grund af de hårde fysiske forhold, som oleokemikalier udsættes for under behandlingen. Derfor er det blevet mere vigtigt for industrien at reagere bedre på forbrugernes behov ved at studere de kemiske transformationer, der er involveret i forarbejdningen af olier og fedtstoffer. Dette skyldes at en god forståelse af procesfænomener fører til et effektivt design.

Formålet med denne undersøgelse er at indsamle, validere og forbedre egenskaber og modeller af udvalgte oleokemiske processer for at få en bedre forståelse for dem og dermed at sikre høj proces effektivitet. Fokusset var i sær på hydrolysen af rapsolie ved subkritiske betingelser. Udfordringerne af manglen på præcise modeller til denne reaktion og proces blev overvundet ved at indsamle data gennem eksperimenter, detaljeret matematisk modellering, usikkerheds- og følsomhedskvantificering, termodynamisk analyse af reaktioner og blandinger, simulering af teknologier og scenarier og analyse af væskestrømsadfærd i industrielle omgivelser. Ved at anvende disse metoder var det muligt at repræsentere netop det studerede system. På denne måde blev produktionen af fedtsyrer analyseret med hensyn til dens fænomener, designvariabler og procesparametre. Endvidere blev resultaterne anvendt til at validere og forbedre egenskabs- og procesmodellering.

Da manglen på pålidelige data er et afgørende problem i behandlingen af vegetabilske olier, viste en kombineret forsøgs- og Process Systems Engineering tilgang at være af væsentlig værdi for at tilvejebringe nødvendig information

til detaljeret modellering og karakterisering af produktionen af fedtsyrer. Resultaterne er vigtige og værdifulde for at forbedre forståelsen af design og driftsvariabler, som øger muligheden for vegetabilsk olieudnyttelse. Dette er tilfældet fordi de indeholder oplysninger, som kan bruges til simulering, design og optimering af reaktionerne samt til udvinding af oleokemikalier.

Preface

This thesis is submitted as a partial fulfillment of the requirements for the degree of Doctor of Philosophy at the Technical University of Denmark.

The work has been carried out at Alfa Laval Copenhagen A/S and at the Process and Systems Engineering Centre (PROSYS) at the Department of Chemical and Biochemical Engineering from June 2016 to June 2019, under the supervision of Associate Professor Gürkan Sin (DTU), Dr. Bent Sarup (Alfa Laval Copenhagen A/S), Professor Anker Degn Jensen (DTU) and Associate Professor Jens Abildskov (DTU).

This project received funding as part of the Marie Skłodowska-Curie Innovative Training Network "**ModLife: Advancing Modeling for Process-Product Innovation, Optimization, Monitoring and Control in Life Science Industries**" in the Horizon 2020 Program of the European Commission (H2020-MSCA-ITN-2015 call, Project No. 675251).

Kongens Lyngby, June 14, 2019

Héctor Alexánder Forero-Hernández (s163136)

Acknowledgements

I would like to thank my supervisors Assoc. Prof. Gürkan Sin, Dr. Bent Sarup (Alfa Laval Copenhagen A/S), Assoc. Prof. Jens Abildskov, and Prof. Anker Degn Jensen for the patience, guidance, encouragement, and help they have provided throughout my time as their PhD student. Their friendly guidance and advice have been invaluable throughout all the stages of this work.

Special thanks to Dr. Viacheslav Artyushenko, Dr. Olga Bibikova, Dr. Irina Mokovic, and Natalie Schwenk from Art Photonics GmbH (Berlin - Germany) for their kindness during my external stay in their laboratories, where I had all the professional and logistical support to achieve the objectives pursued.

I would also like to express my gratitude to Dr. Ana Carolina Fernandes, Dr. Joachim Bachmann Nielsen and BSc. Roxana García for the help I received from them to carry out experiments. In the same way, my appreciation goes to laboratory coordinator Ida Lysgaard Thygesen for providing the resources and support needed. A special acknowledgement to the administrative staff at PROSYS and DTU. Especially to Eva Mikkelsen, Gitte Læssøe, Anja Ninnet Jensen, and Annette Juel Baunsgaard who were always ready to give their kind assistance whenever I required it.

I would also like to express my warmest gratitude to Alexandr Zubov, Mark Jones, Łukasz Ruszczynski, Frederico Montes, Resul Al, Rasmus Fjordbak Nielsen, Katrin Pontius, Franz Bähner, Merve Öner, Daria Semenova, Pau Cabañeros López, Jérôme Frutiger, Robert Spann, Jess Bjørn Rasmussen, Björn Gutschmann, Manon Weiske, Isuru Udugama, Simoneta Caño de las Heras, and all the colleagues at PROSYS for their generous and sincere companion during this time.

This challenge has been a truly life-changing experience for me, and it would not have been possible to do without the support I have received from all the wonderful people I have met during my life. To my lifelong friends Camilo Botero, Manuel Velez-Arboleda, Jefersson Gómez-Carrillo, and Juan Sebastián Calderón-Rave: thank you for always being there whenever I needed it. Your friendship means the world to me. To my friends and colleagues

Carlos Andrés García-Velásquez, Laura Vanessa Daza-Serna, and Sebastián Serna-Loaiza: thank you for listening to me, your help, and feedback. To all my friends around the world: thank you for your thoughts, wishes, phone calls, e-mails, texts, and visits.

A very special acknowledgement goes to my girlfriend Mia who has been by my side throughout this PhD in almost every minute of it, and without whom, I would not have had the strength to complete this journey. I would also like to acknowledge her family, especially Uffe, Helle, Mathias, Svend-Erik, Aase, and Rita for welcoming me warmly and for all the beautiful moments we have shared.

Finally, I wish to express my deepest appreciation to my parents Hector and Luz Marina, and my sisters Natalia and Tatiana for their unconditional love. Without your endless support and understanding, I would not have come this far. Muchísimas gracias por todo. Mi amor siempre estará con ustedes.

Now away we go toward the topmost mountains. Many still, small voices, as well as the noon thunder, are calling, "Come higher". Farewell blessed dell, woods, gardens, streams, birds, squirrels, lizards, and a thousand others. Farewell. Farewell...

— John Muir (mountaineer). *July 8, 1911*

Contents

Summary i

Resumé iii

Preface v

Acknowledgements vii

Contents xi

1 Introduction 1
- 1.1 Hydrolysis of vegetable oils . . . 6
- 1.2 Scope and objectives of the PhD study . . . 11

2 Experimental investigation of the hydrolysis of rapeseed oil 13
- 2.1 Hydrolysis of vegetable oils . . . 14
- 2.2 Design of experiments . . . 14
- 2.3 Materials and methods . . . 18
- 2.4 Experimental analysis . . . 20
- 2.5 Optimization of reaction conditions by RSM . . . 23
- 2.6 Conclusions . . . 33

3 Thermodynamic analysis of the hydrolysis of triglycerides 35
- 3.1 Thermodynamic equilibrium . . . 35
- 3.2 Modeling of the Gibbs free energy . . . 39
- 3.3 Methodology . . . 47
- 3.4 Thermodynamic analysis - Results . . . 48
- 3.5 Conclusions . . . 56

4 A simplified kinetic and mass transfer modelling of the thermal hydrolysis of vegetable oils 59
- 4.1 Problem statement . . . 59

4.2 Methods 63
4.3 Results and discussion 64
4.4 Conclusions 65

5 Development of a model for the hydrolysis of rapeseed oil 69
5.1 Model development 71
5.2 Experimental materials and methods 76
5.3 Parameter estimation, uncertainty and sensitivity analysis . . . 78
5.4 Implementation of methodologies 83
5.5 Results and discussion 84
5.6 Conclusions 92

6 Simulation of a rapeseed oil processing plant 95
6.1 Preliminary considerations 96
6.2 Flow-sheets and simulations 98
6.3 Sizing of equipment 110
6.4 Economic evaluation 116
6.5 Results - Sizing of equipment 119
6.6 Economic analysis of different scenarios 120
6.7 Conclusions 125

7 An analysis of fluid flow behavior in an industrial scale spray column – a coupled CFD and kinetics study 127
7.1 Process description 127
7.2 Computational Fluid Dynamics 128
7.3 Simulation settings 133
7.4 Results 134
7.5 Conclusions 140

8 Conclusions and future work 141

9 Supporting Information 145

Bibliography 167

CHAPTER 1

Introduction

About two-thirds of the World's production of oils and fats are intended for human and animal consumption, the remaining being used in a wide variety of industrial applications. Recently, a great interest has been shown in the transformation of oils and fats, aiming at the use of them in the production of compounds of high added value.

Oils and fats are hydrophobic substances whose main components are triglycerides, esters resulting from the binding of glycerol with fatty acids (Awadallak et al. 2013). Oils and fats belong to the chemical class of *lipids* and may be of animal or vegetable origin. Oils and fats can be differentiated by their physical state at room temperature (Balcao and Malcata 1998).

Generally, vegetable oils are extracted from the seeds or grains of plants known as oleaginous. Oils for human consumption are subjected to a refining process whose purpose is to improve their characteristics by removing undesired components as phospholipids, waxes, oxidation products, pigments and other contaminants (pesticides and solvents).

According to data from the US Department of Agriculture (USDA), the major internationally traded vegetable oils are derived from palm, soybean, rapeseed, sunflower, palm kernel, peanut, cottonseed and coconut as shown in Figure 1.1, with a sustained growth through the years (Willer et al. 2018). Recently, there has been a significant increase in the productivity due to the adoption of new seed varieties, application of fertilizers and pesticides and new management practices. Demand for vegetable oils is steadily growing, due to population and income growth, particularly in populous countries such as India, China, Indonesia, Bangladesh, Pakistan, Nigeria and Egypt. Emerging markets generally consume more than 70% of the global production of vegetable oils. India and China, the two largest consumer countries, account for more than a third of world oil imports.

As seen in Figure 1.2 approximately 70% of the vegetable oil produced is consumed by the food industry, 15% for cosmetics production, and only 10% for the oleochemical industry. The oleochemical industry can be subdivided into three basic branches: fatty acids (approximately 7.6 million tons),

fatty alcohols (approximately 2.8 million tons) and glycerin (approximately 3.6 million tons).

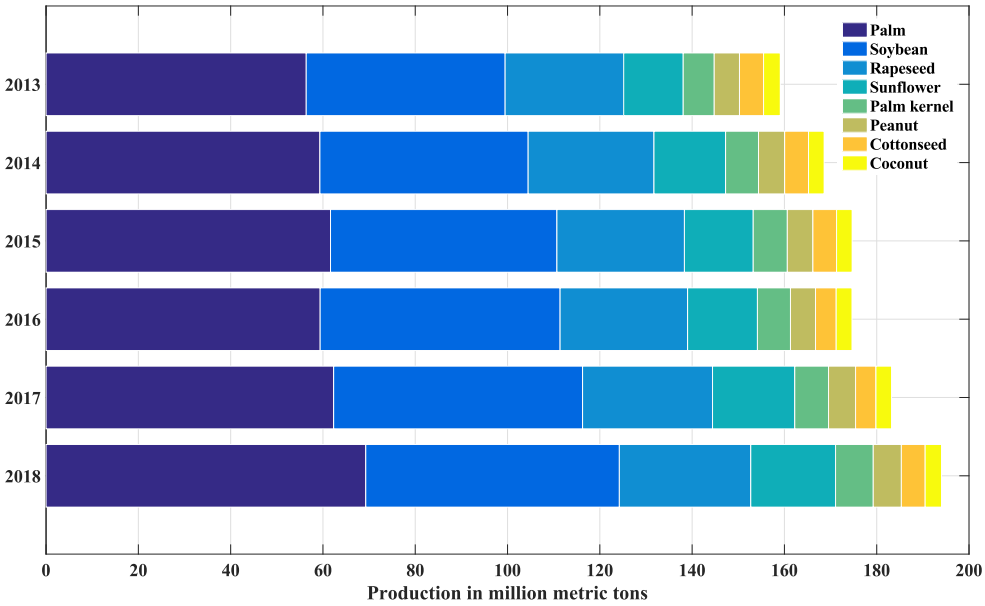

Figure 1.1: Global production of vegetable oils.

Although the industrial applications of oleochemicals are currently concentrated in the fatty acids, new applications have been established in the most diverse fields, such as the pharmaceutical industry, fine chemicals, cosmetics, specialized oleochemicals, leathers, pulp and paper pulp and in the treatment of industrial waste. In this sense, the development of the oleochemical industry emerges as a new force to further boost the growth in demand for vegetable oils.

The volume of the global market of fatty acids is expected to grow from 12.86 million tons in 2016 to 16.82 million tons in 2022, while the market value is expected to increase from 17.96 billion US$ in 2015 to a value of 28.73 billion US$ by 2022 as seen in Figure 1.3 (BCC Research 2016). In order for this market to continue to rise, it is required for producers to maintain the pace with the demand from the industries so as to guarantee the establishment of the productive chains of the sector.

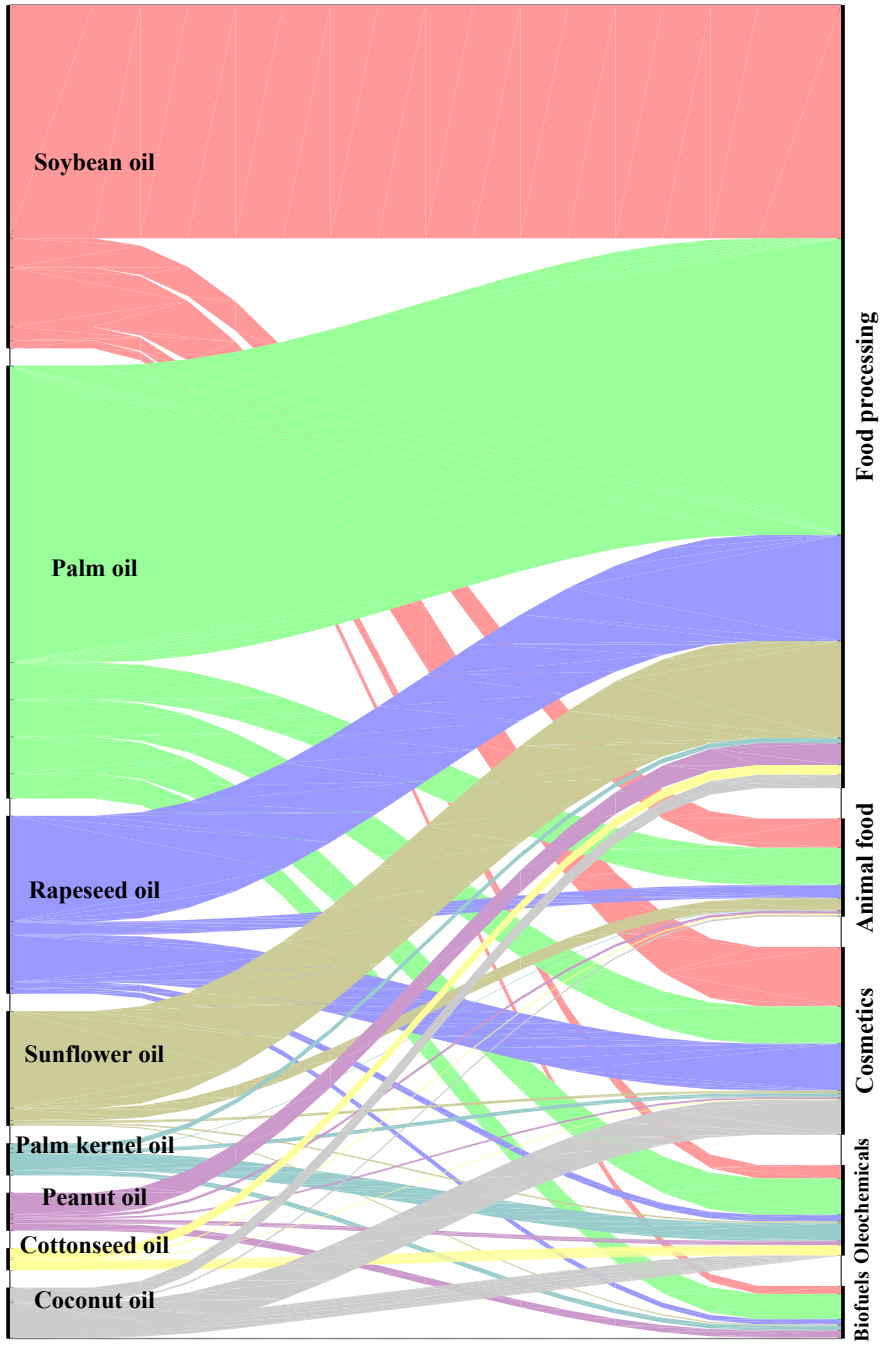

Figure 1.2: Main applications of vegetable oils.

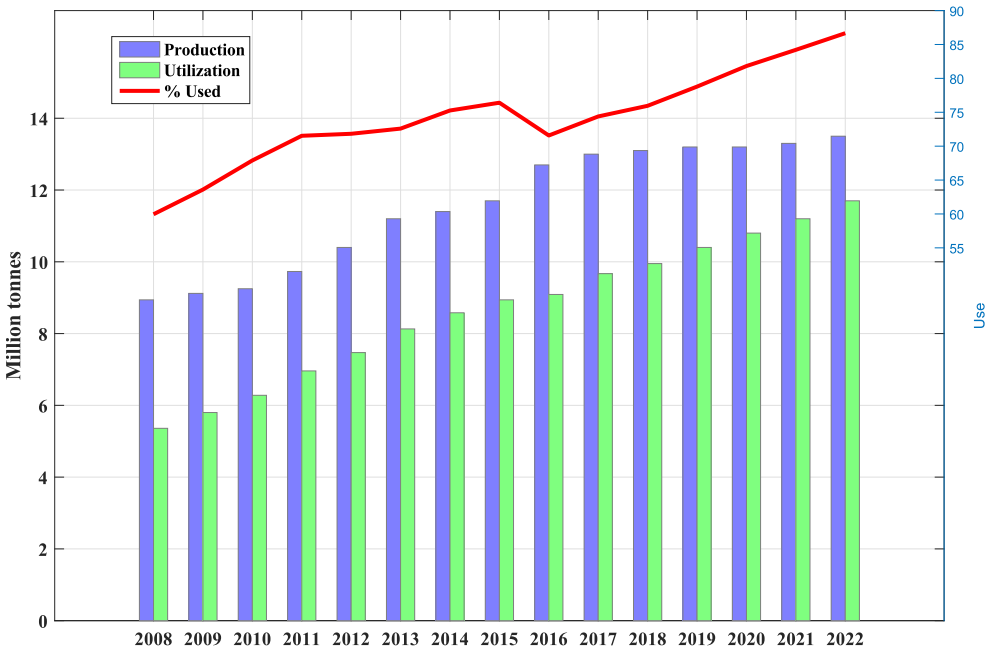

Figure 1.3: Production capacity and use of fatty acids.

Fatty acids are the leading oleochemical type segment due to its high demand in pharmaceutical and food industries, soaps and detergents, candles, waxes, lubricants, paints and coatings. Furthermore, industries related to fatty acids such as plastics, rubbers, and surface-active agents are speeding up their industrial structure to keep up with the growing market.

Given the importance of vegetable oils in the preparations of further chemical compounds, specifically fatty acids, and with a fast-growing market for bio-based products, there is every reason to expect this demand to grow around the world. Hence, it has become more imperative for the industry to better respond to consumer needs by understanding the chemical transformations of vegetable oils.

Triglycerides and fatty acids contained in vegetable oils have two important functions in human metabolism: to supply energy and to transport organic chemical agents soluble in oils such as vitamins and oil-soluble hormones. In the same way, lipids play a key role in nutrition since they are important sources of essential fatty acids, vehicle for fat-soluble vitamins and participate in the synthesis of many endogenous substances. However, its excessive consumption is directly related to cardiovascular diseases, obesity and insulin

resistance (Phuah et al. 2012).

In addition to the problems related to the consumption of oils and fats and their importance in human nutrition, there has been a growing interest in performing research of technologies for the modification of oils and fats. The structure of the oils and fats can be redesigned by means of several chemical transformations such as hydrogenation (chemical modification of fatty acids), hydrolysis (cleavage of the ester bond) and interesterification (reorganization of fatty acids in the triglyceride main chain) (J. Satyarthi, Srinivas, and Ratnasamy 2011).

Figure 1.4 shows the division of the processing of vegetable oils to oleochemicals into three parts: **1)** includes the processing of oil seeds into oil which can be used in the oleochemical industry, **2)** involves the conversion of triglycerides into fatty acids or methyl esters and **3)** comprises the modification, synthesis and refining of the products obtained in **2**.

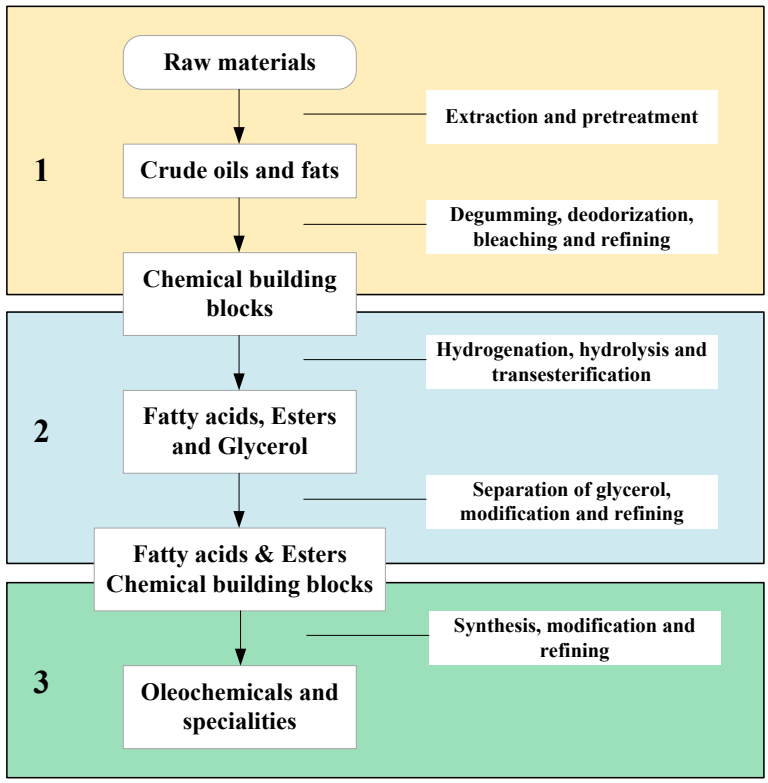

Figure 1.4: Processing of vegetable oils to oleochemicals.

1.1 Hydrolysis of vegetable oils

Hydrolysis is one of the first steps in obtaining chemical derivatives of vegetable oils, which leads to glycerol, monoglycerides, diglycerides and mixtures of fatty acids. Transformations of oils and fats are predominantly based on conventional chemical processes. In the case of hydrolysis, the most employed process is the *Colgate-Emery process* (Bailey and Shahidi 2005).

Figure 1.5 shows the reaction mechanism of the hydrolysis reaction. The reaction is initiated by the nucleophilic attack of a molecule of water on the triglyceride, forming a molecule of fatty acid and a molecule of diglyceride. Then, a new molecule of water makes another cleavage, breaking the diglyceride into a monoglyceride and one more molecule of fatty acid. Finally, the monoglyceride molecule is also hydrolyzed, forming glycerol and the last free fatty acid molecule. Therefore, in this reaction 3 molecules of water are necessary for each molecule of triglyceride to be hydrolyzed. In a complete hydrolysis three molecules of fatty acid and one molecule of glycerol are generated (Minami and Saka 2006).

The hydrolysis of triglycerides is described as an equilibrium reaction characterized by a progressive rise in the reaction rate due to the enhanced solubility of water in the triglycerides at high temperatures (Moquin and Temelli 2008). The main factors affecting this reaction are temperature, type of catalyst, excess of water used for the reaction and the amount of glycerol released to the resulting aqueous phase (Sharma, Chaurasia, and Dalai 2013). The reaction proceeds in stages, which occur simultaneously at different speeds. Kinetic studies report that the hydrolysis reaction of vegetable oils conducted in a subcritical environment provides favorable operating conditions for an autocatalytic action of free fatty acids formed, which act as acid catalysts, accelerating their own reaction (Minami and Saka 2006).

Conventional industrial hydrolysis of oils and fats is generally conducted under subcritical pressures close to 45 bar and temperatures around 250°C for a maximum period of 2 hours with high yields (96-99%). The resulting products are extremely dark fatty acids and an aqueous solution rich in glycerol, which need to be re-distilled for color removal and purification (Abdelmoez, Mostafa, and Mustafa 2013). The hydrolysis of triglycerides can be carried out batchwise (Twitchell process) or continuously (Colgate Emery process) (Sonntag 1979).

Currently, the continuous hydrolysis of triglycerides allows the industrial production of fatty acids by the action of water vapor in a spray column at high pressures (Hill 1949). The reaction is non-catalyzed with conversions of

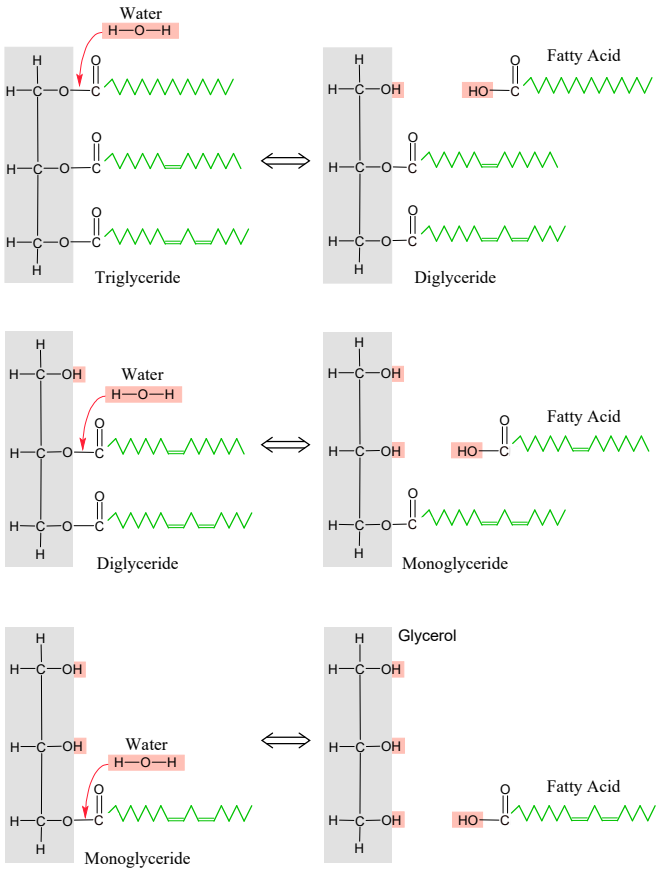

Figure 1.5: Reaction mechanism of the hydrolysis of triglycerides to fatty acids.

triglycerides up to 99% after 1 to 3 hours in the reactor (Kent et al. 2007). The glycerol formed during the hydrolysis is continuously extracted from the reaction medium.

The company Emery-Oleochemicals industrially produces oleic acid by hydrolysis of vegetable oils or animal fats with a purity of 70-75%. This step of hydrolysis of vegetable oil also produces about 10% by weight of pure glycerol at 80-85%. Holliday et al conducted hydrolysis experiments on soybean oil, linseed oil and coconut oil using sub- and supercritical conditions. In this study, the authors report that at subcritical conditions, conversions above 97% were obtained in a period of 15 to 20 minutes, while the reactions conducted above the critical temperature formed the corresponding free fatty acids, but also re-

sulted in degradation, pyrolysis and polymerization reactions (R. L. Holliday, J. W. King, and G. R. List 1997).

King et al performed subcritical hydrolysis experiments using soybean oil in a visible window cell, where it was possible to verify a higher miscibility between oil and water under these conditions. The authors found that the application of subcritical conditions of water replaces the use of catalysts, reaching conversions also higher than 97%, however, the system requires higher reaction temperatures than the catalytic process (J. King, R. Holliday, and G. List 1999).

Pinto and Lancas used corn oil to conduct the reaction in subcritical water, reaching 99% free fatty acid conversion at 280°C. In this study the authors also refer to water as a reagent and reaction solvent with high solubility in the oil (Pinto and Lanças 2006).

Micic et al performed a hydrolysis optimization study in subcritical water. In their work, the authors considered the hydrolysis step as a pretreatment of the raw material for esterification. In their analysis of optimization of the parameters in the pretreatment, the parameters with the greatest influence on the hydrolysis reaction were the residence time alongside the temperature and water-to-oil molar ratio (Micic et al. 2015).

In practice, supercritical conditions are avoided due to the the high energy demanded to maintain the reaction process above the critical point of the water, being replaced by the subcritical operating conditions, where properties similar to the supercritical state are already reached. Some authors, cited below, have already reported the ability of water to act as a reagent and solvent for the hydrolysis reaction under subcritical or supercritical conditions. The great advantage of applying the subcritical medium to the hydrolysis reported in these studies is the elimination of the need for the use of a catalyst, avoiding subsequent steps of separation and recovery of it.

Enzymatic approaches have also been proposed by using *Rhizomucor miehei* and *Candida rugosa*. The reaction in the presence of enzymes has several advantages over conventional processes since generated products have a higher purity and its implementation requires a lower energy input (Gunstone, Harwood, and Dijkstra 2007). However, the high price of enzymes makes their application unrealistic.

Recently, several studies have explored the use of different operating conditions in the hydrolysis of vegetable oils. It is worth mentioning the wide range of temperatures covered and use of different catalysts to enhance the yield. Table 1.1 shows a brief compilation of such studies and their findings.

Table 1.1: Recent applications of the hydrolysis of vegetable oils.

Raw material	Conditions	Catalyst	Yield	Reference
Canola oil	Water-to-oil ratio: 1:1 (%v/v) T: 250 to 320°C P: 20 MPa Time: 60 min	Non-catalyzed	94%	Minami and Saka 2006
Palm oil Castor oil Pine oil Lard	Catalyst: 10% (%m/%v) pH: 8.0 T: 40°C Time: 120 min	Lipase	97%	Sousa et al. 2010
Used oil	Water-to-oil ratio: 1:1 (%v/v) Catalyst: 0 to 0.1% (m/m) pH: 6.8 – 7.4 T: 30°C Time: 10 hours	*Candida rugosa*	99%	Talukder, Wu, and Chua 2010
Soybean oil	Water-to-oil ratio: 1:1 (%v/v) Catalyst: 0 to 7.7% (v/v) T: 47 to 63°C Time: 19 hours	*Therm. lanuginosus*	92%	Cavalcanti-Oliveira et al. 2011
Soybean oil Castor oil	Water-to-oil ratio: 5:1-20:1 (mole) Catalyst: 0 to 20% (m/m) T: 250 to 300°C Time: 60 min	Niobium oxide	87%	LL Rocha et al. 2010
Macaúba palm oil	Water-to-oil ratio: 4:1-14:1 (mole) Catalyst: 0 to 24% (m/m) Agitation: 700 rpm T: 152 to 300°C	Zeolite H – USY	88%	Machado 2013

Microalgae oil	Water-to-oil ratio: 3:1 (mole) T: 200 to 300°C Time: 11 hours	Nb_2O_5	95%	Chenard Diaz et al. 2013
Soybean oil Macaúba palm oil	Water-to-oil ratio: 1:1-5:1 (mole) T: 200°C Catalyst: 4% (m/m) Agitation: 800 rpm P: 13.6 bar Time: 180 to 300 min	ICdO and ISnO	84%	Alves et al. 2014
Macaúba palm oil	Water-to-oil ratio: 1:1 (v/v) Catalyst: 2.5% (m/v) pH: 4.0 T: 30 °C Time: 24 to 72 hours	*Rhizomucor Lipozyme*	92%	Aguieiras et al. 2014
Waste cooking oill	Water-to-oil ratio: 100:1 (mole) Catalyst: 1% (w/w) Agitation: 700 rpm T: 250 °C Time: 120 minutes	Sulfuric acid	95%	Santos et al. 2017
Soybean oil	Water-to-oil ratio: 19:1 (mole) Catalyst: 5% (w/w) Agitation: 60-600 rpm T: 90 to 120 °C Time: 800 minutes	BEA Zeolite	91%	Mowla and Stockenhuber 2019

1.2 Scope and objectives of the PhD study

In processes where chemical reactions occur to obtain a desired product, the overall yield of the process will depend strongly on the operational performance of the units and their constituent models. Hence, for a given process, non-accurate properties and models result in lower productivities, excessive size of units and/or recycle of unconverted reagents. Thus, for the development of the conceptual design of a chemical plant, it is convenient to have an adequate representation in order to describe the phenomena which takes place in the system.

In the literature, the experimental data available which concerns the reactions needed for the design and analysis of processes which involves lipid technology are, in the best case scenario, scarce and not conclusive. Moreover, the mathematical models used to correlate the behavior of reactions with phenomena are not accurate enough and are not used for validation. Hence, these models are not predictive in nature, which limit their scientific and industrial applicability.

Therefore, it is of great interest to develop models and validation strategies which allow the integration of methodologies so as to ensure excellence in process design. Hence, the aim of this project is to collect, validate, and improve properties and models of selected oleochemical processes, so as to get a better understanding of them to ensure high process efficiency. In particular, the batch hydrolysis of rapeseed oil at subcritical conditions was studied.

The methodologies used comprise from the development of experiments, application of different methods to assess kinetic and thermodynamic properties, modeling of reacting phenomena, and evaluation and validation of properties and models.

The main results of the project can be summarized as:

- Systematic identification of the gaps in the property models and the need for data for further improvement and validation.
- Generation and collection of kinetic data relevant for oleochemicals.
- Improvement in property models for predicting phase and chemical equilibrium of mixtures relevant to oleochemicals.
- Comprehensive uncertainty analysis of prediction accuracy of improved models.

- Validation of the models demonstrated for selected oleochemical processes namely fat-oil splitting.

The general structure of the thesis is presented below as a brief overview. Every chapter introduces the methodologies used and provides further details on the results obtained.

- **Chapter 1** serves as an introduction to oleochemicals and the subcritical hydrolysis of triglycerides. Furthermore, the chapter presents the scope of the thesis.

- **Chapter 2** presents the experimental investigation of the hydrolysis of rapeseed oil in a batch reactor. Additionally, this chapter includes the analysis of the effect of operating variables on the reaction and their optimization.

- **Chapter 3** highlights the results a thermodynamic analysis for the calculation of combined chemical and phase equilibrium in the hydrolysis of vegetable oil under subcritical conditions.

- **Chapter 4** proposes a simplified kinetic and mass transfer model for the hydrolysis of vegetable oils in a batch reactor. In this chapter, a bootstrap based uncertainty analysis was performed to find the accuracy of estimated parameters and model outputs.

- **Chapter 5** describes the comprehensive development, uncertainty and sensitivity analysis of an extended biphasic model for the batch hydrolysis of vegetable oil.

- **Chapter 6** shows a preliminary design and techno-economic simulation of a fatty acids chemical plant under different technological and operating scenarios.

- **Chapter 7** provides details on current and future work, specifically an application of computational fluid dynamics to the hydrolysis of vegetable oil at industrial scale.

- **Chapter 8** describes the general conclusions of this thesis and perspectives for future work.

CHAPTER 2

Experimental investigation of the hydrolysis of rapeseed oil

In industrial processes there are several factors or variables which affect the yield of the process or the quality of the final product. The task of optimizing a given process can be lengthy and costly if an appropriate tool is not used. In this regard, *statistical design and analysis of experiments* have been considered effective and indispensable tools for the development of processes, especially when a large number of variables are involved.

These tools are a set of mathematical and statistical techniques whose application allows one to select the combination of optimum conditions to obtain the best response for a given input to the process.

The main advantages of using such methods are to reduce the number of trials performed with experimental designs so as to obtain more accurate results, and to examine the interdependence between variables to decrease the amount of tests required when performing experiments.

The objective of this chapter is to determine the optimum conditions of the reaction of hydrolysis of rapeseed oil by varying the temperature, ratio of reactants and agitation, to determine which of these variables exerts greater influence on the yield of fatty acids. To fulfill this objective, a *Response Surface Methodology* (RSM) was used to study the effect of the operating conditions on the yield of reaction to fatty acids. An ANOVA variance analysis was performed to evaluate the significance of the parameters and their interactions based on the Fisher test and its associated probability. *t*-student tests were also performed for the regression coefficients in the obtained quadratic model. Through the application of this methodology, it was possible propose the combination of process variables which optimized the reaction.

2.1 Hydrolysis of vegetable oils

The hydrolysis of oils and fats is an important processing route for the chemical industry. In this regard, several authors have performed studies for the hydrolysis reaction of triglycerides (Hartman 1951; Minami and Saka 2006; Patil, Raghunathan, and Shankar 1988a; Patil, Raghunathan, and Shankar 1988b; Namdev et al. 1988). This reaction can proceed in multiphasic systems such as liquid-liquid system or gas-liquid (Jeffreys 1961; Archuleta 1991). The reaction between triglycerides and water in subcritical state is influenced by both mass transfer among phases and by the kinetics of the reactions. Lascaray found that the conversion of this reaction is dependent of the temperature (Lascaray 1949; Lascaray 1952). Sturzenegger and Sturm described the autocatalytic behavior of the reaction in a batch reactor, with the assumption that the reaction occurs in the bulk of the oil phase after diffusion. Such behavior had been attributed to the elevated ion product of water at high temperature (Sturzenegger and Sturm 1951). The authors also determined the effect of temperature, pressure, and initial ratio of reactants. Additionally, the authors proposed a shunt reaction mechanism. More recently, Alenezi et al. 2009 studied the kinetics of the hydrolysis of sunflower oil under subcritical conditions in a PFR, which also included information on the different conditions which affects the reaction. Additionally, the hydrolysis at low/middle temperatures over solid acid catalysts was discussed by J. K. Satyarthi, D. Srinivas, and P. Ratnasamy 2011. In their study, the rates of hydrolysis were increased by the action of solvents and phase transfer agents.

This chapter presents the hydrolysis of rapeseed oil by using subcritical water to produce fatty acids. A non-catalytic batch process was studied with-ing a temperature range of 180°C - 280°C for two water-to-oil molar ratios and two agitation rates. The factors which affect the yield were also studied.

2.2 Design of experiments

The use of factorial planning of experiments is a useful strategy in mapping the experiments to be carried out. Depending on the type of study in question, different types of experiment planning can be applied, with planning generally having 3 levels of variation for each factor. Nevertheless, studies with 2 or 4 levels are also available in the literature. The main designs of factorial planning experiments are orthogonal tests, Box-Behnken design, Central Composite Design, and Doehlert Matrix (S. C. Ferreira et al. 2007).

2.2.1 Box-Behnken Design of Experiments

This method is a three-level model for the adjustment of the model of surface responses (Box and Behnken 1960). It combines 2^k factors into an incomplete block in terms of number of experiments, which makes it an efficient and economical option in relation to the corresponding 3^k design (Box and Behnken 1960; Bezerra et al. 2008). Thus, it is advantageous to use them because these vertices may represent constraints from the physical or experimental point of view (Box and Behnken 1960). All factors are adjusted in three levels $(-1, 0, 1)$ with equal intervals in each level.

2.2.2 Response Surface Model methodology

The response surface methodology (RSM) is a mathematical and statistical tool used in the modeling and analysis of systems, whose response is affected by several factors or variables which are to be optimized. If the response of a model presents a curvature, the model can be described by a polynomial of second degree, which is translated by the equation:

$$y = \beta_0 + \sum_{i=1}^{k} \beta_i X_i + \sum_{i=1}^{k} \beta_{ii} X_i^2 + \sum_{i<j} \beta_{ij} X_i X_j + \varepsilon \tag{2.1}$$

Where β_0, β_i, β_{ii} and β_{ij} are the coefficients of the model. X_k are the variables of the process and ε is the error associated to the system (S. C. Ferreira et al. 2007). These parameters are determined by least squares regression method. Given the complexity of the matrix calculations involved, these are usually determined by using computer tools. The process-coded variables are obtained from the real variables by the equation:

$$X_k = \frac{x_k - x_0}{\Delta x_k} \tag{2.2}$$

Where x_k is the true value of the coded variable X_k, x_0 the true value of the center point, and Δx_k the step for each level (Bezerra et al. 2008).

The good estimation of the parameters of the model depends on the choice of the type of model and the design of experiments chosen. In fact, RSM is a sequential model because the response surface, which describes the process, may be far from the optimal point, i.e., the chosen operating conditions may be far from the conditions that would provide an optimal operation point. This occurs when the relationships between the operating variables and their impact on the process is unknown. In this situation, this approach serves only

as an indication of the location of the operating zone (S. C. Ferreira et al. 2007).

2.2.3 Analysis of Variance (ANOVA)

The proposed model should be investigated by analyzing its variance (ANOVA) to determine the significance of the fit to the physical situation in question (Miller Jr 1997). The main purpose of ANOVA is the comparison between the combinations of the different levels and the errors inherent in measurements. An ANOVA implies that the data follows a normal distribution and has the same variance. The technique begins by decomposing the variance of the responses into two fundamental components, variance in the group and between the groups, with the objective of testing the equality of effects by comparing two different estimates of the variance (H. Keselman et al. 1998).

Source	Sum of squares	DoF	Mean of squares
Regression	$SS_R = \sum i^m \sum_j^{n_i} \left(\widehat{y}_i - \bar{y}\right)^2$	$p-1$	$MS_R = \frac{SS_{reg}}{p-1}$
Residuals	$SS_E = \sum i^m \sum_j^{n_i} \left(y - \widehat{y}_i\right)^2$	$n-p$	$MS_E = \frac{SS_{reg}}{n-p}$
Lack of fit	$SS_{lf} = \sum i^m \sum_j^{n_i} \left(\widehat{y}_i - \bar{y}_i\right)^2$	$m-p$	$MS_{lf} = \frac{SS_{lf}}{m-p}$
Pure error	$SS_{pe} = \sum i^m \sum_j^{n_i} \left(y_{ij} - \bar{y}_i\right)^2$	$n-m$	$MS_{pe} = \frac{SS_{pe}}{n-m}$
Total	$SS_{TT} = \sum i^m \sum_j^{n_i} \left(y_{ij} - \bar{y}\right)^2$	$n-1$	

Table 2.1: ANOVA for the fit of experimental data by using multiple regression.

Where n_i is the number of observations, m the total number of combinations in the design, p the number of model parameters, $\widehat{y}_i$ the estimated value for the model for each level i, $\bar{y}$ the global mean, y_{ij} replicates at each level, and $\bar{y}_i$ replicates at each level.

2.2.4 Regression significance tests

The regression significance test is a test to determine the linearity between the response variable and the regression variables. This hypothesis is called *null hypothesis* and can be expressed as:

$$H_0 : \beta_1 = \beta_2 = \cdots = \beta_k = 0 \quad \text{versus} \quad H_1 : \beta_j \neq 0, \ \text{for at least one } j \quad (2.3)$$

The rejection of the null hypothesis H_0, implies the existence of at least one parameter of the regression, X_i, which has a great significance in the

model. The test involves an ANOVA in which SS_{TT} is the total sum of squares. The procedure for non-rejection of the null hypothesis is given by the Fisher statistic F_0, which is determined by the ratio of the mean squares of the regression MS_R and the mean squares of the residuals MS_E (Dunning 1993). H_0 is rejected if F_0 is greater than $F_{\alpha,k,n-k-1}$, or if the p-value is less than the significance α for the desired confidence interval.

Non-rejection of H_0 indicates that X_j can be eliminated from the model. The t_{student} test is used to conclude on the significance of the regression coefficients. This methodology provides parameters which allows one to evaluate the variability of the fit, which is a measure of the variance of the response obtained by using the regression parameters (Dunning 1993; Bezerra et al. 2008).

The inclusion of central points in the design of experiments allows one to obtain the pure experimental error, which divides, in this way, the distribution of the residuals in the component into pure error and lack of fit (S. C. Ferreira et al. 2007). The statistical test for significance of mismatch is based on the ratio of the mean squares of mismatch MS_{lf} and measured two squares of the pure error MS_{pe}, which in turn is the value of the Fisher statistic F_0. It allows one to compare the value F_0 with the value of $F_{\alpha,k,n-k-1}$, where $m-p$ are the degrees of freedom in the lack of adjustment and $n-m$ the degrees of freedom of pure error. If $F_0 \leq F_{\alpha,k,n-k-1}$ there is no evidence to support the lack of adjustment (Dunning 1993).

2.2.5 Evaluation of the model

The fit between the quality of the model and the experimental data is important in order to ensure that the model gives a true measure of the real system. In this regard, the *Predicted Residual Error Sum of Squares* PRESS can be checked for suitability by plotting the residuals or PRESS. The PRESS allows the calculation of a $R^2_{\text{prediction}}$ which indicates the predictive capacity of the regression model. It is determined by the equation:

$$R^2_{\text{prediction}} = 1 - \frac{\text{PRESS}}{S_{yy}} = 1 - \frac{\sum_{i=1}^{n} (y_i - \widehat{y_i})^2}{S_{TT}} \tag{2.4}$$

The predictive capacity of a model based on this criterion has shown quite satisfactory results (Bezerra et al. 2008).

2.3 Materials and methods

2.3.1 Chemicals

Rapeseed oil was purchased from Scandic Food A/S (Nørre Aaby, Denmark). Deionized water (18 Ω) was used for the hydrolysis experiments. Potassium hydroxide [CAS 1310-58-3], potassium biphthalate [CAS 877-24-7], phenolphthalein [CAS 77-09-8], and toluene [CAS 108-88-3] were used for Acid Value-analysis and were purchased from Sigma-Aldrich Denmark ApS (Brøndby, Denmark).

2.3.2 Batch experiments

Hydrolysis reactions were run in a 300 ml Hastelloy C-276 jacketed reactor with ceramic band heaters (Parker Autoclave Engineers, Model 300 ml HC EZE-Seal), which included a coil to cool the contents in the reactor. The reactor is equipped with a PID controller to monitor and control temperature and agitation speed. The reactor has a sampling port for withdrawal of liquid samples during the reaction every 30 minutes. A scheme of the set-up used is depicted in Figure 5.2. 15 experiments were carried out based on a Box-Behnken design for three factors (temperature, oil-to-water ratio, and agitation speed) and an experimental runtime of six hours as shown in Table 5.1 (Box and Behnken 1960).

The initial time of each experiment was defined as the time when the mixture reached the operating temperature (approximately 18 minutes). In this initiation time, no agitation was provided to the system so as to prevent the reaction. Collected samples were cooled and let to settle in a graduated vial for phase separation and then separated by decantation.

2.3.3 Analysis of samples

2.3.3.1 Acid value

This analytical procedure allows the quantification of free fatty acid content in a sample. In this procedure, a sample of oil is neutralized with a standard alkaline solution. The determination of fatty acids is given by its percentage (by weight) in relation to the weight of the sample. The American Oil Chemists' Society AOCS *Cd 3d-63* method was applied to measure acid value as a way to obtain the yield of the hydrolysis reaction (AOCS 2017). In

Experimental conditions			
Experiment	**Temperature (°C)**	**Water-to-oil ratio**	**Agitation (rpm)**
1	180	15	360
2	180	40	360
3	280	15	360
4	280	40	360
5	180	27.5	120
6	180	27.5	600
7	280	27.5	120
8	280	27.5	600
9	230	15	120
10	230	15	600
11	230	40	120
12	230	40	600
13	230	27.5	360
14	230	27.5	360
15	230	27.5	360

Table 2.2: Experimental design (validation sets are highlighted).

this study, an acid-base titration with potassium hydroxide as titrating base was performed by using diluted phenolphthalein in toluene as indicator. The following equation was then applied to calculate the acid value (AV):

$$AV_{\text{mg KOH / g sample}} = \frac{56.11 \cdot V_{\text{KOH}} N_{\text{KOH}} f_c}{m_{\text{sample}}} \tag{2.5}$$

Where V_{KOH} is the volume in mL of KOH used in the titration, N_{KOH} is the normality of KOH, f_c a correction factor of the acidity or alkalinity of the sample and m_{sample} is the mass of the sample.

Calculation of the correction factor (f_c) was performed by using potassium biphthalate as the primary standard:

$$f_c = \frac{m_{\text{BK}}}{MW_{\text{BK}} V_{\text{KOH}} N_{\text{KOH}}} \cdot 1000 \tag{2.6}$$

Where m_{BK} is the mass in g of potassium biphthalate, MW_{BK} is the molecular weight in $\frac{g}{mol}$ of potassium biphthalate, V_{KOH} is the volume in mL of KOH used in the titration, and N_{KOH} is the normality of KOH.

The reaction yields were determined with Equation (2.7) which is the ratio of the acid value in the sample divided by the acid value of a sample of pure fatty acid obtained from rapeseed oil and multiplied by 100%.

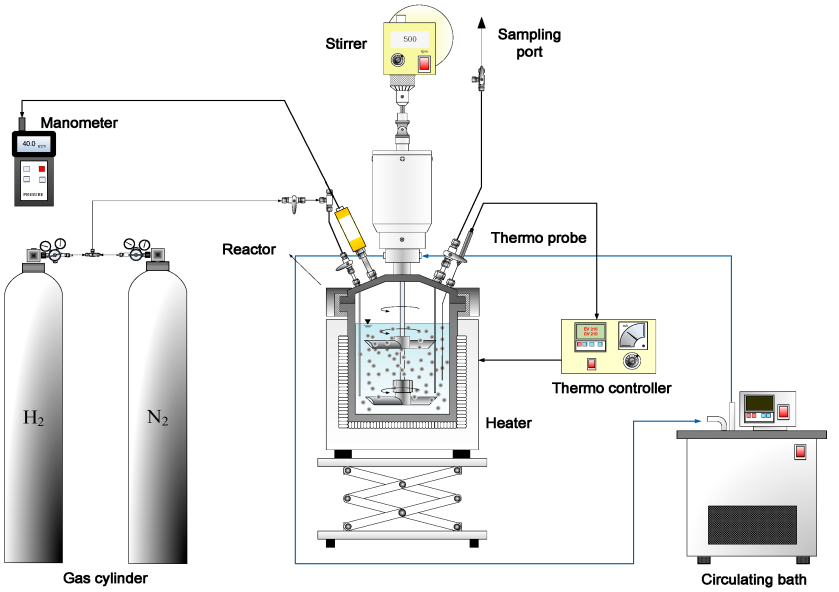

Figure 2.1: Reactor setup used for the hydrolysis of rapeseed oil.

$$\text{Yield}_{\text{sample}} = \frac{\text{Acid value}_{\text{sample}}}{\text{Acid value}_{\text{fatty acid}}} \cdot 100 \tag{2.7}$$

2.4 Experimental analysis

Samples obtained during the reaction were characterized by measuring acid value for calculating yields of reaction. The statistical treatment of the data was elaborated by using Matlab and Minitab. Figure 2.2, Figure 2.3, and Figure 2.4 present the variation of yield versus time of reaction at the different conditions proposed by the design of experiments in Table 5.1.

Generally, the variation of the reaction yield as a function of time had a similar profile in the conditions studied. The yield increased exponentially with time until it reached approximately 75% and then slowly moved to a plateau.

On the other hand, the inflection points in the curves obtained for both low and high yields may be related to the presence of diglycerides and monoglycerides, which in addition to forming hydrogen bonds, can be combined in the mixture with small amounts of water and glycerol. This assumption is

based on the fact that the tests performed with low yield always presented the formation of emulsions.

Figure 2.2 shows that at low temperatures and regardless the water-to-oil molar ratio and agitation, there is no significant growth in the yield during the first hours of the reaction. In this stage, water in the aqueous bulk needs to diffuse through the aqueous film. This mass transfer process depends highly on temperature, since the miscibility between water and oil is enhanced at temperatures above 160°C due to a reduction of the dielectric constant of water. As the reaction progresses with a sigmoidal behaviour, the yield has a sharp rise where it reaches conversions of up to 80%. Experiment 4 shows a faster and exponential increase in the yield than in other experiments. It can be said that in the beginning of the hydrolysis the transfer of water from the bulk of the aqueous phase to the bulk of the oil phase is accelerated due to the high temperature (Patil, Raghunathan, and Shankar 1988b; J. King, R. Holliday, and G. List 1999). These experiments reach a plateau after 2h of reaction where they maintain a sustained, but not significant, increase in the yield.

Figure 2.3 shows that at high temperatures (280°C) the yield function proceeds faster than at lower temperatures where it reaches conversions of up to 80%. However, it is also possible to observe at low temperatures, small amounts of water, and high agitation speed, where greater yields can be achieved (Experiments 6, 9 and 10). This may be the result of an increased interfacial area due to high agitation speed. The early stages in the reaction can be considered to be solubility limited when the dispersion of water in oil is being generated and the interfacial area is limited (Forero-Hernandez et al. 2017).

Figure 2.4 presents the yields obtained at 230°C with a change in the water-to-oil ratio and agitation speed. The yields show a growth rate lower than the ones observed in the experiments conducted under similar conditions of temperature in Figures 2.2 and 2.3. In regards to the behavior of the water quantity, it is possible to observe that for the initial times, the smaller the amount of water, the higher the reaction yield. However, during the course of reaction, higher yields will be obtained with greater amounts of water with a point of inflection that will depend on the kinetics and the thermodynamics of the reaction.

This data provides important information to design and optimize an industrial process, which is a necessary tool when making decisions and choosing the amount of water, temperature, and agitation speed, to obtain the maximum possible yield at a certain fixed reaction time.

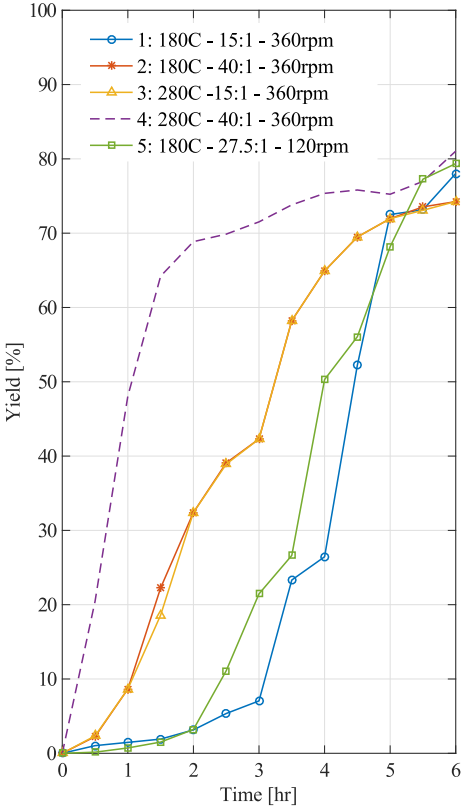

Figure 2.2: Experiments 1-5.

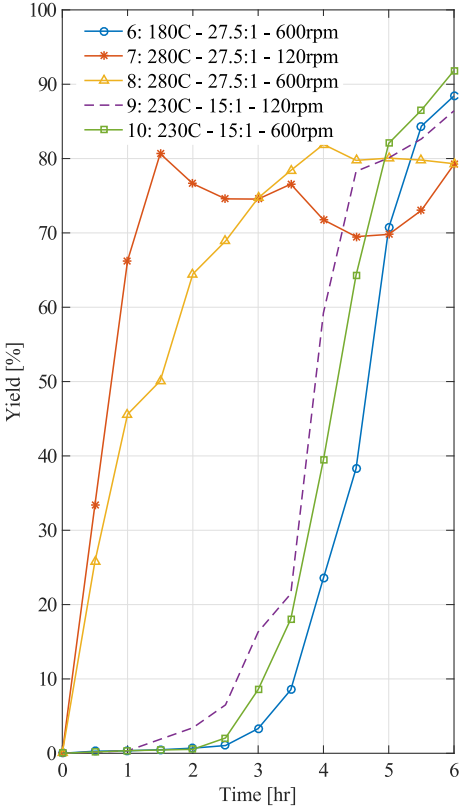

Figure 2.3: Experiments 6-10.

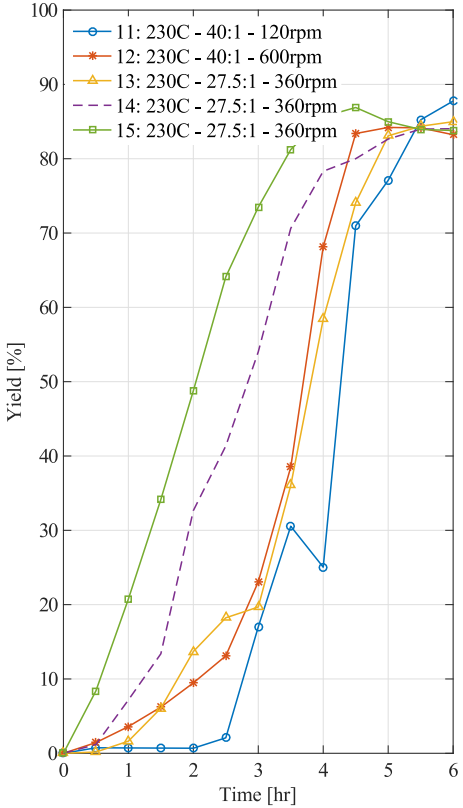

Figure 2.4: Experiments 11-15.

2.5 Optimization of reaction conditions by RSM

The objective of the application of the RSM in this chapter is to study the influence of the operating conditions (temperature, water-to-oil molar ratio, and agitation speed) on the yield of the hydrolysis. An ANOVA was performed to quantify the significance of the parameters and their interactions based on the Fisher test and its associated probability. *t-student* tests were also performed for the regression coefficients in each model. Table 5.2 shows the coding associated with each level of the variable related to the design of experiments presented in Table 5.1. The final yields obtained experimentally are shown in Table 5.3.

Variable		**Level**		
		Lower (-1)	**Middle (0)**	**Upper (+1)**
Temperature (°)C	X_T	180	230	280
Water-to-oil ratio	X_{MR}	15	27.5	40
Agitation (rpm)	X_{rpm}	120	360	600

Table 2.3: Box-Behnken design variables.

Table 5.3 presents the experimental yield of oleic acid obtained for each of the experiments performed according to the Box-Behnken design after six hours of reaction. It also shows the predicted value and associated error of the oil yield, when they are calculated with the reduced model represented by Equation (2.8) presented later in the chapter. The fundamentals which support this model and the inferences about the influence of the studied variables on the objective relative to the point under discussion are presented below.

It can be seen that the yield varies between 74.25% and 91.84% in Experiments 2 and 10 respectively. All points in the model have a relative error of less than 2%.

2.5.1 Pareto diagram

The statistical representation of data is presented in a Pareto diagram (Figure 2.5), so as to investigate the effect of the studied variables on the yield. This analysis allows one to identify, in descending order, the said influences by showing the proximity of the absolute values of the estimated effects. It is possible to observe that the generation of fatty acids results from the combination of the variables temperature, water-to-oil molar ratio, and agitation. However, the individual effect of the agitation influences negatively the yield,

Experimental conditions						
Exp.	X_T	X_{MR}	X_{rpm}	**Yield** $_{\text{exp}}(\%)$	**Yield** $_{\text{calc}}(\%)$	**Error** (%)
1	180	15	360	78.03	77.52	0.644
2	180	40	360	74.25	75.28	-1.397
3	280	15	360	74.26	73.22	1.397
4	280	40	360	81.04	81.54	-0.62
5	180	27.5	120	79.36	79.88	-0.658
6	180	27.5	600	88.43	87.41	1.15
7	280	27.5	120	79.22	80.23	-1.284
8	280	27.5	600	79.31	78.78	0.658
9	230	15	120	86.43	86.41	0.023
10	230	15	600	91.84	92.35	-0.56
11	230	40	120	87.76	87.24	0.586
12	230	40	600	83.23	83.25	-0.024
13	230	27.5	360	84.98	84.27	0.831
14	230	27.5	360	84.04	84.27	-0.277
15	230	27.5	360	83.8	84.26	-0.568

Table 2.4: Experiment planning according to Box-Behnken design and yield of oleic acid (%).

while the individual effect of the temperature enhances the yield. The non-significant values do not reach the threshold delimited by the significance level ($p \leq 0.05$). The Pareto diagram in Figure 2.5 shows that three two-factor interactions ($X_T X_{MR}$, $X_{MR} X_{RPM}$, and $X_T X_{RPM}$) are statistically significant at 5% significance level and have a high influence in the yield. It is also possible to infer that a high increase in the temperature affects negatively the yield. In this case, it is reasonable to assume, based on the gathered experiments, that high temperatures are not only responsible for the yield of fatty acids but for the generation of other compounds in the mixture. Such an occurrence has been observed in the discussion of the experimental results when the highest temperature was used (280°C). As for the X_{RPM}, one could expect its positive and pronounced influence on the yield since high agitation speed enhances the mass transfer of water in the beginning of the reaction. Factors $X_{MR} X_{MR}$ and X_{MR} are deemed non-influential and can be discarded from the quadratic response model.

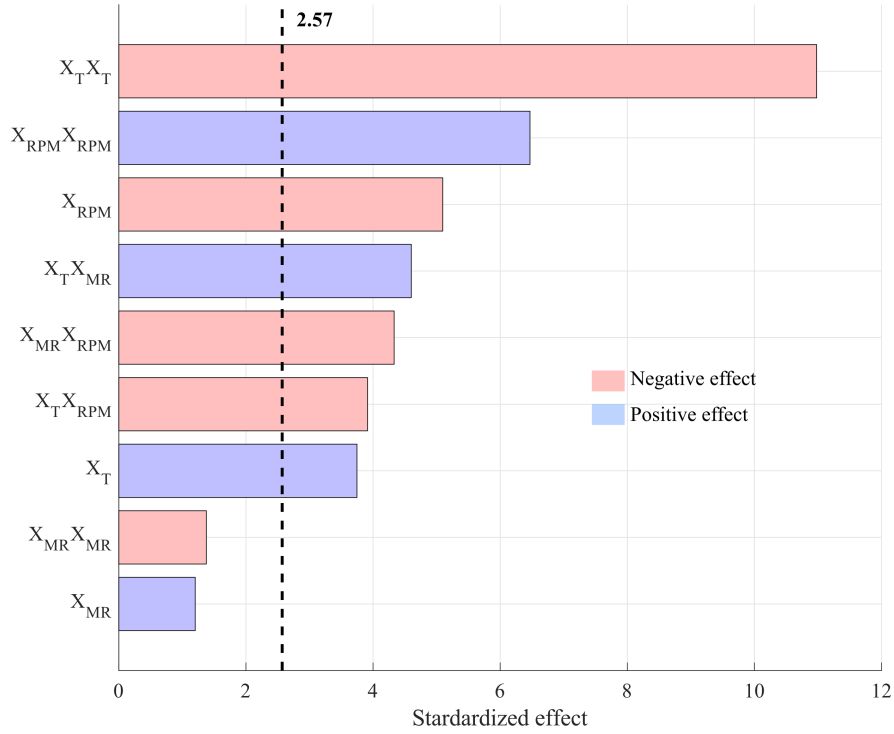

Figure 2.5: Pareto diagram ($p = 0.05$): relative influence of the variables on the yield of fatty acids.

2.5.2 Quadratic regression

Equation (2.8) is obtained from the simplification of Equation (2.1) which is representative of the second-order mathematical model of the response surface:

$$\begin{aligned} Y =& \beta_0 + \beta_1 X_T + \beta_2 X_{MR} + \beta_3 X_{rpm} + \beta_{11} X_T^2 + \beta_{22} X_{MR}^2 + \beta_{33} X_{rpm}^2 \\ &+ \beta_{12} X_T X_{MR} + \beta_{13} X_T X_{rpm} + \beta_{23} X_{MR} X_{rpm} \end{aligned} \tag{2.8}$$

The regression coefficients obtained for Equation (2.8) are shown in Table 2.5. These coefficients were determined statistically with a 95% confidence interval. The quality of the model with reference to the experimental data can be explained by the similarity between the correlation coefficients $R^2 = 0.9699$ and $R^2_{\text{adjusted}} = 0.9398$, as seen in the probability plot presented in Figure 2.6.

Coefficients in bold have statistical significance ($p \leq 0.05$) and represent the scenarios in which the rejection of the null hypothesis was verified in

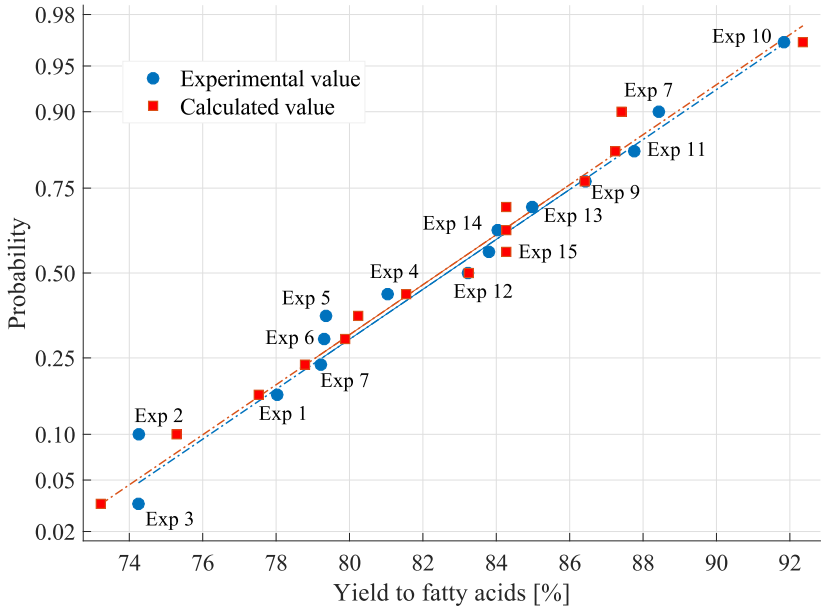

Figure 2.6: Probability plot.

the test. The coefficients that did not satisfy the constraint were eliminated from the model. New coefficients were then calculated and coupled with the decoding of the significant parameters of Equation (2.8). Thus, it allowed one to formulate a new quadratic function in Equation (2.9). The fitting of the reduced model with respect to the experimental points is evidenced by the small difference between the correlation coefficients $R^2 = 0.982$ and $R^2_{\text{adjusted}} = 0.9495$ and their statistical significance as shown in Table 2.6.

$$\begin{aligned}\text{Yield}(\%) = &- 59.45 + 1.188\ \text{T} - 0.0089\ \text{rpm} - 0.002623\ \text{T}^2 + 0.000067\ \text{rpm}^2 \\ &+ 0.004224\ \text{T MR} - 0.000187\ \text{T rpm} - 0.000828\ \text{MR rpm}\end{aligned} \tag{2.9}$$

2.5.3 ANOVA

The analysis of variance allows one to study the quality of the model fit to the experimental data, since it compares the variance which results from the combination of the variables with the random errors inherent to the measurement of the responses. When the design of the experiments used involves performing replicates from the central point, the error associated with the replicates

Variable	Regression coefficients		p (t-Student)
	β_0	84.273	
X_T	β_1	1.52	**0.01344**
$X_T X_T$	β_{11}	-6.557	**0.00011**
X_{MR}	β_2	0.488	0.28831
$X_{MR} X_{MR}$	β_{22}	-0.822	0.22728
X_{rpm}	β_3	-2.067	**0.00378**
$X_{rpm} X_{rpm}$	β_{33}	3.863	**0.00131**
$X_T X_{MR}$	β_{12}	2.64	**0.00583**
$X_T X_{rpm}$	β_{13}	-2.245	**0.01126**
$X_{MR} X_{rpm}$	β_{23}	-2.485	**0.00749**
R^2	0.9699	R^2_{adjusted}	0.9398

Table 2.5: Regression coefficients for the general model of the response surface relative to fatty acids yield.

Variable	Regression coefficients		p (t-Student)
	β_0	83.7677	
X_T	β_1	1.52	**0.0109**
$X_T X_T$	β_{11}	-6.4935	**0.00002**
X_{rpm}	β_3	-2.0675	**0.00229**
$X_{rpm} X_{rpm}$	β_{33}	3.9265	**0.00052**
$X_T X_{MR}$	β_{12}	2.64	**0.00395**
$X_T X_{rpm}$	β_{13}	-2.245	**0.00891**
$X_{MR} X_{rpm}$	β_{23}	-2.485	**0.0054**
R^2	0.9825	R^2_{adjusted}	0.9495

Table 2.6: Regression coefficients for the general model of the response surface relative to fatty acids yield.

can be determined and thus divided in relation to the lack of fit. From Table 2.7, it can be concluded that the error associated with the lack of fit is not significant, since its distribution value $F = 4.98$ is less than the critical value of $F_{0.05,3,2} = 19.16$. It means that most of the variation observed is described by the equation which represents the proposed quadratic model. In regards to the significance of the other parameters and their interactions, it can be observed that it coincides with the significance observed in the Pareto Diagram (Figure 2.5 and Table 2.7).

2.5.4 Response surface

Figure 2.7 shows the response surface and contours of fatty acids yields as a function of water-to-oil molar ratio and temperature obtained by applying Equation (2.9). It is observed that increasing both process variables enhances the yield. It can be understood that at these conditions, there is enough water for the reaction to proceed as well as high solubility between the oil and water due to the action of temperature. On the other hand, an excessive amount of water makes the recovery of glycerol from the resulting aqueous phase difficult. Therefore, the optimal feed ratio has to be established empirically, where each individual process has to be considered. In this case, both the surface and contour plots show that there is agreement with the previously mentioned relation to these two-factor interactions and the Pareto Diagram (Figure 2.5).

	SS	**DoF**	**MS**	**F**	**p**
X_T	18.483	1	18.483	14.04	**0.01334**
$X_T X_T$	158.732	1	158.732	120.55	**0.00011**
X_{MR}	1.901	1	1.901	1.44	0.28831
$X_{MR} X_{MR}$	2.493	1	2.493	1.89	0.22728
X_{rpm}	34.196	1	34.196	25.97	**0.00378**
$X_{rpm} X_{rpm}$	34.196	1	34.196	41.85	**0.00131**
$X_T X_{MR}$	27.878	1	27.878	21.17	**0.00583**
$X_T X_{rpm}$	20.160	1	20.160	15.31	**0.01126**
$X_{MR} X_{rpm}$	24.701	1	24.701	18.76	**0.00749**
Lack of fit	5.806	3	1.935	4.98	0.17189
Pure error	0.778	2	0.389		
Total SS	364.971	14			
R^2	0.982		R^2_{adjusted}		0.9495

Table 2.7: ANOVA analysis of the fatty acids yield. Values in bold represent significant factors.

Figure 2.8 presents the response of yield to the combined effect of agitation and temperature, where yields of up to 80% are obtained. It can be inferred that high obtention of fatty acids is strongly favored when high agitation rate is provided to the reacting system for low to mid temperatures. Agitation is generally applied in multiphasic systems to increase the interfacial area by creating droplets. This helps to enhance the mass transfer and consequently the reaction rate. As shown in the the Pareto Diagram (Figure 2.5), the combined interaction of these has a negative effect on the yield. Figure 2.9 shows that there is a negative effect between the water-to-oil molar ratio and agitation speed. At a low mixing rate, an increase in the molar ratio enhanced the yield up to 84% (120 rpm and 38:1 molar ratio). On the other hand, at high mixing rates the opposite effect occurred. Hence, an increase in the agitation would promote the mixing of the reactants which then favours the reaction, since the distribution of the reacting components as well as the mass transfer of the reactants is better. On the other hand, high agitation rates would increase the turbulence in the mixture, which would increase the yield.

The optimization of the quadratic function in Equation (2.9) allowed one to find the optimum value for the yield of fatty acids. The optimal value for each operational condition was chosen "within" the ranges defined by the experiments while the % yield of fatty acids was defined as the variable to maximize. In this way, the optimum working conditions with their respective yield were established. The maximum predicted yield 93.83% was found to be achieved at 254°C, 40:1 water-to-oil molar ratio, and 120 rpm.

In similar studies, King and List obtained high conversions of triglycerides at temperatures between 270-340 °C and low water-to-oil molar ratio (5:1) (J. King, R. Holliday, and G. List 1999). Pinto and Lancas studied hydrolysis of corn oil by using a water-to-oil mass ratio of 85:15. In both studies conversions varied between 80% and 96%. Recently, supercritical CO_2 has been used as a solvent for the hydrolysis of triglycerides in order to improve the solubility of water in the triglycerides obtaining conversions near to 100% in temperatures between 250°C and 350°C. However, processes at this conditions require high investment and operating costs, which limits the industrial applications of this technology.

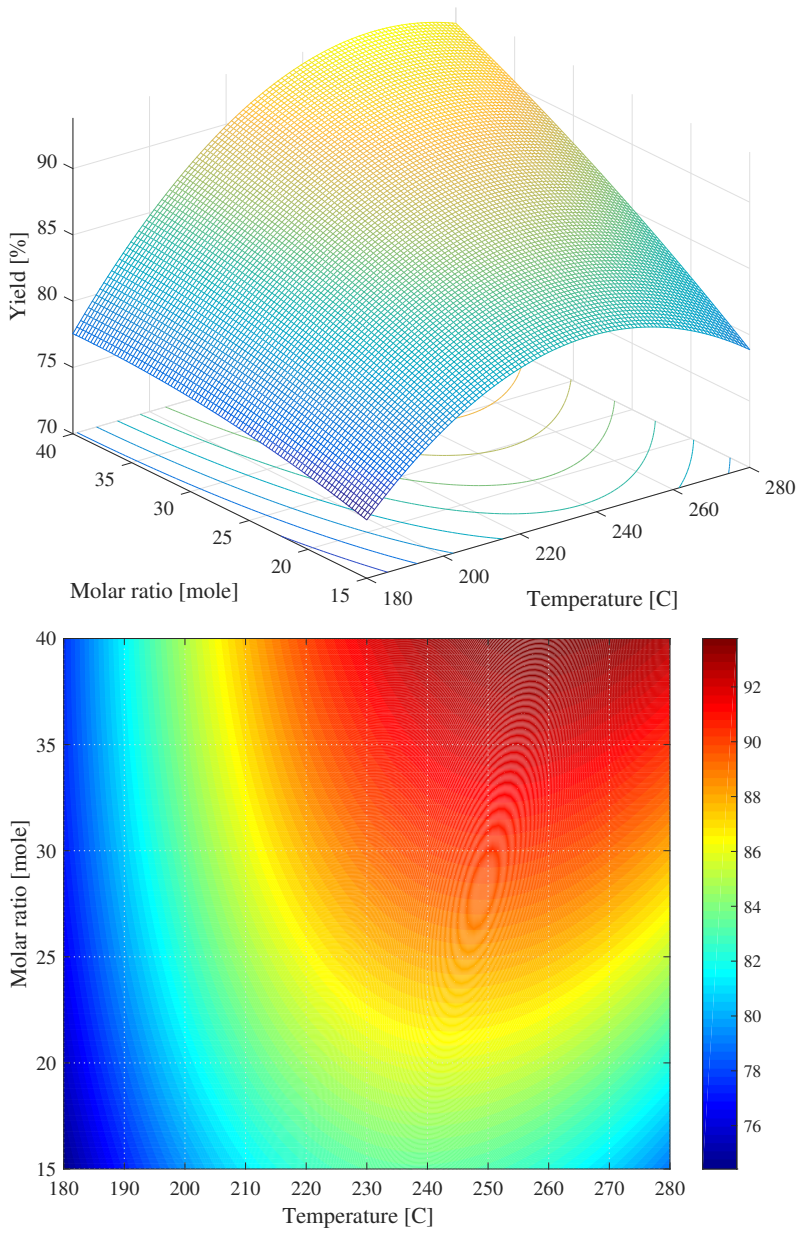

Figure 2.7: Surface & Contours - Effect of molar ratio and temperature on the yield.

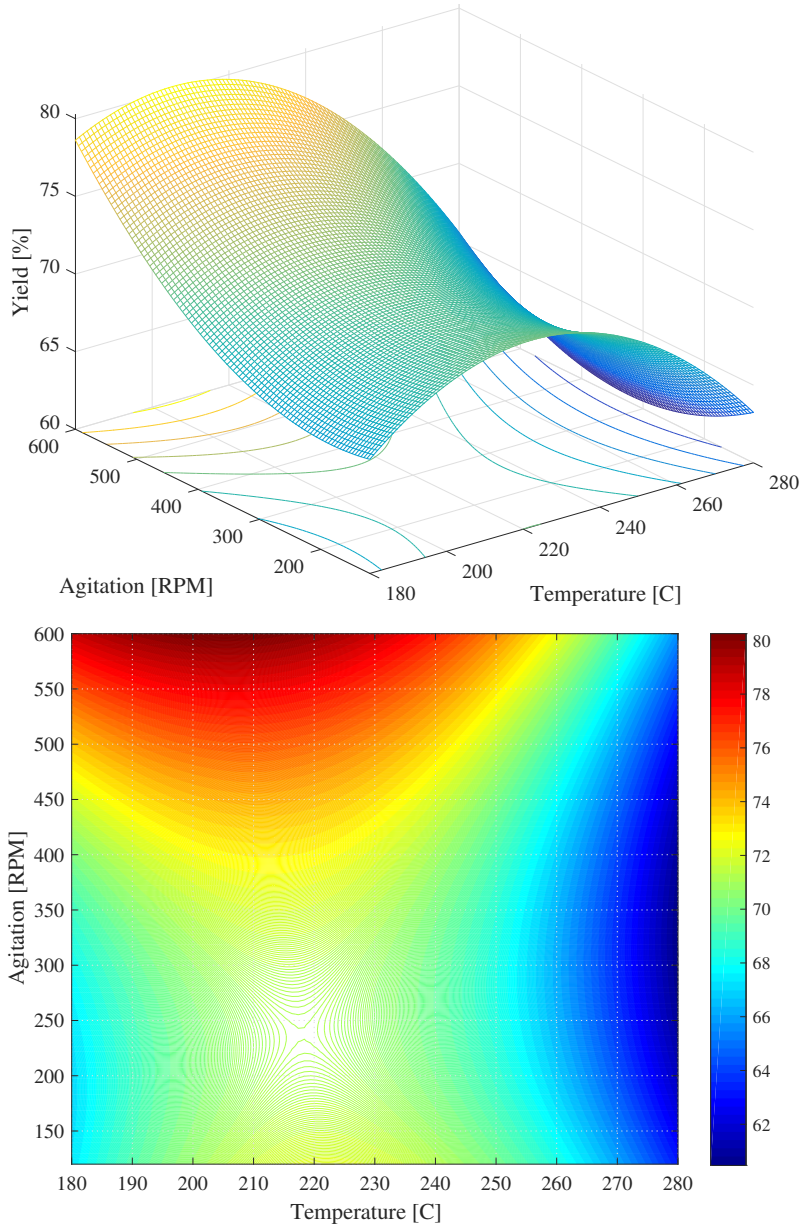

Figure 2.8: Surface & Contours – Effect of agitation and molar ratio on the yield.

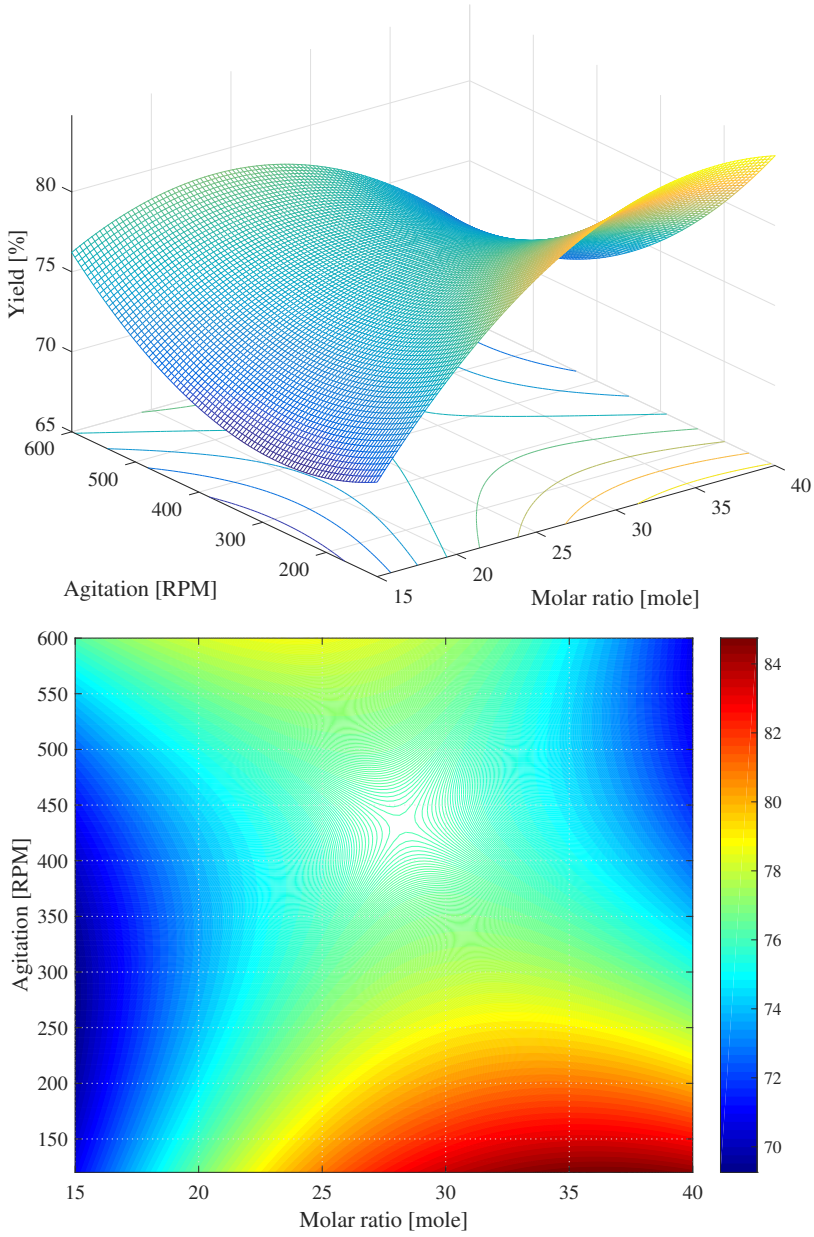

Figure 2.9: Surface & Contours – Effect of agitation and molar ratio on the yield.

2.6 Conclusions

To analyze the hydrolysis of rapeseed oil experiments were performed in a batch reactor, obtaining high yields of fatty acids. To estimate the most favorable operating conditions for fatty acids production, it was necessary to carry out several tests in a stirred reactor based on a Box-Behnken design. Consequently, ANOVA and RSM were applied to the obtained data in the experiments, so as to study the effect of various hydrolysis operating variables. The results showed that by carrying out the reaction together with the optimized conditions allows one to reach yields of fatty acids of up to 93.83%. This analysis provided a powerful tool to optimize the hydrolysis conditions which constitutes an important improvement in the yield obtained in the experiments.

CHAPTER 3

Thermodynamic analysis of the hydrolysis of triglycerides

The study of chemical reactions is of great importance for many industrial processes. For the study of a reaction it is necessary to know to what extent will it take place according to the different concentrations of the reactants, the extent to which the reaction will be carried out by variations in temperature and pressure, etc. This information can be obtained in a laboratory by carrying out a series of experiments and measurements under the conditions of interest.

This direct treatment of the problem forces one or several people to perform a large number of measurements and to use reactants, laboratory devices. Most importantly, it takes a lot of time. Therefore, it is useful to have a theory of chemical and phase equilibrium that allows to carry out a relatively small number of experiments in a system, and then apply the results of this small number of experiments together with its theory to evaluate the properties and behavior of the same system under different operating conditions. Although this theory never completely eliminates direct experimentation, the treatment of the problems can be systematized so that only few experiments are necessary.

3.1 Thermodynamic equilibrium

The equilibrium is a static condition, with no tendency to modify, on a macroscopic scale, a system over time. An equilibrium system can be described as one in which all forces are fully balanced. Therefore, the thermodynamic equilibrium is defined by the absence of a driving force for mass transfer, energy or momentum (William Smith and Ronald Missen 1985).

According to Prausnitz, Lichtenthaler, and Azevedo 1998, when two phases are brought into contact, they tend to change their components until the com-

position of each phase reaches a constant value. In that state, the compositions of the components in the mixture depend on many variables, such as temperature, pressure, chemical nature and total initial amounts of the substances.

The conditions necessary for the determination of the chemical equilibrium and the combined phases is expressed through the following constraints (Stanley I Sandler 2017):

$$T^1 = T^2 = \ldots = T^{NP} \tag{3.1}$$

$$P^1 = P^2 = \ldots = P^{NP} \tag{3.2}$$

$$\mu_i^1 = \mu_i^2 = \ldots = \mu_i^{NP} \tag{3.3}$$

$$\sum_{i=1}^{NC} v_i^j \mu_i^k = 0 \quad M = 1, 2, \ldots, NC \;\; \& \;\; k = 1, 2, \ldots, NP \tag{3.4}$$

Here i denotes a chemical species NC in total, k is a certain phase NP in total, j represents the index of a chemical reaction, M is the number of independent chemical reactions, v_i^j is the stoichiometric coefficient of component i in the j reaction, and μ_i^j is the chemical potential of a component in a given phase. This chemical potential is the driving force responsible for the transfer mass transfer between the different phases seeking to achieve equilibrium.

Generally, the pressure and constant temperatures are used in such a way that the conditions given by Equations (3.1) and (3.2) are automatically satisfied. Therefore, the only necessary condition for equilibrium in this case is that the chemical potential of a component in a specific phase should be equal to the chemical potential of the same component in any of the other phases (Equation (3.3)). In addition, it is necessary that the mass balance of each species is respected, according to the stoichiometry of the reactions involved.

These conditions, though necessary, are not sufficient; a sufficient condition for equilibrium is given by Gibbs energy G, which must be a minimum at temperature T and at system pressure P (Stanley I Sandler 2017):

$$\Delta G|_{T,P} \leq 0 \tag{3.5}$$

This equilibrium criterion provides a method for calculating the chemical and phase equilibrium for a multi-component, multi-phase and isobaric system

by minimizing the Gibbs free energy function, which will be the focus of this chapter.

The minimization of the Gibbs free energy, coupled with optimization methods, has been used by several researchers to calculate phase and chemical equilibrium. White, S. M. Johnson, and Dantzig 1958 were the pioneers in this field. The authors used the minimization of the Gibbs free energy for systems in ideal state. Gautam and Seider 1979 applied different quadratic programming algorithm to determine the distribution of compositions in equilibrium of multiphase systems. However, the method presented problems, with local minimum occurrences that made it impossible to predict the correct distribution of phases.

Castillo and Grossmann 1981 proposed a new method for the simultaneous calculation of phase and chemical equilibrium in which a nonlinear programming approach was used, which allows one to calculate the number and composition of the phases in equilibrium. With this approach, any thermodynamic model that can predict fugacities can be easily incorporated into the method (Castillo and Grossmann 1981).

C. M. McDonald and Floudas 1994 showed that when a liquid phase is modeled by the UNIFAC thermodynamic method, the Gibbs energy minimization tends to local minimums due to the high nonconvexity of this equation (C. M. McDonald and Floudas 1994). However, they demonstrated that this equation can be rewritten to simplify the calculation as the subtraction of two convex functions. For this purpose, the authors used a modification of the ABB algorithm to obtain global solutions.

Other researchers have used stochastic methods rather than deterministic methods to solve the problem of minimizing Gibbs function. Zhu and Xu 1999 and Zhu, Wen, and Xu 2000 used the Simulated Annealing algorithm coupled with NRTL and UNIQUAC thermodynamic methods equations to find the global optimum of the Gibbs free energy function.

In recent years, some relevant work has been done for performing thermodynamic analyses. Rossi, Cardozo-Filho, and Guirardello 2009 presented two methodologies for calculating chemical and phase equilibria by minimizing Gibbs energy. The first methodology was the direct implementation of the problem using nonlinear programming for the convex thermodynamic models, and the second methodology was the linearization of the Gibbs function to guarantee the location of the global optimum when convex and non-convex thermodynamic models were used; in the same way, they used two approaches to the equilibrium problem: a $\gamma - \phi$, using the Wilson, NRTL and UNIQUAC equations, and another $\phi - \phi$, where they used the Peng-Robinson cubic state

equation with the quadratic van der Waals mixing rule. Voll et al. 2011 used the thermodynamic models UNIFAC and Wilson modified for the analysis of the esterification reaction of fatty acids by minimizing Gibbs energy.

3.1.1 Thermodynamic models

At a fixed temperature, the excess molar Gibbs energy (g^E) depends on the temperature, composition of the mixture and, to a much lesser extent, the pressure. Thus, the effect of pressure on g^E is only significant for high pressures. At low or moderate pressures, far from critical conditions, the pressure effect is small enough to be neglected (Prausnitz, Lichtenthaler, and Azevedo 1998). Therefore, the thermodynamic models for the excess molar Gibbs energy depend only on the temperature and composition of the mixture. These models are based on different theories which are models based on the concept of local composition.

Modifications of these methods have been presented as a good way to calculate the activity coefficients. For example, the modified UNIFAC (Dortmund) presented changes with the introduction of empirical coefficients to the combinatorial term and to the interaction parameter, allowing it to vary with temperature (Juergen Gmehling, J. Li, and Schiller 1993; Jürgen Gmehling, Lohmann, et al. 1998; Jürgen Gmehling, Wittig, et al. 2002). Such modifications help to enhance the prediction of models with respect to experimental data due to the higher number of adjustable parameters. In addition, there are still changes in models based on statistical mechanics that provide a better prediction of liquid-vapor equilibrium data of binary mixtures (Stanley I Sandler 1985; Lee, Lombardo, and S. Sandler 1985).

A brief description of the thermodynamic model used in this chapter is presented in the Supporting Information.

3.1.2 Estimation of thermodynamic properties

For the calculation of the chemical and phase equilibrium by direct minimization of Gibbs energy, it is generally necessary to have knowledge of the thermochemical properties of all the substances in the system under analysis. These properties are the heat capacity, enthalpy, standard Gibbs free energy of formation as well as the saturation pressure. However, it is not always possible to find experimental values in the literature of these properties for the compounds of interest. When it is not possible to make the experimen-

tal measurements necessary to obtain said properties, estimation methods are generally employed in this and similar situations.

Methods of estimating such properties of pure components are generally based on group contribution methods. These types of methods use basic structural information of the chemical molecule, such as a simple list of functional groups, adding parameters to these groups, and the calculation of the thermophysical, thermochemical and transport properties is done as a function of the sum of the parameters of each group (Poling, Prausnitz, O'connell, et al. 2001).

3.2 Modeling of the Gibbs free energy

As mentioned previously, the thermodynamic equilibrium is given by Equation (3.5) at constant temperature and pressure. These conditions allow to calculate the phase equilibrium with or without chemical reaction in an isothermal and isobaric system as an optimisation problem. Considering the equilibrium criterion, an expression for the Gibbs energy as a function of state variables such as temperature, pressure and composition of compounds can be proposed. This expression is given by (Stanley I Sandler 2017):

$$G = \sum_{i=1}^{NC} \sum_{k=1}^{NP} n_i^k \mu_i^k \tag{3.6}$$

Where NC and NP are the number of components and phases; n_i^k and μ_i^k are the number of moles and the chemical potential of a component i in a given phase k, being the chemical potential a function of the composition of phase k, temperature and pressure. The chemical potential is defined as a function of the molar partial Gibbs energy:

$$\mu_i = \left(\frac{\partial (ng)}{\partial n_i} \right)_{T,P,n_{j \neq i}} = \bar{g}_i \tag{3.7}$$

Where g is the molar Gibbs energy and $\bar{g}_i$ is the partial molar Gibbs energy of the component i.

Differentiating $\frac{g}{T}$ in relation to T, gives:

$$\frac{\partial}{\partial T} \left(\frac{g}{T} \right)_P = \frac{1}{T} \left(\frac{\partial}{\partial T} \right) - \frac{g}{T^2} \tag{3.8}$$

Inserting (J. M. Smith 1950):

$$g = h - Ts \tag{3.9}$$

Where h and s are the molar enthalpy and entropy, gives:

$$\frac{\partial}{\partial T}\left(\frac{g}{T}\right)_P = -\frac{s}{T} - \frac{h - Ts}{T^2} = -\frac{h}{T^2} \tag{3.10}$$

Multiplying Equation (3.10) by n and differentiating in relation to n_i:

$$\frac{\partial}{\partial n_i}\left(\frac{\partial}{\partial T}\left(\frac{ng}{T}\right)_P\right)_{T,P,n_{j\neq i}} = \frac{\partial}{\partial n_i}\left(\frac{nh}{T^2}\right)_{T,P,n_{j\neq i}} \tag{3.11}$$

$$\frac{\partial}{\partial T}\left(\frac{\mu_i}{T}\right)_P = -\frac{\bar{h}_i}{T^2} \tag{3.12}$$

Hhere $\bar{h}_i$ is the partial molar enthalpy. Thus, the chemical potential for a component i at a temperature T and a known reference pressure P_0 can be obtained by integrating Equation (3.12):

$$\frac{\mu_i\left(P_0, T\right)}{T} = \frac{\mu_i\left(P_0, T_0\right)}{T_0} + \int_{T_0}^{T} \frac{-\bar{h}_i\left(P_0, T'\right)}{T'^2} \mathrm{d}T' \tag{3.13}$$

By integrating the Gibbs-Duhem equation for a pure component, the chemical potential can also be obtained at a temperature T and a given pressure P knowing $\mu_i\left(P_0, T_0\right)$, thus:

$$\text{Gibbs-Duhen Equation} \quad \mathrm{d}\mu = -s\mathrm{d}T + \upsilon \mathrm{d}P \tag{3.14}$$

Where s and υ are the entropy and the molar partial volume, respectively.

Integrating the Gibbs-Duhem equation with respect to P and keeping the temperature constant:

$$\mu_i\left(P, T\right) = \mu_i\left(P_0, T\right) + \int_{P_0}^{P} \upsilon_i\left(P', T\right) \mathrm{d}P' \tag{3.15}$$

Substituting (3.13) in (3.15):

$$\mu_i\left(P, T\right) = T\ \frac{\mu_i\left(P_0, T_0\right)}{T_0} + T \int_{T_0}^{T} \frac{-\bar{h}_i\left(P_0, T'\right)}{T'^2} \mathrm{d}T' + \int_{P_0}^{P} \upsilon_i\left(P', T\right) \mathrm{d}P' \tag{3.16}$$

Thus, the chemical potential of an i component at any P and T can be obtained from the chemical potential at a known pressure P_0 and temperature

T_0, according to Equation (3.16). However, in the case of a liquid, enthalpy is a function only of temperature, therefore:

$$\mu_i(P,T) = \left(\frac{T}{T_0}\right)\mu_i(P_0,T_0) + T\int_{T_0}^{T}\frac{-\bar{h}_i(P_0,T')}{T'^2}\mathrm{d}T' + \int_{P_0}^{P}\upsilon_i(P',T)\,\mathrm{d}P' \tag{3.17}$$

The partial molar enthalpy for a pure component can be calculated by the following thermodynamic relation:

$$\left(\frac{\partial\bar{h}_i}{\partial T}\right)_P = Cp_i \tag{3.18}$$

Where Cp_i of an ideal gas can be expressed as a third order polynomial:

$$Cp_i = A_i + B_iT + C_iT^2 + D_iT^3 \tag{3.19}$$

In which A_i, B_i, C_i and D_i are parameters of component i, obtained from a thermodynamic database of pure substance.

Substituting Equation (3.19) in (3.18):

$$\left(\frac{\partial\bar{h}_i}{\partial T}\right)_P = A_i + B_iT + C_iT^2 + D_iT^3 \tag{3.20}$$

Integrating Equation (3.20) and substituting in Equation (3.17):

$$\begin{aligned}\mu_i(P,T) = \left(\frac{T}{T_0}\right)\mu_i(P_0,T_0) + \int_{P_0}^{P}\upsilon_i(P',T)\,\mathrm{d}P' + T\int_{T_0}^{T}\frac{-\bar{h}_i(P_0,T')}{T'^2}\mathrm{d}T' \\ + T\int_{T_0}^{T}\frac{-\left(A_iT' + \frac{B_i}{2}T'^2 + \frac{C_i}{3}T'^3 + \frac{D_i}{4}T'^4\right)}{T'^2}\mathrm{d}T' \\ + T\int_{T_0}^{T}\frac{-\left(A_iT_0 + \frac{B_i}{2}T_0^2 + \frac{C_i}{3}T_0^3 + \frac{D_i}{4}T_0^4\right)}{T'^2}\mathrm{d}T'\end{aligned} \tag{3.21}$$

Integrating Equation (3.21):

$$\mu_i(P,T) = \left(\frac{T}{T_0}\right)\mu_i(P_0,T_0) + \int_{P_0}^{P} \upsilon(P',T)\,\mathrm{d}P' + \bar{h}_i T_0\left(1-\frac{T}{T_0}\right) - A_i\left(T\ln\left(\frac{T}{T_0}\right)+T_0-T\right) - \frac{B_i}{2}(T-T_0)^2 - \frac{C_i}{6}\left(T^3-3TT_0^2+2T_0^3\right) - \frac{D_i}{12}\left(T^4-4TT_0^3+3T_0^4\right) \tag{3.22}$$

For practical purposes, the chosen reference state is the ideal gas at an atmosphere of pressure and the ambient temperature ($P_0 = 1$ atm and $T_0 = 298.15$ K). Thus, $\mu_i(P_0,T_0) = \Delta g^0_{f,i}$ and $\bar{h}_i(T_0) = \Delta h^0_{f,i}$ which are the standard molar Gibbs energy of formation and the standard molar enthalpy of formation, defined at 298.15K and 1 atm.

Equation (3.22) can be rewritten as:

$$\mu_i(P,T) = \mu_i^0(T) + \int_{P_0}^{P} \upsilon_i(P',T)\,\mathrm{d}P' \tag{3.23}$$

Where:

$$\mu_i^0(T) = \left(\frac{T}{T_0}\right)\Delta g^0_{f,i} + \Delta h^0_{f,i}\left(1-\frac{T}{T_0}\right) - A_i\left(T\ln\left(\frac{T}{T_0}\right)+T_0-T\right) - \frac{B_i}{2}(T-T_0)^2 - \frac{C_i}{6}\left(T^3-3TT_0^2+2T_0^3\right) - \frac{D_i}{12}\left(T^4-4TT_0^3+3T_0^4\right) \tag{3.24}$$

Considering ideal behaviour in vapor phase:

$$\upsilon_i^{gi} = \frac{RT}{P_i} \tag{3.25}$$

Solving the integral in Equation (3.23):

$$\mu_i^{gi}(P,T) = \mu_i^0(T) + RT\ln\left(\frac{P_i}{P_0}\right) \tag{3.26}$$

This equation is valid only for an ideal gas mixture, nevertheless it can be generalized to a mixture of real gases introducing the concept of fugacity, thus:

$$\mu_i^g(P,T) = \mu_i^0(T) + RT\ln\left(\frac{\hat{f}_i^g}{f_i^0}\right) \tag{3.27}$$

Assuming that the molar volume of component i for the liquid is practically constant, the integration of Equation (3.23) results in:

$$\mu_i^l(P,T) = \mu_i^0(T) + \upsilon_i^l(P - P_0) \tag{3.28}$$

From the Gibbs-Duhem Equation (3.14), it can be easily demonstrated that:

$$\upsilon_i(P - P_0) = g_i - g_i^0 = RT\ln\hat{a}_i \tag{3.29}$$

Where $\hat{a}_i$ is the activity of species i in mixture, and is defined by:

$$\hat{a}_i = \frac{\hat{f}_i}{f_i^0} \tag{3.30}$$

Substituting Equation (3.29) in (3.28):

$$\mu_i^l(P,T) = \mu_i^0(T) + RT\ln\frac{\hat{f}_i^l}{f_i^0} \tag{3.31}$$

Thus, Equation (3.6) can be rewritten in terms of the fugacity ($\hat{f}_i^k$), applying the definition of the chemical potential. Thus, for an isothermal and isobaric process, for a component in any gaseous, liquid or solid, pure or mixed, ideal or non-ideal system, can be expressed as:

$$\mu_i^k(P,T) = \mu_i^0(T) + RT\ln\frac{\hat{f}_i^k}{f_i^0} \tag{3.32}$$

In what k could be the solid, liquid or gaseous phase, $\mu_i^0(T)$ is the reference chemical potential of component i and can be calculated by Equation (3.24), f_i^0 is the reference fugitivity of component i, T is temperature and R is ideal gas constant. Therefore, the equation for the Gibbs energy will be:

$$G = \sum_{i=1}^{NC}\sum_{L=1}^{NP} n_i^k\left(\mu_i^0(T) + RT\ln\frac{\hat{f}_i^k}{f_i^0}\right) \tag{3.33}$$

The equations of fugacities for the liquid and vapor phases can be represented by Equations (3.44) and (3.35):

$$\hat{f}_i^g = \hat{\phi}_i y_i P \tag{3.34}$$

$$\hat{f}_i^L = \gamma_i x_i^L f_i^{0,L} \tag{3.35}$$

In which y_i and x_i^L are the molar fractions of the vapor and liquid phase of the component i, $\hat{\phi}_i$ and γ_i^L are the coefficients of fugacity and activity of the component i respectively, P the pressure and $f_i^{0,L}$ is the fugacity of reference of the liquid phase, which is given by the following equation:

$$f_i^{0,L} = P_i^{\text{sat}} \phi_i^{\text{sat}} \text{POY}_i \tag{3.36}$$

Where P_i^{sat} is the saturation pressure of component i, ϕ_i^{sat} is the saturation coefficient of component i and POY_i is the Poynting factor given by:

$$\text{POY}_i = \exp\left(\frac{\upsilon_i^{\text{sat}}}{RT}\left(P - P_i^{\text{sat}}\right)\right) \tag{3.37}$$

Where υ_i^{sat} is saturation molar volume.

At low or moderate pressures, the Poynting factor is close to the unit $\text{POY}_i \cong 1$, assuming ideal gas behavior in the vapor phase; $\hat{\phi}_i \cong 1$ and $\phi_i^{\text{sat}} 1$. Therefore, fugacities in the liquid and vapor phase can be rewritten as follows:

$$\hat{f}_i^g = y_i P \tag{3.38}$$

$$\hat{f}_i^L = \gamma_i^L x_i^L P_i^{\text{sat}} \tag{3.39}$$

Substituting these expressions in Equation (3.33):

$$G = \sum_{i=1}^{NC} \sum_{L=1}^{NPL} n_i^L \left(\mu_i^0(T) + RT \ln \frac{\gamma_i^L x_i^L P_i^{\text{sat}}}{f_i^0}\right) + \sum_{i=1}^{NC} n_i^g \left(\mu_i^0(T) + RT \ln \frac{y_i P}{f_i^0}\right) \tag{3.40}$$

Due to the chosen reference state, the reference fugacity can be equated to the reference pressure P_0, hence Equation (3.40) after making some rearrangements is as follows:

$$G = \sum_{i=1}^{NC}\sum_{L=1}^{NPL} n_i^L \mu_i^0(T) + RT\sum_{i=1}^{NC}\sum_{L=1}^{NPL} n_i^L \ln P_i^{\text{sat}} + RT\sum_{i=1}^{NC}\sum_{L=1}^{NPL} n_i^L \ln x_i^L + RT\sum_{i=1}^{NC}\sum_{L=1}^{NPL} n_i^L \ln \gamma_i^L + \sum_{i=1}^{NC} n_i^g \mu_i^0(T) + RT\sum_{i=1}^{NC} n_i^g \ln y_i + RT\sum_{i=1}^{NC} n_i^g \ln P \tag{3.41}$$

In the Gibbs energy minimization approach as a nonlinear programming problem, it is preferred to use expressions based on the Gibbs energy in excess (g_L^E) than with activity coefficients, so that for a liquid phase L, g_L^E can be expressed as:

$$g_L^E = RT\sum_{i=1}^{NC} x_i^L \ln \gamma_i^L \tag{3.42}$$

Or in terms of the number of moles:

$$n_t^L g_L^E = RT\sum_{i=1}^{NC} n_i^L \ln \gamma_i^L \tag{3.43}$$

Where the number of total moles in a liquid phase is:

$$n_t^L = \sum_{L=1}^{NPL} n_i^L \tag{3.44}$$

Thus, Equation (3.41) can be rewritten as:

$$\frac{G}{RT} = \frac{1}{RT}\sum_{i=1}^{NC}\mu_i^0(T)\left(n_i^g + \sum_{L=1}^{NPL} n_i^L\right) + \sum_{i=1}^{NC}\sum_{L=1}^{NPL} n_i^L \ln P_i^{\text{sat}} + \sum_{i=1}^{NC}\sum_{L=1}^{NPL} n_i^L \ln x_i^L + \sum_{L=1}^{NPL} n_t^L \frac{g_L^E}{RT} + \sum_{i=1}^{NC} n_i^g \ln y_i + \sum_{i=1}^{NC} n_i^g \ln P \tag{3.45}$$

In this equation, NC and NPL are the number of components and the number of liquid phases, n_i^L and n_t^L are the number of moles of component i in a liquid phase L and the number of total moles in that liquid phase, n_i^g is the number of moles of component i in the gas phase, μ_i^0 is the chemical

potential of component i in the ideal gas state and g_L^E is the molar Gibbs energy in excess in a liquid phase L.

Equation (3.45) is the Gibbs energy for the simultaneous chemical and phase equilibrium. Therefore, the equilibrium calculation problem can be solved by employing optimization methods to minimize the Gibbs energy function (Equation (3.45)). In this approach some constraints must be satisfied (R.W. Missen and W.R. Smith 1982):

- *Non-negativity of the number of moles*

$$n_i^k \geq 0 \quad \text{for } i = 1, 2, \ldots, NC \text{ and } k = 1, 2, \ldots, NP \tag{3.46}$$

- *Conservation of the number of moles*

  - Phase equilibrium:

$$\sum_{k=1}^{NP} n_i^k = n_i^0 \quad \text{for } i = 1, 2, \ldots, NC \tag{3.47}$$

  - Chemical and phase equilibrium by balance of element (non-stoichiometric formulation):

$$\sum_{i=1}^{NC} a_{mi} \left(\sum_{k=1}^{NP} n_i^k \right) = \sum_{i=1}^{NC} a_{mi} n_i^0 \quad \text{for } m = 1, 2, \ldots, \text{NE} \tag{3.48}$$

    Where n_i^0 is the initial number of moles of component i in the system and a_{mi} is the number of elements m in component i.

  - Chemical and phase equilibrium (stoichiometric formulation):

$$\sum_{k=1}^{NP} n_i^k = n_i^0 + v_i \epsilon \quad \text{for } i = 1, 2, \ldots, \text{NC} \tag{3.49}$$

    Where n_i^0 is the initial number of moles of component i in the system, v_i is the stoichiometric coefficient of element i in the reaction, and ϵ is the coordinate of the reaction.

The equilibrium constant is related to the thermodynamic properties of the mixture through the following equation:

$$K_{eq} = \exp\left(-\frac{G}{RT}\right) \tag{3.50}$$

Additionally, considering only formation of liquid phases the model can be simplified in a way where the variable part of the Gibbs energy equation is minimized (Z):

$$Z = \sum_{i=1}^{NC}\sum_{L=1}^{NPL} n_i^L \ln x_i^L + \frac{1}{RT}\sum_{L=1}^{NPL} n_t^L g_L^E \tag{3.51}$$

In view of this, the equation above is much simpler than the equation of the original model (Equation (3.45)), since it does not need information of properties of the pure component. However, it can only be used in the specific case of phase equilibrium involving several liquid phases.

3.3 Methodology

In the present work, the phase equilibrium with chemical reaction was performed using a methodology based on the minimization of the Gibbs free energy for the hydrolysis reaction system, using Matlab's Global Optimization Toolbox (The Mathworks Inc. 2016; Kolda, Lewis, and Torczon 2003). In this way, the development of this chapter has a purely theoretical and computational character. Before presenting the steps of the methodological development, it is important to say that, in order to facilitate calculations in the minimization process, vegetable oil was treated as a single triglyceride (triolein) and the generated fatty acids as a single species (oleic acid).

Phase equilibrium with chemical reaction uses the assumption that two liquid phases are formed during the reaction. The existence of these possible phases is determined during optimization (minimization) by applying stability tests (Michelsen 1989). In this study the excess function of the modified UNIFAC (Dortmund) thermodynamic model was introduced to the Gibbs function model so as to calculate the phase equilibria in the hydrolysis reaction, due to its wide and successful utility in calculating liquid-liquid equilibrium (Juergen Gmehling, J. Li, and Schiller 1993; Jürgen Gmehling, Lohmann, et al. 1998; Jürgen Gmehling, Wittig, et al. 2002).

The programming of these algorithms was developed by minimizing Equation (3.49). This minimization was subject to the constraints of non negativity and conservation of the number of moles. It should also be mentioned that the optimization variables were the number of moles of the liquid phases (n_i^L)

and the Gibbs energy of the system (G). In the same way, some parameters of these algorithms like R (ideal gas constant), T and P remained constant throughout the optimization, others like P_i^{sat} and μ_i^0 were calculated before the optimization through some functions or thermodynamic relations. Properties such as saturation pressure, heat capacity of the ideal gas, enthalpy and Gibbs energy of formation (P_i^{sat}, Cp_i, $\Delta h_{f,i}^0$ and $\Delta g_{f,i}^0$), which were required to complete the minimization, were calculated using polynomial fittings of experimental data of property versus temperature. Correlation parameters for these polynomials have been obtained from the *CAPEC Lipids Database* (Diaz-Tovar, Gani, and Sarup 2011).

3.4 Thermodynamic analysis - Results

In this section the results of the thermodynamic simulation of the reaction of hydrolysis of triolein for the formation of oleic acid and glycerol are presented. As described in the previous section, Gibbs free energy is the most commonly used function to identify the chemical and phase equilibrium in a reacting system. In this type of analysis, when all species of the system are given, the distribution of products is established knowing the chemistry of the reactions when the Gibbs free energy is at its minimum. This method was also used to characterize the multiphasic behavior of the system.

In industry, the hydrolysis of vegetable oils is employed to generate fatty acids under subcritical conditions. Vegetable oil and water are combined in a reactor and heated-up to about 180°C - 280°C under an autogenous pressure of about 20-80 bar due to the vapor pressure of water. At such conditions the miscibility of oil in water is enhanced, then the non-catalyzed reaction can take place. The generated fatty acids, can be purified by distillation while the glycerol and water can be separated by mechanical means. The reactions are reversible, consecutive and parallel:

$$\mathrm{TG} + \mathrm{H_2O} \underset{\mathrm{k_{-1}}}{\overset{\mathrm{k_1}}{\rightleftharpoons}} \mathrm{FA} + \mathrm{DG} \qquad \text{(Reaction 1)}$$

$$\mathrm{DG} + \mathrm{H_2O} \underset{\mathrm{k_{-2}}}{\overset{\mathrm{k_2}}{\rightleftharpoons}} \mathrm{FA} + \mathrm{MG} \qquad \text{(Reaction 2)}$$

$$\mathrm{MG} + \mathrm{H_2O} \underset{\mathrm{k_{-3}}}{\overset{\mathrm{k_3}}{\rightleftharpoons}} \mathrm{FA} + \mathrm{Gly} \qquad \text{(Reaction 3)}$$

The complexity of models with several individual kinetic constants are simplified by lumping the three reactions into one step where the TG is converted into FA. Hence, a hydrolysis of vegetable oil is expressed as shown in (Reaction 8):

$$\mathrm{TG} \; + \; 3\mathrm{H_2O} \underset{\mathrm{k_{-1}}_{\mathrm{overall}}}{\overset{\mathrm{k_1}_{\mathrm{overall}}}{\rightleftharpoons}} 3\,\mathrm{FA} + \mathrm{Gly} \qquad \text{(Reaction 4)}$$

This reaction is modeled as a reversible heterogeneous reaction due to the biphasic nature of the mixture. In addition, the lumped reaction can be deemed as endothermic (Gunstone, Harwood, and Dijkstra 2007). The concentration of diglycerides DG and monoglycerides MG in the reactions can be considered as negligible.

The study of the feasibility of the reactions is of key relevance in order to identify the possible distribution of products present during the hydrolysis. The calculation of the equilibrium composition of a mixture is important when studying reactions at harsh conditions because experiments are costly and often do not provide relevant information. It is worth noting that combined chemical and phase equilibrium data for systems containing vegetable oil, water, fatty acids and glycerol were not found in the literature; therefore, the results of the tests presented are predictive in nature.

3.4.1 Equilibrium compositions

To study the simultaneous effect of water-to-oil molar ratio and temperature on the consumption of triolein and generation of oleic acid and glycerol, the feed ratio is varied from 0.5:1 to 7.5:1 and the temperature from 190°C to 290°C, and consequently, calculations were performed for each of the variables and their combinations. The results obtained for the compositions in the equilibrium for the studied compounds are grouped in Figures 3.1 and 3.2.

The results indicate that temperature significantly affects equilibrium composition of the reaction. When the temperature is raised from 190°C to 220°C, the overall composition of oleic acid in the equilibrium increases from 45% to 75%. On the other hand, the highest compositions in the equilibrium were obtained at a lower temperature when water-to-oil molar ratio of 3:1 was used, which is not in agreement with the optimal ratios used in practice. It is also important to highlight that at low feed ratios the triolein is not entirely consumed for all temperatures. In Figure 3.1 it is observed that, when

a water-to-oil molar feed ratio range of 4.5:1 is used the highest conversions of triolein is obtained. Thus, a high feed ratio could appreciably enhance the conversion of triolein to products.

Starting from this feed condition, it is also observed that high temperatures do not have a significant influence the equilibrium conversion (see Figure 3.3). As seen in Figure 3.2, at low feed ratios and regardless the temperatures a relatively large amount of glycerol is produced. In practical scenarios this is highly inconvenient, since more complicated evaporation schemes might be needed to separate glycerol from the resulting aqueous mixture. In the case of water added to the system, a small feed ratio is sufficient to reach complete consumption. This can be explained by the fact that at above 170°C water has a lower dielectric constant, allowing to solubilize non-polar organic compounds such as triolein, favoring then the reaction as discussed in previous chapters.

3.4.2 Equilibrium conversions

Calculated conversion of the hydrolysis of triolein is quite high when an excess of water is used as shown in Figure 3.3; however, in none of the reported cases the conversion is entirely complete ($\approx 100\%$). It can be said that the conversion in the equilibrium is quite close to completion using the stoichiometric ratio of the reaction. From an experimental point of view, several authors have studied the influence of high temperature on the conversion of vegetable oils to fatty acids. In a pioneering work, Mills and McClain reported triglycerides conversions of 60% and 70% at 260°C and 280°C for the hydrolysis of sunflower oil under subcritical conditions. Conversions were enhanced when the feed ratio was raised from 3:1 to 10:1. On the other hand, when the amount of water was high (33:1 molar ratio) there was no significant change in the conversion reaching 90% (Mills and McClain 1949). Ilham and Saka studied the influence of temperature for the non-catalytic hydrolysis of Jatropha oil, obtaining conversions close to 80% at 215°C and 97% at 305°C (Ilham and Saka 2010). Furthermore,Kusdiana and Saka 2004 reported a similar study in which conversions where increased when high molar ratios of water to rapeseed oil were used. In their studies, conversions of 60% were obtained at a molar ratio of 13:1 while conversions of 85% were obtained at 54:1 demonstrating that a high excess of water does not have a significant effect on conversion. In spite of this, the difference was expected since in the simulations the reaction rate and its kinetics are not taken into account, so the obtained conversions in the thermodynamic analysis are the maximum point that can reach the reaction.

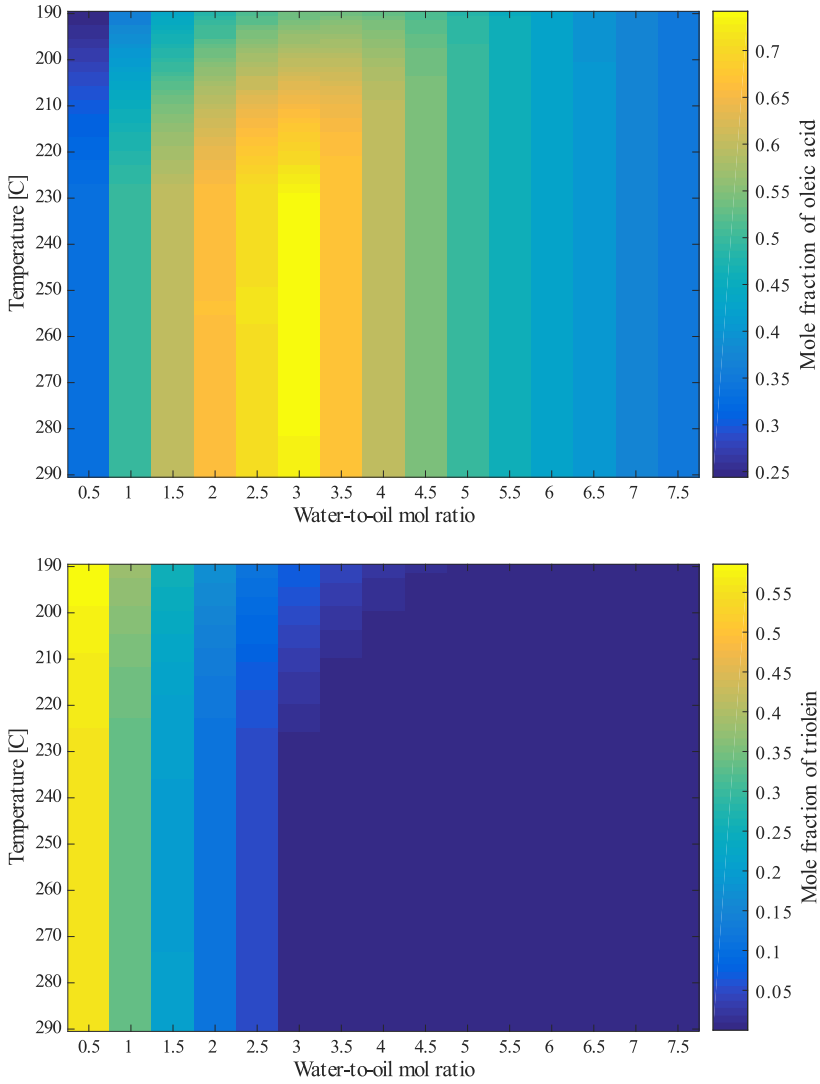

Figure 3.1: Mole fraction of oleic acid and triolein in the thermodynamic equilibrium.

3.4.3 Equilibrium constants

The equilibrium constants of the reaction considered during the hydrolysis are plotted as a function of temperature for different feed ratios in Figure 3.4. For a given temperature, when the variation of the Gibbs free energy

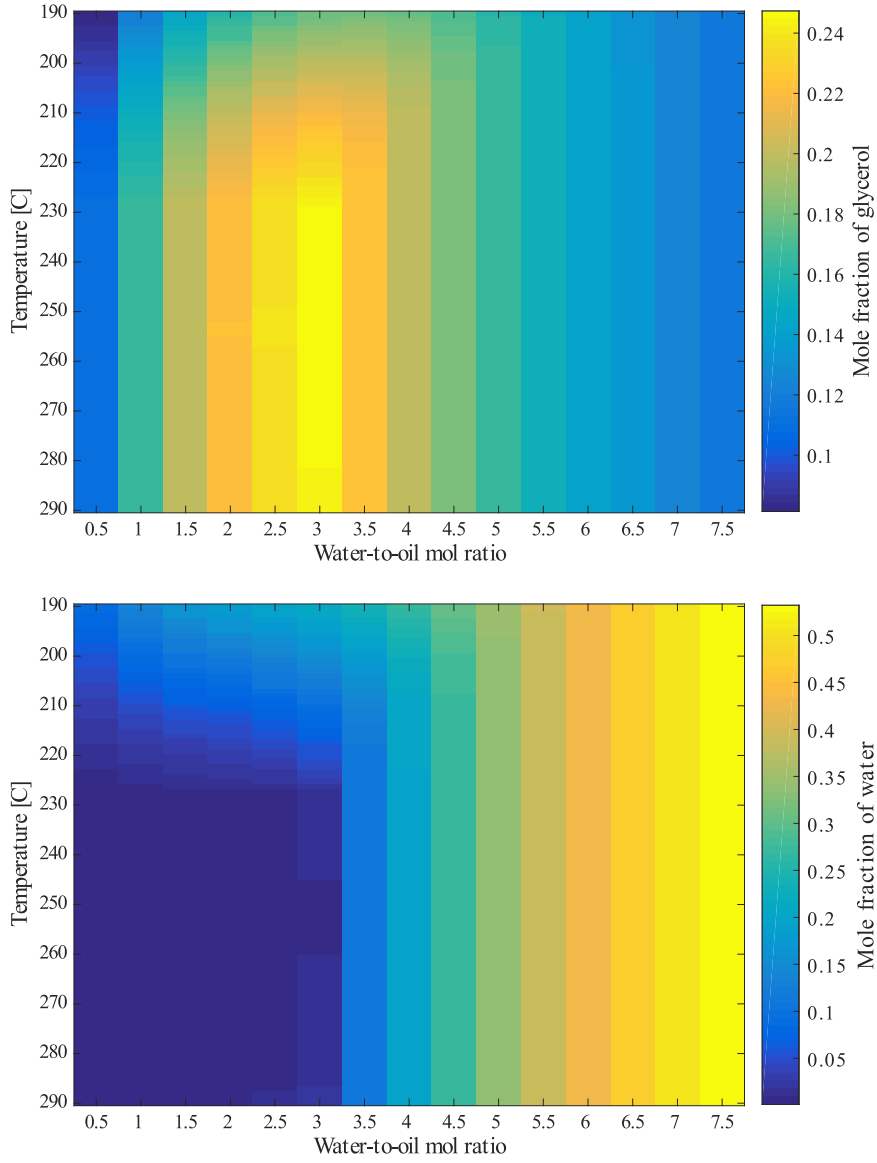

Figure 3.2: Mole fraction of glycerol and water in the thermodynamic equilibrium.

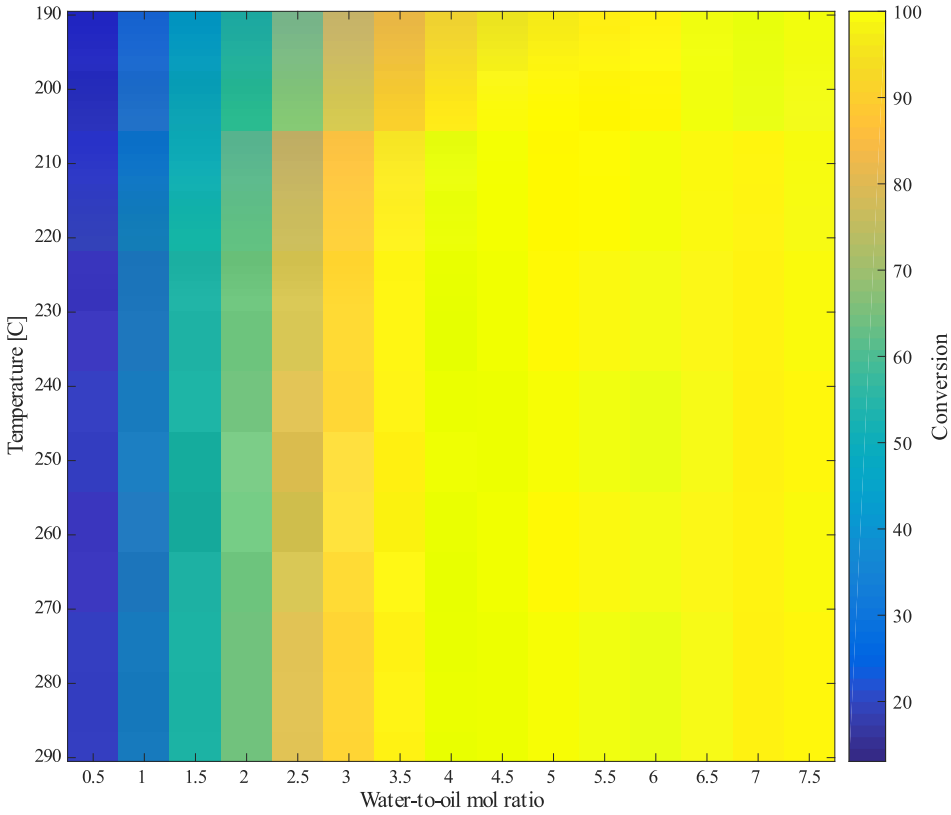

Figure 3.3: Conversion of triolein to products in the equilibrium at different reaction conditions.

has a negative value, the chemical reactions are said to move towards the side of the products, corresponding to a very high equilibrium constant K_{eq}. On the other hand, the reactions are thermodynamically limited when the variation in the Gibbs free energy is positive, hence the equilibrium constant tends to a negative value. In this case, the reaction moves towards the side of the reactants. When the equilibrium constant is much higher than 1, the reactions can not be shifted to the opposite side by changing the reactants contents. However, for K_{eq} values close to 1, a variation in the conditions of the reaction has a considerable influence on the distribution of products.

Figure 3.4 shows that at almost all the conditions, the reactions occurs fast resulting in a significant effect on the composition of the product. Figure 3.4 also shows that the reaction is favoured to the products in middle-to-high

temperatures as well as feed ratio due to positive values of $\ln K_{eq}$. Thus, any increase in temperature or the amount of water displaces the equilibrium to the formation of products. According to Jogunola et al. 2011, catalyzed hydrolysis generally have a low equilibrium constant. For example, for an oil-to-water molar ratio of 8:1, the authors found an equilibrium constant less than 0.2. In their study, in order to enhance conversion, it was necessary to shift the equilibrium towards acid formation by employing an excess of water. However, the major disadvantage of this action lies in the fact that it can lead to problems in the separation since due to the presence of water in excess. Such disadvantages are represented by oversizing and low performance of the system. Another way of shifting the equilibrium in the formation of products is by increasing the temperature since the reaction is endothermic. It is worth mentioning that extremely high temperatures could degrade the formed acids.

3.4.4 Phase splitting

Phase equilibrium calculations were performed with the values of the global composition of the mixture obtained by minimization of the Gibbs energy. The phase equilibrium was calculated considering a non-ideal liquid phase mixture. This non-ideality was corrected using the UNIFAC Dortmund for the calculation of activity coefficient calculations as described in the methodology.

As seen in Figure 3.5, all the resulting mixtures involved in the hydrolysis are virtually heterogeneous. In the prediction of the phases formed by the simulations after the reaction it is observed that a biphasic system is formed, consisting of an oleic acid-rich phase with small amounts of triolein, and another liquid phase with the remaining amount of water and formed glycerol. In this case, both temperature and feed ratio have a big effect on the formation of the two phases. A similar behavior during the transesterification of soybean oil was obtained by Voll et al. 2011.

Under high amounts of water, the efficiency and speed of the reaction are relatively high according to the analyses presented in previous sections, hence the purification stages of the products can be simplified by removing the excess of water by decantation. Overall, an increase in temperature affects the simulated phase splitting since the formation of fatty acids improves the possibility of forming a single-phase reaction by dissolving larger amounts of glycerol in fatty acids-rich phases. However, glycerol species have a significant tendency to split from fatty phases, even with mixtures containing very high amounts of fatty acids creating then a second liquid phase with water for the given range of operating conditions (Dossat, Combes, and Marty 1999).

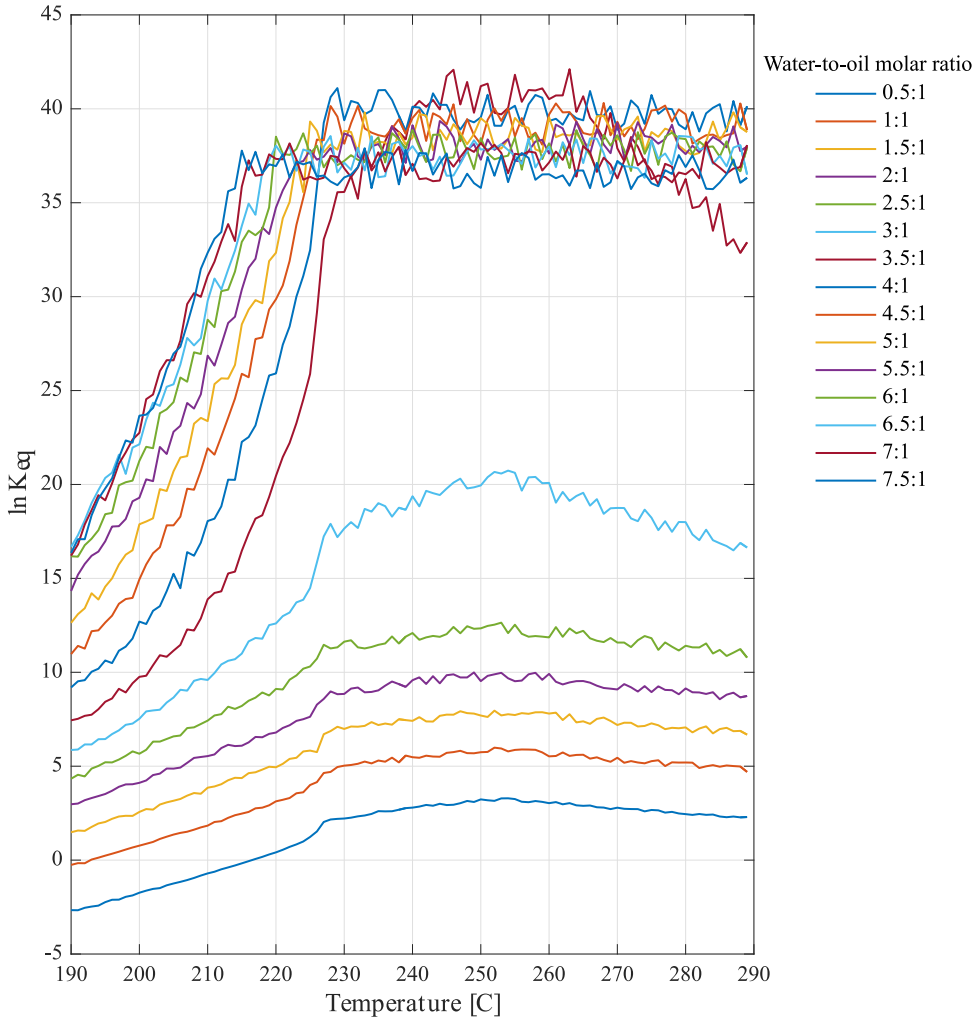

Figure 3.4: Equilibrium constant for the hydrolysis of triolein.

Phase equilibrium helps to describe the state of the mixture after hydrolysis reaction with relative good accuracy, while the thermodynamic chemical equilibrium is less predictive since this analysis is the maximum theoretical value a reaction can reach. In real conditions, the conversion of reactants to products is affected by factors that cannot be taken into account in this analysis such as reaction time, catalyst, and pressure. It is therefore of great interest to develop experiments that bring together both theoretical and experimental

estimates of conversion.

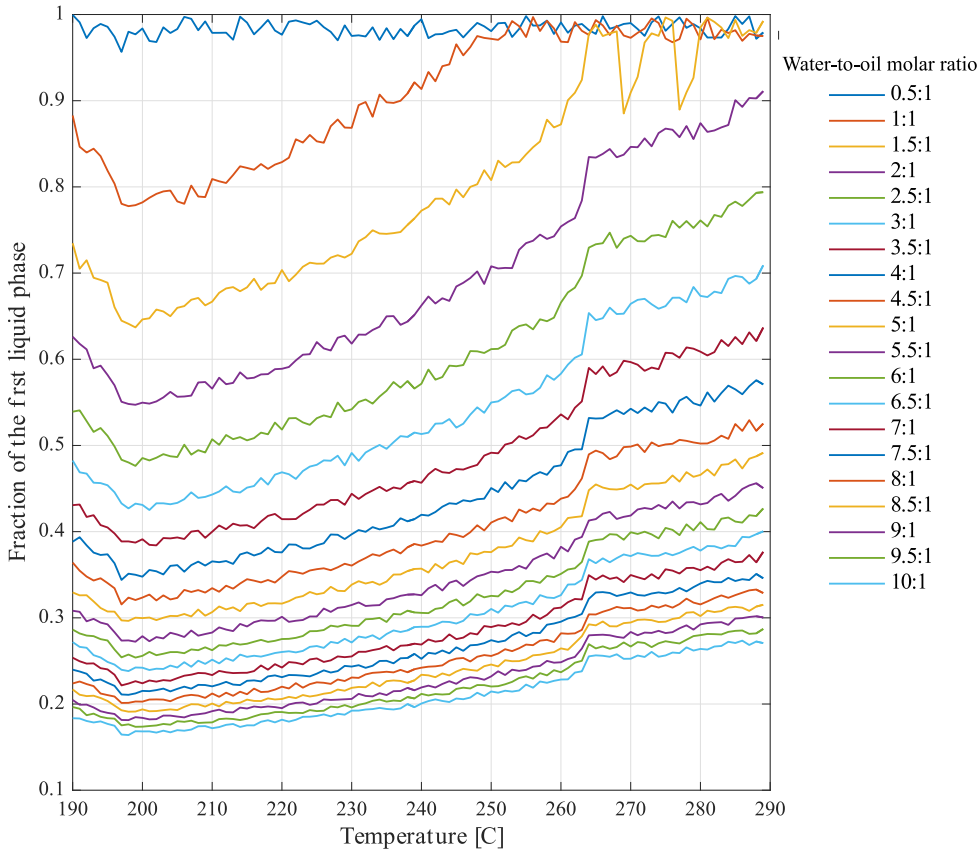

Figure 3.5: Fraction of oleic acid-rich phase as a function of temperature and water-to-oil molar ratio.

3.5 Conclusions

Thermodynamic analysis of hydrolysis reactions is important for the industrial application of the fat-oil splitting process, because it provides theoretical information that could be used to compare different modelling approaches under different operating conditions for producing fatty acids. Although the literature contains many reports regarding the hydrolysis of triglycerides and fatty acid and its kinetic features, there is little information on the thermodynamic

behavior of the process. The performed thermodynamic analysis indicates that the Gibbs energy minimization methodology for the calculation of combined chemical and phase equilibrium is robust and reliable for the prediction of phase formation and its composition in the equilibrium for the hydrolysis of vegetable oil under subcritical conditions. At equilibrium, high conversions are theoretically possible for the hydrolysis of simple triglycerides at relatively low values of water-to-oil molar ratios and temperature. Both properties have great influence on the reaction since any increase in them displaces the equilibrium to the formation of products.

CHAPTER 4

A simplified kinetic and mass transfer modelling of the thermal hydrolysis of vegetable oils

This chapter is based upon the following article:

Forero-Hernandez, Hector Alexander; Jones, Mark Nicholas; Sarup, Bent; Abildskov, Jens; Jensen, Anker Degn; Sin, Gürkan: *A simplified kinetic and mass transfer modelling of the thermal hydrolysis of vegetable oils.* Proceedings of the 27th European Symposium on Computer Aided Process Engineering (ESCAPE 27) Vol. 40 1. ed. Elsevier, 2017. p. 1177-1182.

4.1 Problem statement

Modeling batch kinetic data is important for the industrial application of the fat-oil splitting process, because it provides information that could be used to compare different modeling approaches under different operating conditions for producing fatty acids. In this sense, access to accurate data and parameters is relevant in predicting optimal reaction conditions. Hence, it is important to find good values for insufficient or missing properties in order to have an effective design.

Batch autoclaving of vegetable oils is employed to generate fatty acids. Fat and water are combined in a batch autoclave and heat to about 180°C-250°C under an autogenous pressure of about 20-45 *bar*. At such conditions, the non-catalyzed hydrolysis reaction takes place, where the oil is almost completely miscible in water and the hydrolysis takes place in a very short time. The

liberated fatty acids, washed free of glycerine by the water, can be separated by mechanical means.

The reactions are reversible, consecutive and parallel:

$$\mathrm{TG} + \mathrm{H_2O} \underset{\mathrm{k_{-1}}}{\overset{\mathrm{k_1}}{\rightleftharpoons}} \mathrm{FA} + \mathrm{DG} \qquad \text{(Reaction 5)}$$

$$\mathrm{DG} + \mathrm{H_2O} \underset{\mathrm{k_{-2}}}{\overset{\mathrm{k_2}}{\rightleftharpoons}} \mathrm{FA} + \mathrm{MG} \qquad \text{(Reaction 6)}$$

$$\mathrm{MG} + \mathrm{H_2O} \underset{\mathrm{k_{-3}}}{\overset{\mathrm{k_3}}{\rightleftharpoons}} \mathrm{FA} + \mathrm{Gly} \qquad \text{(Reaction 7)}$$

The complexity of models with several individual kinetic constants are simplified by lumping the three reactions into one step where the TG is converted into FA. Hence, a hydrolysis of vegetable oil is expressed as shown in (Reaction 8):

$$\mathrm{TG} + 3\mathrm{H_2O} \underset{\mathrm{k_{-1G}}}{\overset{\mathrm{k_{1G}}}{\rightleftharpoons}} 3\,\mathrm{FA} + \mathrm{Gly} \qquad \text{(Reaction 8)}$$

This reaction is modeled as an irreversible pseudo-homogeneous reaction which is followed by a reversible equilibrium reaction below. The concentration of diglycerides DG and monoglycerides MG in the reactions can be considered as negligible.

4.1.1 Modelling of vegetable oil hydrolysis reaction

In the modeling of the hydrolysis reaction, time dependent reaction regimes should be included. The reaction mechanism is assumed to be mass transfer controlled which is followed by a chemical reaction controlled regime. Studies on modeling the reaction kinetics with the initial mass transfer rate have been carried out by Namdev et al. 1988 as well as by Aniya et al. 2015. Three regimes of hydrolysis are identified:

1. A mass transfer controlled regime on the interface due to immiscibility of the emulsion oil formed by oil and water.

2. An irreversible fast chemical reaction controlled regime in the stable emulsion due to an increase in the concentration of water in the oil

phase and formation of products that act as co-solvent in the reaction mixture.

3. A reversible equilibrium chemical reaction controlled regime near to the hydrolysis equilibrium stage due to reduction of reactants and formation of products.

4.1.1.1 Mass transfer controlled regime

As Patil et al. (1988) reported, the initial phase of the reaction mixture is heterogeneous due to the low miscibility of the continuous phase (oil) in dispersed phase (water). The transfer of TG from the bulk of oil with mass transfer in the film formed with the droplets of water must be equal to the rate of its disappearance in the reaction, modelled as follows:

$$-r_{TG} = \frac{\mathrm{d}C_{TG}}{\mathrm{d}t} = k_c a \left(C_{TG} - C_{TG,S}\right) = k_c C_{TG} \tag{4.1}$$

Where k_c is the mass transfer coefficient ($\frac{m}{min}$), a is the specific interfacial area ($\frac{m^2}{m^3}$). C_{TG} and $C_{TG,S}$ are TG concentration in bulk and at interface respectively. As the reaction rate is faster than that of mass transfer, the interfacial concentration of oil results in $C_{TG,S} \to 0$. The TG concentration in bluk can be expressed in terms of conversion X_{TG} as:

$$C_{TG} = C_{TG,0} \left(1 - x_{TG}\right) \tag{4.2}$$

Equation (4.1) can be simplified in terms of the conversion of TG:

$$\frac{\mathrm{d}x_{TG}}{\mathrm{d}t} = k_c^{'} \left(1 - x_{TG}\right) \tag{4.3}$$

Mass transfer coefficient $k_c^{'}$ is a function of properties such as density, viscosity and diffusivity.

4.1.1.2 Pseudo-homogeneous reaction regime

Due to excess of water, the conversion of triglycerides to fatty acids follows pseudo-homogeneous second order reaction kinetics that can be represented:

$$-r_A = \frac{\mathrm{d}C_{TG}}{\mathrm{d}t} = k_1 C_{TG}^2 \tag{4.4}$$

Where k_1 is the irreversible reaction rate constant to the pseudo homogeneous regime, equation (4.4) can also be expressed in terms of conversion as:

$$-\frac{\mathrm{d}x_{TG}}{\mathrm{d}t} = k_1 C_{TG,0}\,(1 - x_{TG})^2 \tag{4.5}$$

4.1.1.3 Equilibrium reaction regime

When the hydrolysis is reaching the chemical equilibrium, the forward and reverse reaction rates follow second order reaction kinetics as described by:

$$-r_{TG} = -\frac{\mathrm{d}C_{TG}}{\mathrm{d}t} = k_2 C_{TG} C_W - k_3 C_{FA} C_{Gly} \tag{4.6}$$

Where k_2 and k_3 represent the forward and reverse reaction rate constants; C_W, C_{FA} and C_{Gly} are the concentrations of water, fatty acids and glycerol in the reacting mixture. By using stoichiometry and establishing that $C_W = C_{TG,0}\,(M - 3x_{TG})$, $C_{FA} = 3C_{TG,0}x_{TG}$, $C_G = C_{TG,0}x_{TG}$, equation (4.7) can be modified as:

$$\frac{\mathrm{d}x_{TG}}{\mathrm{d}t} = k_2 C_{TG,0}\,(1 - x_{TG})\,(M - 3x_{TG}) - 3k_3 C_{TG,0} x_{TG}^2 \tag{4.7}$$

k_1, k_2 and k_3 are kinetic parameters to be estimated and M is the initial water-to-oil molar ratio.

Since these regimes occur sequentially, this process corresponds to three chemical resistances in series and can be compared to Ohm's Law of electrical resistance in series $R_{\text{equivalent}} = \sum R_i$, which is defined as:

$$-r_{TG} = -r_{TG,\text{mass transfer}} = -r_{TG,\text{pseudo homogeneous}} = -r_{TG,\text{equilibrium}} \tag{4.8}$$

$$\frac{\mathrm{d}X_{TG}}{\mathrm{d}t} = \frac{C_{TG0}\,(1 - X_{TG})}{\underbrace{\frac{1}{k_c'}}_{\text{Mass transfer}} + \underbrace{\frac{1}{k_1\,C_{TG0}\,(1 - X_{TG})}}_{\text{Pseudo homogeneous}} + \underbrace{\frac{1}{k_2\,C_{TG0}\,(1 - X_{TG})\,(M - 3X_{TG}) - 3k_3\,C_{TG0}X_{TG}^2}}_{\text{Equilibrium}}} \tag{4.9}$$

In Equations (4.9) k_c', k_1, k_2 and k_3 are parameters to be estimated.

4.2 Methods

4.2.1 Parameter estimation

The mass transfer coefficient and the kinetic parameters parameters k_c', k_1, k_2 and k_3 were estimated using the Levenberg-Marquardt Algorithm for the non-linear regression problem. As results, the Levenberg-Marquardt Algorithm presents the simultaneously estimated parameters, the value of the residuals and the Jacobian matrix by minimizing the objective function to get the lowest sum of squared residuals for the parameters:

$$SS = \sum_i \left[(Y_{obs})_i - \left(\hat{Y}_{pred} \right)_i \right]^2 \tag{4.10}$$

4.2.2 Sampling the bootstrap method

The bootstrap method used in this case is described by Saisana, Saltelli, and Tarantola 2005 and Sin, Gernaey, and Lantz 2009 as follows:

- stimation of parameters k_c', k_1, k_2 and k_3 for the data set using the Levenberg-Marquardt Algorithm.
- Synthetic data is generated by bootstrap sampling (random sampling with replacement) in order to get a fictional data set. These generated data sets contain x_1^*, $x_2^*, \ldots,$ x_n^* points, where each x_i^* is generated randomly from the provided data points. The response y is estimated for the randomly generated data set by using statistical estimation:

$$y = T\left(x_1,\ x_2, \ldots, x_n\right) \tag{4.11}$$

- The resampling step is repeated n times to acquire a set of values for the calculated response.
- Calculation of mean, standard deviation/variance and 95% percentiles for the outputs (Sin, Meyer, and Gernaey 2010).

4.2.3 Application of bootstrap method to the model for assesing uncertainty in estimates

For 8 conversion values of triglycerides and time history were used to estimate k_c', k_1, k_2 and k_3. The model and the estimation of parameters were imple-

mented and simulated in Matlab. The method for performing the uncertainty analysis was also implemented in Matlab based on the work by Sin, Gernaey, and Lantz 2009. Sampling input uncertainty 100 samples were selected. Parameters were considered to be correlated due to the available information on the correlation matrix. Normal bivariate distributions and the 95% confidence regions were plotted for the estimated parameters.

4.3 Results and discussion

Experimental data for the hydrolysis of sunflower oil at 300°C are used from Alenezi et al. 2009. Data is provided in terms of conversion of sunflower oil into fatty acids, as shown in Table 4.1.

Time (min)	0	5.62	6.3	7.19	10.1	12.7	17	25.5
Conversion	0	00.0982	0.129	0.189	0.361	0.619	0.79	0.913

Table 4.1: Experimental data for the hydrolysis of sunflower oil (Alenezi et al. 2009).

Parameters were estimated at the above presented conditions, having a root mean squared error (RMSE) of values of 0.0028 indicating a good fit. Synthetic data was generated by bootstrap sampling (random sampling with replacement) from residual vector and adding it to the model prediction obtained in the parameter estimation. For each synthetic data, parameter estimation is repeated. The results including mean rates of reaction estimates, their standard deviation, correlation matrix as well as 95% bootstrap confidence interval are presented in Table 4.2.

	+95%	**Mean**	**-95%**	σ	**Correlation matrix**			
$k_c^{'}$	0.38	0.426	0.48	0.0635	1	-1	0.982	0.79
k_1	0.324	0.358	0.406	0.0232	-1	1	0.982	-0.79
k_2	0.131	0.147	0.166	0.0002	0.982	-0.982	1	0.844
k_3	0.0084	0.015	0.022	0.0012	0.79	-0.79	0.844	1

Table 4.2: Estimates of model parameters.

The plot of the estimated parameters obtained by the bootstrap method is shown in Figure 4.1. The scatter plot contains pairwise views of the sampling distribution of the four model parameters used for estimation. The

graph presents the variability of these estimates and how the coefficients are correlated.

In this scatter plot, it is safe to say that there is a correlation between all the parameters as seen in Table 4.2, indicating that the information that determines the mass transfer controlled regime also determines the chemical reaction regime. The linearity tendency suggests that the data follows a normal distribution. The model mean (calculated using values of parameter estimators) and the measured data fall inside the bootstrap prediction band and it is presented in Figure 4.2. The parameter estimation results showed that while the parameter have low standard deviation, the pairwise correlation between estimates is significant (more than 0.7).

This shows that the available experimental data is not fit to separately identify the mass transfer coefficient and kinetic parameters requiring further and better experiment information. On the other hand, the uncertainty analysis indicated that model prediction uncertainty represented as the 95% confidence regions due to parameter estimation errors is rather slight. Therefore, it is recommended that the model be used for process analysis and improvement accompanied by Monte Carlo uncertainty analysis.

4.4 Conclusions

In this work a simplified kinetic for hydrolysis of vegetable oils in a batch reactor was proposed and the parameters in the model were estimated from data in the literature. A bootstrap based uncertainty analysis was performed to find the accuracy of estimated parameters and model output from batch thermal hydrolysis of oil data. The bootstrap method was successfully applied to calculate the accuracy of estimates of kinetic parameters as well as their confidence intervals for the hydrolysis of vegetable oils and recommended for estimation of the variance of parameters in chemical kinetics modelling. The results showed that the presented model was able to predict accurately the experimental data with a narrow confidence interval. Since the lack of experimental data is a crucial issue in the hydrolysis of vegetable oils, this model-based analysis of data is of substantial value to provide necessary information for detailed modelling and characterization of the process.

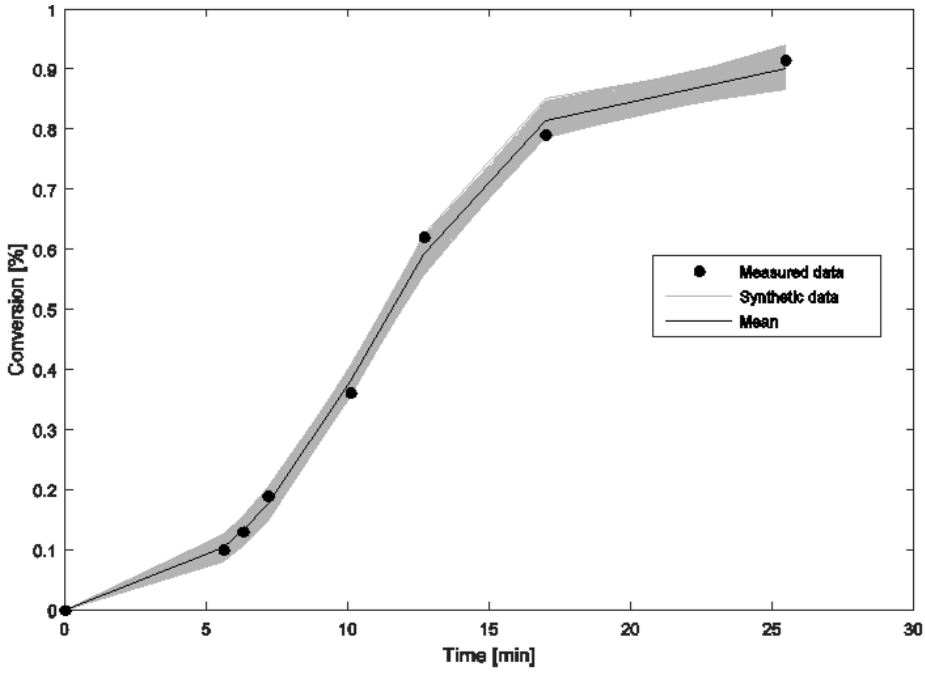

Figure 4.1: Comparison between experimental data and fitted model.

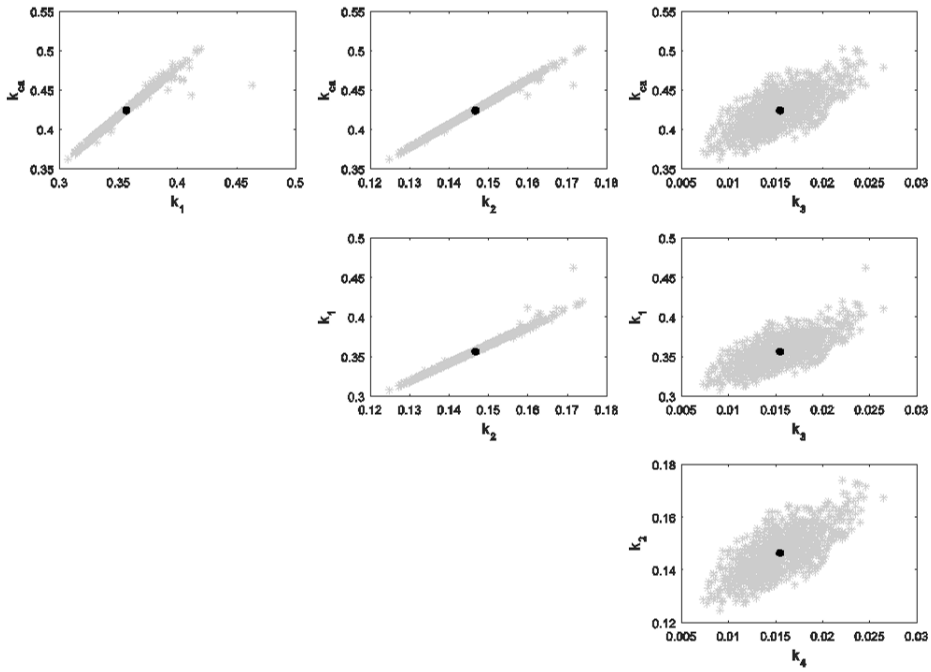

Figure 4.2: Scatter plots of bootstrap estimated parameters.

CHAPTER 5

Development of a model for the hydrolysis of rapeseed oil

This chapter is based upon the following article:

Forero-Hernandez, Hector Alexander; Jones, Mark Nicholas; Sarup, Bent; Abildskov, Jens; Jensen, Anker Degn; Sin, Gürkan: *Comprehensive Development, Uncertainty and Sensitivity Analysis of a Model for the Hydrolysis of Rapeseed Oil.* Submitted to: *Computers & Chemical Engineering Journal.* Under review.

The hydrolysis of oils and fats is an important processing route for the chemical industry. In this regard, several authors have developed kinetic models for the hydrolysis reaction of triglycerides (Hartman 1951; Minami and Saka 2006; Patil, Raghunathan, and Shankar 1988a; Patil, Raghunathan, and Shankar 1988b; Namdev et al. 1988). The process for hydrolyzing oil by using water is influenced by both mass transfer between the phases and by the kinetics of the reactions.

Lascaray 1952; Lascaray 1949 found that the conversion of this reaction is dependent of the temperature. Sturzenegger and Sturm 1951 described the autocatalytic behavior of the reaction in a batch reactor, with the assumption that the reaction occurs in the bulk of the oil phase. Such behavior had been attributed to the elevated ion product of water at high temperature (Sturzenegger and Sturm 1951). Patil, Raghunathan, and Shankar 1988a; Patil, Raghunathan, and Shankar 1988b; Namdev et al. 1988 proposed a model to describe the biphasic hydrolysis by using a combined mass transfer and kinetic approach. The authors also investigated the reaction in both batch and continuous mode and proposed a three-step reversible reaction mechanism

for the hydrolysis of tri-, di- and monoglycerides (Patil, Raghunathan, and Shankar 1988a; Patil, Raghunathan, and Shankar 1988b; Namdev et al. 1988). Minami and Saka 2006 developed a second-order chemical reaction model and suggested an autocatalytic mechanism due to the action of generated fatty acids in the aqueous phase that subsequently act as acid catalyst in subcritical water (Minami and Saka 2006). More recently, Alenezi et al. 2009 presented a kinetic study for the hydrolysis of sunflower oil under subcritical conditions in a PFR, where information on the different kinetic regimes the reaction exhibits as well as on the rate parameters was also provided. Additionally, the hydrolysis at low/middle temperatures over solid acid catalists was discussed by J. K. Satyarthi, D. Srinivas, and P. Ratnasamy 2011. In their study, the rates of hydrolysis were increased by the action of solvents and phase transfer agents.

Nevertheless, after a revision of the technical process development of hydrolysis of triglycerides one finds that some basic facts related to the thermodynamics, mass transfer, and kinetics inherent to the biphasic nature of the process have only been partially recognized due to the rather harsh physical conditions at which tri-, di-, and monoglycerides are exposed to during their hydrolysis. Hence, only limited information is available (Metzger and Bornscheuer 2006). Besides, another disadvantage of the available models in the open literature is, to the best of our knowledge, that none of the recent studies has been analyzed and thoroughly validated.

Kinetic modeling of biphasic reactions, specifically the hydrolysis of vegetable oils at subcritical conditions, is complicated due to the heterogeneous nature of the system. Therefore, it is the aim of this chapter to present the development and validation of a biphasic model with dedicated experiments based on measurable properties of the overall hydrolysis reaction.

This model describes batch runs with a reasonable number of parameters and degree of accuracy. Monte Carlo simulations were run to identify the working bounds and the cases where the model is most accurate under uncertainty in the parameter estimates and model outputs. Furthermore, a sensitivity analysis method based on variance was used in order to quantify how much of the variance in the model output each uncertain parameter is responsible for.

5.1 Model development

5.1.1 System phenomena relevant for modeling

The hydrolysis of triglycerides is generally considered a three-step set of consecutive, reversible reactions in which one mole of glyceride is generated and consumed as seen in (Reaction 9) - (Reaction 11). In water at high temperature, this hydrolysis reaction with its backward reaction occurs without any catalyst. In this system of reversible reactions, a molecule of Triglyceride (TG) is hydrolyzed to one molecule of Diglyceride (DG) and one molecule of Fatty Acid (FA). DG is subsequently hydrolyzed to Monoglyceride (MG) which is further hydrolyzed to Glycerol (Gly), producing three molecules of FA in total (Patil, Raghunathan, and Shankar 1988b; C. E. Goering et al. 1982).

The following reactions present the three-step vegetable oil hydrolysis reaction:

$$\mathrm{TG} + \mathrm{H_2O} \underset{\mathrm{k_{-1}}}{\overset{\mathrm{k_1}}{\rightleftharpoons}} \mathrm{FA} + \mathrm{DG} \qquad \text{(Reaction 9)}$$

$$\mathrm{DG} + \mathrm{H_2O} \underset{\mathrm{k_{-2}}}{\overset{\mathrm{k_2}}{\rightleftharpoons}} \mathrm{FA} + \mathrm{MG} \qquad \text{(Reaction 10)}$$

$$\mathrm{MG} + \mathrm{H_2O} \underset{\mathrm{k_{-3}}}{\overset{\mathrm{k_3}}{\rightleftharpoons}} \mathrm{FA} + \mathrm{Gly} \qquad \text{(Reaction 11)}$$

However, as presented by Noureddini et al, the reaction described by (Reaction 12) can take place at high temperatures (180°C-280°C) (Noureddini, Harkey, and Gutsman 2004).

$$\mathrm{TG} + \mathrm{MG} \underset{\mathrm{k_{-4}}}{\overset{\mathrm{k_4}}{\rightleftharpoons}} 2\,\mathrm{DG} \qquad \text{(Reaction 12)}$$

As a result of its heterogeneous nature, the hydrolysis reaction is affected not only by the chemical kinetics but also by the rate of mass transfer between the oil and water phase. Other important variables which are affecting the process are temperature, pressure, density, viscosity, and geometry of reactor. Since the polar water and non-polar TG form two immiscible phases, one component must diffuse into the other before the reaction between them can happen. Thus, both a mass transfer of water from the bulk of the aqueous

phase to the organic phase and a chemical reaction take place in the process. Lascaray 1952 observed that in the beginning of the reaction, a water in oil emulsion is formed and the reaction proceeds slowly due to mass transfer limitations. As the reaction continues, the emulsion breaks down and the reaction rate increases significantly. This is because the fatty acid content in the oil increases due to the reaction, which then acts as an acid catalyst. Consequently, the overall reaction rate expression should consist of the mass transfer rate, the chemical reaction rate and include explicitly the solubility of water in the oil phase depending on its composition.

According to the two-film theory, an interface separates the phases and there is one film in either phase that adheres to the interface (Astarita 1967; Trambouze, Van Landeghem, and Wauquier 1989). Mass transfer and reaction occur through the following consecutive steps as proposed by Attarakih et al. 2012 for a high-pressure oil-hydrolysis countercurrent spray reactor:

1. Water in the aqueous bulk diffuses through the aqueous film.
2. Water diffuses through the liquid/liquid interface.
3. Water diffuses through the oil film to the oil phase bulk where the reaction takes place.
4. Water reacts with the tri-, di-, and monoglycerides forming fatty acids and glycerol.
5. Fatty acids dissolve in the oil phase with the unreacted tri-, di-, and monoglycerides while glycerol diffuses back to the aqueous phase. The aqueous bulk is composed of water, glycerol, and very low amounts of TG, DG, MG, and FA.

The representation of the mass transfer mechanism is shown in Figure 5.1.

5.1.2 Mathematical formulation

The general modeling objective followed in this work is that the model should be sophisticated enough to describe the complexities of the hydrolysis of vegetable oil, but the parameters should be based on measurable phenomena to a possible extent.

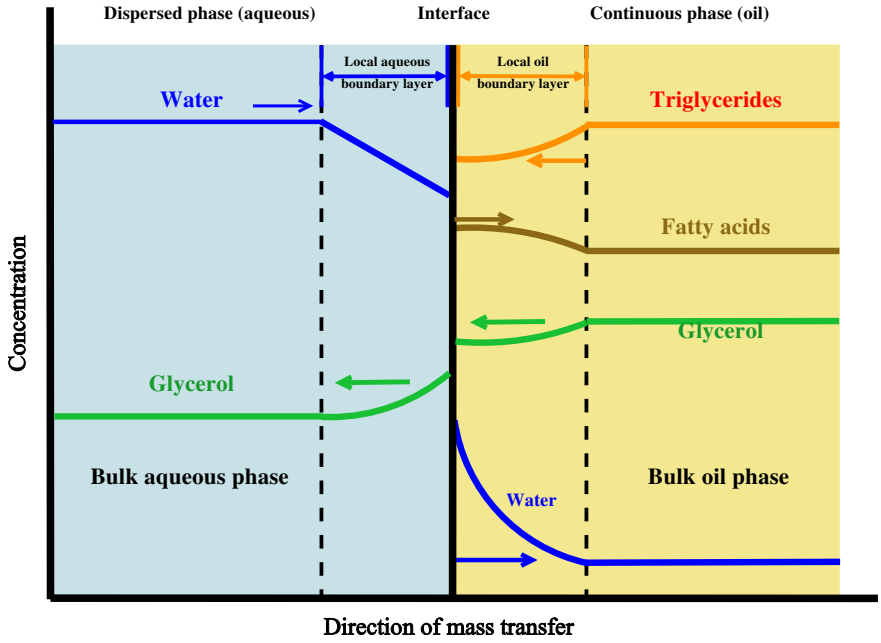

Figure 5.1: Mass transfer and reaction processes based on the two film theory for the hydrolysis of oils.

1. Two phases are present: aqueous (polar) and oil (non-polar) represented by the subscripts *aq* and *oil* respectively. All the reactions occur in oil phase.

2. Reactions are elementary and consecutive.

3. As the reactions are reversible, TG, DG, and MG are present at the chemical equilibrium.

4. Partition of water and glycerol among the two phases.

5. Mass transfer phenomena is described by Whitman's two-film theory (Whitman 1962).

Based on the reaction scheme presented in (Reaction 9) to (Reaction 12), the following kinetic equations are proposed:

$$\begin{gathered} \mathrm{TG} \ + \ \mathrm{H_2O} \underset{\mathrm{k_{-1}}}{\overset{\mathrm{k_1}}{\rightleftharpoons}} \mathrm{FA} + \mathrm{DG} \\ R_1 = k_1 \cdot C_{TG} \cdot C_{H_2O} - k_{-1} \cdot C_{DG} \cdot C_{FA} \end{gathered} \tag{5.1}$$

$$\begin{gathered} \mathrm{DG} \ + \ \mathrm{H_2O} \underset{\mathrm{k_{-2}}}{\overset{\mathrm{k_2}}{\rightleftharpoons}} \mathrm{FA} + \mathrm{MG} \\ R_2 = k_2 \cdot C_{DG} \cdot C_{H_2O} - k_{-2} \cdot C_{MG} \cdot C_{FA} \end{gathered} \tag{5.2}$$

$$\begin{gathered} \mathrm{MG} \ + \ \mathrm{H_2O} \underset{\mathrm{k_{-3}}}{\overset{\mathrm{k_3}}{\rightleftharpoons}} \mathrm{FA} + \mathrm{Gly} \\ R_3 = k_3 \cdot C_{MG} \cdot C_{H_2O} - k_{-3} \cdot C_{Gly} \cdot C_{FA} \end{gathered} \tag{5.3}$$

$$\begin{gathered} \mathrm{TG} \ + \ \mathrm{MG} \underset{\mathrm{k_{-4}}}{\overset{\mathrm{k_4}}{\rightleftharpoons}} 2\,\mathrm{DG} \\ R_4 = k_4 \cdot C_{TG} \cdot C_{MG} - k_{-4} \cdot C_{DG}^2 \end{gathered} \tag{5.4}$$

Where k_i is the reaction rate constant for component i.

In order to model the batch hydrolysis, the expression for every species involved in the reaction should be determined. The reaction rates can be described by the expressions in Equations (5.1) - (5.4). The mole balances for the aqueous and oil phases become:

- Aqueous phase

$$\frac{dn_{H_2O}^{aq}}{dt} = -J_{H_2O}^{aq} \cdot V_{aq} \tag{5.5}$$

$$\frac{dn_{Gly}^{aq}}{dt} = J_{Gly}^{aq} \cdot V_{aq} \tag{5.6}$$

- Oil phase

$$\frac{dn_{TG}^{oil}}{dt} = (-R_1 - R_4) \cdot V_{oil} \tag{5.7}$$

$$\frac{dn_{DG}^{oil}}{dt} = (R_1 - R_2 - 2 \cdot R_3) \cdot V_{oil} \tag{5.8}$$

$$\frac{dn_{MG}^{oil}}{dt} = (R_2 - R_3 - R_4) \cdot V_{oil} \tag{5.9}$$

$$\frac{dn_{FA}^{oil}}{dt} = (R_1 + R_2 + R_3) \cdot V_{oil} \tag{5.10}$$

$$\frac{dn_{H_2O}^{oil}}{dt} = \left(-R_1 - R_2 - R_3 + J_{H_2O}^{oil}\right) \cdot V_{oil} \tag{5.11}$$

$$\frac{dn_{Gly}^{oil}}{dt} = \left(R_3 - J_{Gly}^{oil}\right) \cdot V_{oil} \tag{5.12}$$

The equations which describe the mass transfer of water and glycerol from and to the two phases are as follows:

$$J_{H_2O}^{aq} = k_{1L,a} \cdot \left(C_{H_2O}^{aq} - m_{H_2O} \cdot C_{H_2O}^{oil,*}\right) \tag{5.13}$$

$$J_{Gly}^{aq} = k_{2L,a} \cdot \left(C_{Gly}^{aq} - m_{Gly} \cdot C_{Gly}^{oil,*}\right) \tag{5.14}$$

$$J_{H_2O}^{oil} = k_{1L,a} \cdot \left(C_{H_2O}^{oil,*} - C_{H_2O}^{oil}\right) \tag{5.15}$$

$$J_{Gly}^{oil} = k_{2L,a} \cdot \left(C_{Gly}^{oil} - C_{Gly}^{oil,*}\right) \tag{5.16}$$

When one assumes steady-state, the interfacial concentration (C_i^*) can be calculated by solving the following balance for the ith component:

$$J_i^{aq} \cdot V^{aq} = J_i^{oil} \cdot V^{oil} \tag{5.17}$$

By solving Equation (5.17), it is possible to obtain:

$$C_i^{oil,*} = \frac{V^{aq} \cdot k_{iL,a} \cdot C_i^{aq} + k_{iL,a} \cdot V^{oil} \cdot C_i^{oil}}{k_{iL,a} \cdot V^{oil} + V^{aq} \cdot k_{iL,a} \cdot m_i} \tag{5.18}$$

In order to solve the mass transfer equations, it is also necessary to define the partition coefficient for both water and glycerol. In the absence of experimental data for the liquid-liquid system, the UNIFAC model is used to calculate the partition coefficient m. In this study the modified UNIFAC (Dortmund) thermodynamic model is applied for the calculation of the liquid-liquid equilibrium compositions and partition coefficients (Lohmann and Jürgen Gmehling 2001; Juergen Gmehling, J. Li, and Schiller 1993; Jürgen Gmehling, Lohmann, et al. 1998; Jürgen Gmehling, Wittig, et al. 2002; Jakob et al. 2006). These calculations are carried out by using the iterative algorithm proposed by Rachford and Rice 1952, and it is summarized in the Supporting Information section of this work.

Volumes of oil and aqueous phase are calculated by using the following equation:

$$V_{oil} = \sum_{i,oil} \frac{n_{i,oil}}{\rho_i} \qquad V_{aq} = \sum_{i,aq} \frac{n_{i,aq}}{\rho_i} \tag{5.19}$$

Densities of components (ρ_i) are calculated by using polynomial fittings of experimental data of density versus temperature for the desired range. Correlation parameters for these polynomials have been obtained from the *CAPEC Lipids Database* (Diaz-Tovar, Gani, and Sarup 2011). In brief, the mathematical model has 8 variables, i.e. moles, and it contains 10 parameters which are estimated from dedicated experiments.

5.2 Experimental materials and methods

5.2.1 Chemicals

Rapeseed oil purchased from Scandic Food A/S (Nørre Aaby, Denmark) and deionized water (18 Ω) were used for the hydrolysis experiments. n-Heptane [CAS 142-82-5], Acetic acid [CAS 69-19-7], Isopropanol [CAS 67-63-0], and tert-Butyl methyl ether [CAS 1634-04-4] were used for HPLC-Analysis and were purchased from Sigma-Aldrich Denmark ApS (Brøndby, Denmark).

5.2.2 Batch experiments

Hydrolysis reactions were run in a 300 ml Hastelloy C-276 jacketed reactor with ceramic band heaters (Parker Autoclave Engineers, Model 300 ml HC EZE-Seal), which includes a coil to cool the contents in the reactor. The reactor is equipped with a PID controller to monitor and control temperature and agitation speed. The reactor has a sampling port for withdrawal of liquid samples during the reaction every 30 minutes. A scheme of the set-up used is depicted in Figure 5.2. 11 experiments were carried out based on a Box-Behnken design for three factors (temperature, oil-to-water ratio, and agitation speed) and an experimental runtime of 6 hours as shown in Table 5.1 (Box and Behnken 1960).

The initial time of each experiment was defined as the point of time when oil and water reached the operating temperature (approximately 18 minutes).

Experimental conditions			
Experiment	**Temperature (°C)**	**Water-to-oil ratio**	**Agitation (rpm)**
1	**180**	**15**	**360**
2	**180**	**40**	**360**
3	280	15	360
4	280	40	360
5	180	27.5	120
6	**180**	**27.5**	**600**
7	280	27.5	120
8	280	27.5	600
9	230	15	120
10	230	15	600
11	230	40	600

Table 5.1: Experimental design (validation sets are highlighted).

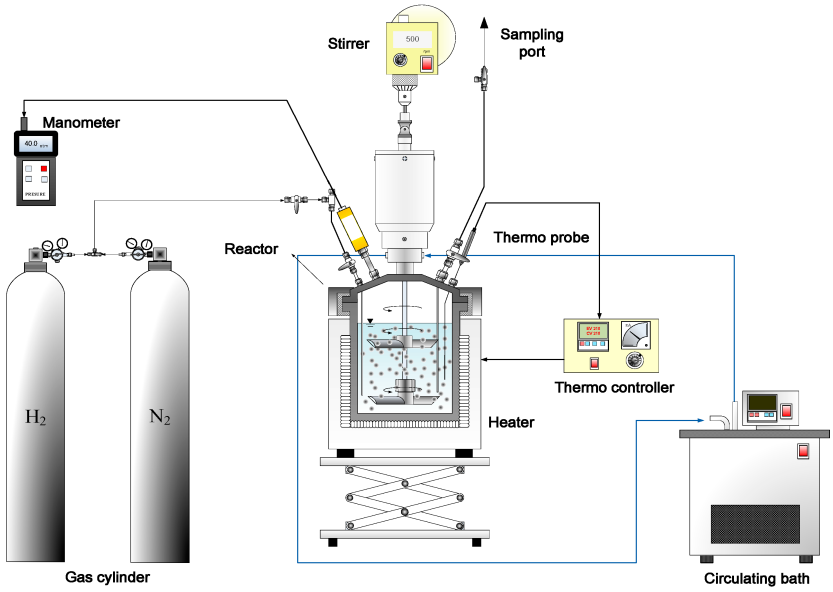

Figure 5.2: Reactor setup used for the hydrolysis of rapeseed oil.

Collected samples were cooled and let to settle in a graduated vial for phase separation and then separated by decantation.

5.2.3 HPLC Analysis

Collected samples were analyzed by following the procedure developed by Foglia and Jones 1997, and modified by Price et al. 2014. 40 μL of the sample were injected in the HPLC (Ultimate 3000, Dionex A/S, Hvidovre, Denmark) to analyze TG, DG, MG, and FA. The separation of the compounds was performed in a cyanopropyl column (0.25 x 0.004 m) (Discovery, Cyano, Sigma Aldrich A/S, Brøndby, Denmark), U3000 auto-sampler, TCC-3000SD column oven, U3400A quaternary pump modules, and a Corona Charged Aerosol Detector (Thermo Scientific, MA, United States). A binary gradient program was run with the use of three solvents (99.6% v/v tert-Butyl methyl ether, 0.4% v/v Acetic acid and, Isopropanol). The detection of the compounds was achieved by a Corona Charged Aerosol Detector from Thermo Scientific Dionex (Chelmsford, MA) with pressurized N_2 .

5.3 Parameter estimation, uncertainty and sensitivity analysis

5.3.1 Sequential and simultaneous parameter estimation

For the datasets collected in the experiments, kinetic and mass transfer parameters were estimated by applying the Levenberg-Marquardt algorithm for the non-linear global fitting problem. Thus, the Levenberg-Marquardt algorithm presents the simultaneously estimated parameters, the value of the residuals and the Jacobian matrix by minimizing the objective function in order to get the lowest sum of squared residuals for the kinetic and mass transfer parameters:

$$\theta = \arg\ \min \sum_{i} \left(y_i^{\exp} - y_i^{pred} \right)^2 \tag{5.20}$$

In Equation (5.20) θ are the estimated parameters, y_i^{exp} the measurement, and y_i^{pred} the obtained value of parameter i.

This preliminary estimation gives an initial guess for the simultaneous estimation of parameters which is carried out as an ordinary non-linear regression problem.

5.3.1.1 Covariance-based uncertainty analysis of parameter estimation and output prediction

The underlying assumption is that the errors are normally distributed. The uncertainty of the parameter estimates is based on the covariance matrix, $COV(\theta)$, which is obtained through first linear approximation as described in the workflow proposed by Sin, Meyer, and Gernaey 2010. The covariance matrix $\mathrm{COV}(\theta)$ is estimated by Equation (5.21):

$$\mathrm{COV}\left(\theta\right) = \frac{S\left(\theta\right)}{N-p}\left(\left(\frac{d\mathbf{y}}{d\theta}\right)^{T} Q_m^{-1}\left(\frac{d\mathbf{y}}{d\theta}\right)\right) \tag{5.21}$$

where $S(\theta)$ represents the minimum error sum of squares calculated from the Levenberg-Marquardt algorithm in the non-linear global fitting problem, $\frac{dy}{d\theta}$ is sensitivity matrix of the outputs obtained in the model ($\mathbf{y}$) with reference to the model parameters (θ). Q_m is the covariance matrix of measurement errors, N is the number of experimental data used for the regression, and p is the total number of estimated parameters. In this way, the correlation between two parameters v and w can be expressed as:

$$\mathrm{COR}\left(\theta_v, \theta_w\right) = \frac{\mathrm{COV}\left(\theta_v, \theta_w\right)}{\sqrt{\sigma_{\theta_v}^2 \sigma_{\theta_w}^2}} \tag{5.22}$$

The histograms of residuals were used to verify that the residuals follow a normal distribution and have a zero mean. This also allows one to evaluate the quality of the fitting by identifying the confidence regions for the parameters through the calculation of normal bivariate distributions.

5.3.1.2 Monte Carlo method for uncertainty analysis of parameter estimation and prediction

In this work, the calculation of the uncertainty in the obtained parameters was carried out by applying the Monte Carlo method. This technique uses randomly sampled parameters so as to evaluate the model outputs and to obtain their distribution. In this way, it is possible to achieve global results in the uncertainty due to the large number of evaluations the model undergoes. Thus, once the input parameter space is defined, the model is evaluated by obtaining the corresponding model outputs $\mathbf{y}$. The procedure for performing uncertainty analysis can be summarized as:

1. **Definition of the input parameter uncertainty**: upper and lower bounds for a model parameter are defined by its confidence intervals $\hat{\theta}$.

2. **Sampling input uncertainty**: quasi-random sampling of the parameter estimates by means of a Latin Hypercube Sampling to distribute samples evenly over the input parameter space (Iman and Conover 1982).

3. **Use of the sampling matrix to evaluate the model**: simulations are performed by using the sampled input matrix obtained in the previous step. In this way, a cumulative distribution function for each model output is obtained. Consequently, mean values of the model and 5^{th} and 95^{th} percentile calculations are used to represent the uncertainty of the model outputs.

5.3.2 Variance based sensitivity analysis - Sobol method

A variance based sensitivity analysis method uses the variance of the model outputs and decomposes it into fractions that can be related to the model parameters. These partial variances can be obtained by the decomposition of a random vector of input parameters. Then, the partial variances are normalized with the total variance to obtain the so-called Sobol sensivity indices (Sobol 1993). The Sobol indices are useful to quantify the importance of a parameter X_i on a model output. The Sobol indices can take values between 0 and 1. In this method, a value closer to 1 means that the contribution of the input parameter on the variance is high. The Sobol sensitivity indices also allow one to identify the total and the interaction effect among parameters on the output variance for a specific input parameter (Klinkert 2018).

The variance calculates measures on how far a set of random numbers are spread out from their mean value. The variance of a model output y is given by:

$$V(y) = V(f(X)) = \sigma^2 = \int (f(X) - \mu)^2 - p(X)\, dX \tag{5.23}$$

where $V(X)$ is the variance, σ the standard deviation, μ the mean, $p(X)$ is the probability density function of X, and X is a random parameter.

The variance can be decomposed by using Sobol's higher dimensional model representations as follows (R. C. Smith 2013):

$$V(y) = \sum_i V_i + \sum_i \sum_{j>i} V_{i,j} \tag{5.24}$$

where V_i and $V_{i,j}$ are the first-order and second-order variance of the model outputs respectively.

Sobol indices can be obtained by normalizing the partial variances with the total variance as:

$$S_i = \frac{V_i}{V(y)} \qquad S_{i,j} = \frac{V_{i,j}}{V(y)} \tag{5.25}$$

where S_i is the first-order sensitivity index which allows one to characterize the influence of parameter X_i on the model output. $S_{i,j}$ is the second-order sensitivity index, which allows the quantification of interactions among parameters X_i and X_j.

S_{Ti} is the total sensitivity index where the input parameter X_i is present, which can be expressed as (Marelli et al. 2019):

$$S_{TI} = S_i + \sum_j S_{i,j} \tag{5.26}$$

These indices can be obtained by using Monte Carlo simulations (e.g. Janssen, Sobol, or Saltelli approximation) (Jansen 1999; Sobol 1993; Saltelli et al. 2010). However, recently developed methodologies make use of metamodels, such as polynomial chaos expansions to overcome the computational costs related to the sampling of the Monte Carlo method.

5.3.3 Polynomial chaos expansions

Polynomial chaos expansion (PCE) is a sampling-based method to determine the evolution of uncertainty in a model, which can be estimated as a sum of orthogonal polynomials. The main advantage of representing the model output as a polynomial is that it allows one to simplify and speed-up the calculations required.

Different polynomial types can be used to approximate the model output. This approximation depends on the type of distribution the input variable X

follows. For example, Legendre polynomials and Hermite polynomials are used for rectangular and standard normal distributions respectively. The model output can be approximated with different polynomial types. The approximated function is defined as:

$$y = f(\mathbf{X}) \approx \sum_{a \in \mathbb{R}^M} \hat{y}_a \phi_a(\mathbf{X}) \tag{5.27}$$

where the coefficients $\hat{y}$ can be found by using Gauss-Legendre quadrature rules (Hildebrand 1987):

$$\hat{y}_a \approx \sum_{k=1}^{N} = f(x_k)\, \phi_a(x_k)\, w_k \tag{5.28}$$

In Equation (5.28) w_k represent the weights and x_k the nodes, which can be calculated by the polynomial distribution function of the independent input parameters. Both the weights and nodes can be determined by finding the roots of the polynomial function (Marelli et al. 2019).

Once this approximation of the model output is obtained, the total and partial variance of the function can directly be computed due to the orthogonality of the polynomials (Marelli et al. 2019; Al et al. 2019). Once the variances are obtained, the Sobol sensitivity indices can be computed.

$$V_t = \sum_{\substack{a \in \mathbb{R}^M \\ a \neq 0}} \hat{y}_a^2 \tag{5.29}$$

$$V_i = \sum_{\substack{a \in \mathbb{R}^a \\ a \neq 0}} \hat{y}_a^2 \tag{5.30}$$

5.3.4 Residual analysis

The residual analysis is relevant for model validation because it allows one to verify whether the model estimates explain the variations in a dependent variable. Ideally the residuals should be small and uncorrelated. If the residuals are correlated or have any special aspect that does not seem random, there is a methodical error in the model. The residuals are calculated as:

$$e = \mathbf{y} - \hat{\mathbf{y}} \tag{5.31}$$

Where e is a vector which contains the residuals, y are the measurements taken in a experiment, and $\hat{y}$ is the output calculated in the model.

5.4 Implementation of methodologies

The implementation of the methodologies, simulations, and programming of the statistical methods were coded in Matlab by using the work-flow presented by Sin, Gernaey, and Lantz 2009; Azim, Subki, and Yusof 2018. (Sin, Gernaey, and Lantz 2009; Sin and Gernaey 2016). The algebraic differential equations proposed in the model were solved by using the built-in routine $ode23s$, while parameter estimations and regressions were performed with the use of the $fminsearch$ and $lsqnonlin$ algorithms in Matlab (Lawrence F. Shampine, Mark W. Reichelt, and Kierzenka 1999; The Mathworks Inc. 2016; Lawrence F Shampine and Mark W Reichelt n.d.; Coleman and Y. Li 1993). The UQLab framework provided implementations of PCE models and Sobol sensitivity indices, which were used in this study (**al2018a**; Marelli et al. 2019). The implementation of the above presented methods is summarized in Table 5.2.

#	Step	Description	Output
1	Parameter estimation	Parameters to fit the model	θ_0
		Identification of parameter	$\hat{\theta}_R$
		Correlation matrix	R_θ
		Confidence interval for parameters	σ
2	Uncertainty analysis	Prediction uncertainty of the model	5^{th} and 95^{th}
3	Sensitivity analysis	Sobol sensitivity indices	S_i and S_{Ti}
		Polynomial chaos expansions	V_i and V_T
4	Residual analysis	Simulations with estimated parameters	
		Probability distribution of residuals	
		Compute the autocorrelation function	

Table 5.2: Uncertainty and sensitivity analysis method.

5.5 Results and discussion

5.5.1 Global fitting, uncertainty in the parameters and correlation

Eight datasets obtained with the above described experimental procedure were used to estimate the model parameters through global fitting, while three are used for model validation. Model fits for the validation sets as well as the parameter estimation are presented in Figure 5.3 and Table 5.3.

The performance of the model fits for the validation sets during the reaction times is shown in Figure 5.3, where data is provided in terms of moles of species. It can be seen that the quality of the model fits is high. These fits were obtained by estimating 8 kinetic and 2 mass transfer parameters present in the developed mathematical model. Since the estimation error obtained by the standard deviation is low, it is possible to say that the estimated values are accurate (Sin and Gernaey 2016).

The proposed model captures the behaviour for the four analyzed component, although the prediction for DG and MG mismatches the experimental data. However in Figure 5.3, the experimental amount of moles of validation set 1 (180°C - 1:15 oil-to-water molar ratio) shows significant mismatches, when it comes to the prediction of MG which is much higher than the amount predicted by the model. The model mismatches observed can be related to changes in the phenomena which were not modeled such as viscosity, large generation of emulsifying agents such as DG, and distribution of phases due to the initial amount of water as reported by Wang et al. 2013. At 180°C - 1:40 oil-to-water molar ratio - 360 rpm, there is a higher amount of FA produced which is in agreement with previous research, since it is known that high amounts of water lead to higher conversion rates (Wang et al. 2013; Minami and Saka 2006; Patil, Raghunathan, and Shankar 1988a).

The mean of the estimated parameters, their standard deviation σ, and correlation coefficients are shown in Table 5.3. Once parameter estimates are obtained, it is necessary to determine how specific they are in relation to the experimental data used. When two parameters are highly correlated, a change in the model output can be mitigated by a change in the value of the other parameter. As seen in Table 5.3, some of the parameters are highly correlated. This prevents find

For example, k_1 has a high negative correlation with $k_{1L,a}$, which means that the kinetic constant related to the consumption of triglycerides has a

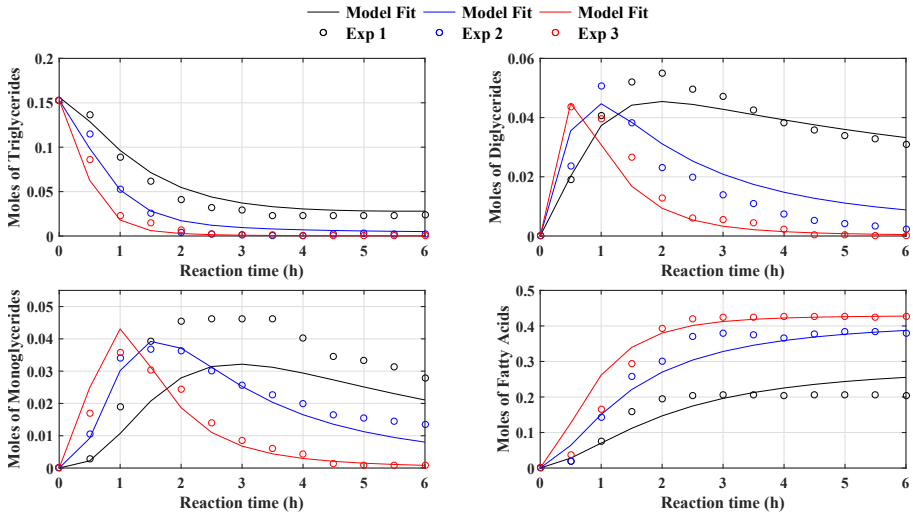

Figure 5.3: Global fitting and experimental data for the hydrolysis at (—) 180°C - 1:15 oil-to-water molar ratio - 360 rpm, (—) 180°C - 1:27.5 oil-to-water molar ratio - 600 rpm and (—) 180 °C-1:40 oil-to-water molar ratio-360 rpm..

θ	Mean		Correlation matrix									
			k_1	k_{-1}	k_2	k_{-2}	k_3	k_{-3}	k_4	k_{-4}	$k_{1L,a}$	$k_{2L,a}$
k_1	2.029	0.101	1.000									
k_{-1}	1.919	0.208	0.655	1.000								
k_2	2.251	0.203	0.112	0.013	1.000							
k_{-2}	4.236	0.528	0.123	-0.137	0.931	1.000						
k_3	1.173	0.057	0.059	0.168	-0.079	-0.059	1.000					
k_{-3}	0.395	0.031	-0.103	-0.292	-0.092	-0.029	0.603	1.000				
k_4	2.464	0.128	-0.138	0.096	-0.111	-0.185	-0.001	-0.155	1.000			
k_{-4}	1.75	0.102	-0.268	-0.431	-0.302	-0.262	-0.111	0.063	0.068	1.000		
$k_{1L,a}$	0.319	0.025	-0.773	-0.424	-0.524	-0.499	-0.063	0.061	0.191	0.292	1.000	
$k_{2L,a}$	0.772	0.13	-0.273	-0.222	0.063	0.182	-0.426	-0.242	-0.336	0.054	0.255	1.000

Table 5.3: Mean, standard deviation, and correlation matrix for the parameter estimation..

negative effect on the mass transfer coefficient of water. Our study also shows that if the value of k_1 increases, $k_{1L,a}$ decreases to obtain a good fit. Similar analyses can be done for k_1 and k_{-1} (consumption and generation of TG in (Reaction 9)), k_{-1} and k_{-4} (consumption and generation of DG in (Reaction 9) and (Reaction 12)), k_2 and k_{-2} (generation and consumption of MG in (Reaction 10)), k_{-2} and $k_{1L,a}$ (consumption of MG in (Reaction 10)

and mass transfer of water respectively), k_3 and k_{-3} (generation and consumption of MG). This correlation is expected, since the hydrolysis proceeds as a set of parallel and sequential reactions, which implies poor identifiability. In this regard, more measurements should be performed so as to be included in the parameter estimation. These measurements can be moles of glycerin and water as well as separate measurements of mass transfer rates between phases without the complexity of ongoing reaction.

5.5.2 Uncertainty analysis of model predictions

The uncertainty of the calculated model outputs (n_{TG}, n_{DG}, n_{MG}, and n_{FA}) during the hydrolysis reaction can be seen in Figure 5.4 and Figure 5.5. In these figures, synthetic data generated by the evaluation of the model by using Latin Hypercube Samples is shown for the validation set (hydrolysis at 180°C - 1:27.5 oil-to-water molar ratio - 600 rpm). It is possible to observe that almost all the experimental values lay inside the working boundaries of the simulations. The tight predictions for n_{TG} and n_{FA} give an overview of the robustness of the model and quality of the fit, while the large predictions calculated for n_{DG} and n_{MG} indicate that either the model which contains deficiencies or the variables were not properly measured. In this case, a better estimation of the parameters and more experiments are necessary to get more accurate predictions for these species.

5.5.3 Sensitivity analysis of model outputs

For the sensitivity analysis with Sobol indices an output was needed, given our interest in determining which parameters contribute to the uncertainty of the model outputs during the time course of the reaction (0.5 - 6 hours), where there are significant variations in the model outputs of the Monte Carlo simulations (Figure 5.4). Global calculations were also made by using the mean values of the outputs. This was done to rank the significance of the parameters obtained at the different conditions used in the validation sets. It should be noted that the analysis can be performed at different time points and different process conditions at which case the parameter ranking can vary. In this case, the selected set of conditions was the hydrolysis at 180°C - 1:27.5 oil-to-water ratio - 600 rpm.

Results for the variance-based sensitivity analysis are expressed by two sensitivity indices: the Sobol first order sensitivity indices S_i indicate the impor-

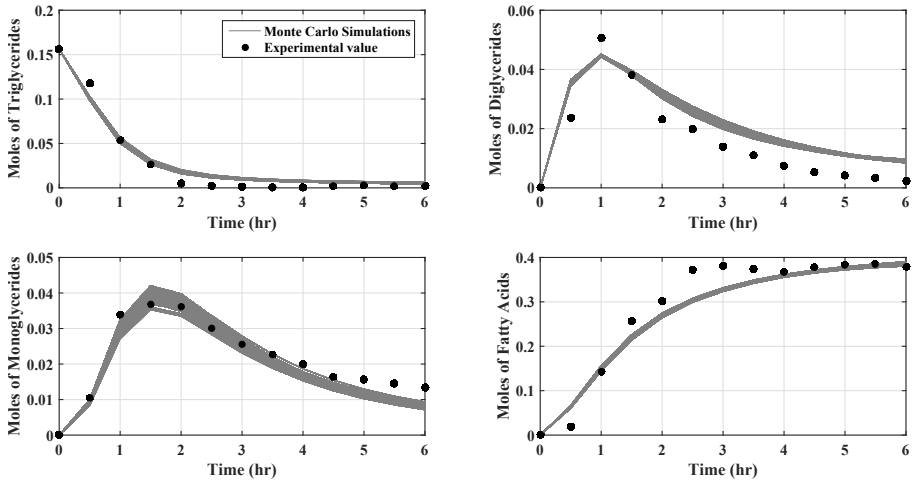

Figure 5.4: Uncertainty propagation generated from the simulations based on Monte Carlo method for the selected dataset (hydrolysis at 180°C - 1:27.5 oil-to-water molar ratio - 600 rpm) (—).

tance of each parameter considered individually, while the total sensitivity indices S_{Ti} account for both the importance of individual parameters and interactions between parameter pairs. In this study, the values of S_{Ti} are similar to S_i.

The highest sum of S_{Ti} obtained for the input parameters of n_{MG} (1.0059), as seen in Table 5.4, shows that the variations in outputs are motivated by first-order effects of the parameters, while the second-order interaction terms contribute to only 0.59% of the variance of the model output (Zubov and Sin 2018) (See also Supporting Information).

Through the analysis of the sensitivity analysis for the mean values of the validation set, it can be noticed that the consumption of n_{TG} is most influenced by kinetic parameters k_1 and k_{-1} in (Reaction 9) along with the mass transfer coefficient of water $k_{1L,a}$. It is explained by the fact that the the mass transfer of water is bound to the reaction with n_{TG}. Hence, the resulting decrease or increase in mass transfer should then affect all the model outputs. For the parameters in the reactions related to the formation and consumption of n_{DG}, the most influential parameters are k_2 and k_{-2} in (Reaction 10), while the remaining parameters are deemed irrelevant. In the case of n_{MG}, kinetic parameters k_3 and k_{-3} in (Reaction 11) have the higher impact. Con-

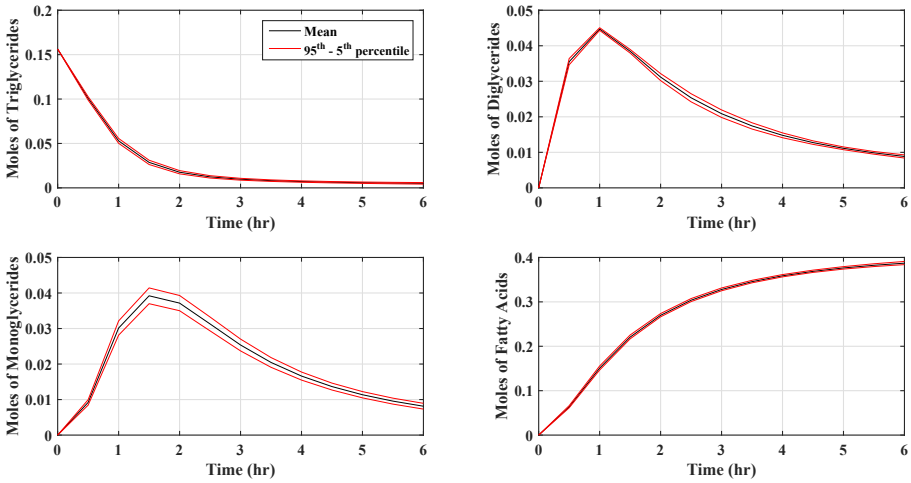

Figure 5.5: Uncertainty propagation represented by the mean (—) and the 5^{th} and 95^{th} percentiles (—) of the Monte Carlo simulations for the selected dataset (hydrolysis at 180°C - 1:27.5 oil-to-water ratio - 600 rpm).

sequently, the most important parameters related to generation of the product n_{FA} are the rate constants for forward reactions alongside the rate constants for reverse reactions (Reaction 9) - (Reaction 11). As seen in Table 5.4, the parameters k_4, k_{-4}, and $k_{2L,a}$ are little or non-influential for the model outputs coupled with the experimental data. Therefore, they can be fixed to any value within their confidence intervals without influencing the model outputs. Non-influential parameters contribute to a small percentage of the total variance, which then provide criteria for model simplification.

In Figure 5.6 and Figure 5.7, we show graphically the first order indices S_i obtained by Sobol's method of the mass transfer phenomena ($k_{1L,a}$ and $k_{2L,a}$) and the different reaction pathways (k_1 and k_{-1}, k_2 and k_{-2}, k_3 and k_{-3}, and k_4 and k_{-4}) to the measured outputs n_{TG} and n_{FA} at different time steps. Detailed data concerning the sensitivity analysis of model outputs n_{MG} and n_{DG} is available in the Supporting Information. These indices give information about the significance of each parameter, where high values indicate higher significance and *vice versa* smaller values indicate negligible or no significance. Nonetheless, total sensitivity indices S_{Ti} give information related to the first-order effects of the parameters in the the model and the mutual interactions among parameters.

Rank	Triglycerides		Diglycerides		Monoglycerides		Fatty acids	
1	k_1	0.5476	k_2	0.7355	k_3	0.6547	k_2	0.3735
2	k_{-1}	0.2339	k_{-2}	0.2149	k_{-3}	0.2185	k_3	0.1778
3	$k_{1L,a}$	0.1181	k_3	0.0234	$k_{2L,a}$	0.0591	k_1	0.1521
4	k_2	0.0671	k_{-3}	0.0073	k_2	0.0344	k_{-2}	0.1096
5	k_{-2}	0.0327	$k_{1L,a}$	0.0068	k_{-2}	0.0257	k_{-3}	0.0622
6	k_{-4}	0.0009	k_1	0.0051	$k_{1L,a}$	0.0049	$k_{1L,a}$	0.0553
7	k_3	0.0006	k_{-1}	0.0045	k_1	0.0043	k_{-1}	0.055
8	k_{-3}	0.0004	$k_{2L,a}$	0.0019	k_{-1}	0.0043	$k_{2L,a}$	0.0167
9	k_4	0.0002	k_{-4}	0.0018	k_4	0	k_4	0
10	$k_{2L,a}$	0.0001	k_4	0.0004	k_{-4}	0	k_{-4}	0
	$\sum S_i = 0.9984$		$\sum S_i = 0.9984$		$\sum S_i = 0.9939$		$\sum S_i = 0.9978$	
	$\sum S_{Ti} = 1.0016$		$\sum S_{Ti} = 1.0016$		$\sum S_{Ti} = 1.0059$		$\sum S_{Ti} = 1.0022$	

Table 5.4: Sensitivity analysis with first order Sobol indices for each model parameter for the hydrolysis at 180°C - 1:27.5 oil-to-water molar ratio - 600 rpm.

In Figure 5.6 and 5.7, we present the global sensitivity analysis results conducted as the reaction progresses. The most important insight provided by these results are the relative importance of mass transfer and kinetics parameters changes as reaction progresses. For example, in Figure 5.6, it is possible to notice that in the early stages of the reaction the consumption of n_{TG} is mainly sensitive to the rate constant for forward (Reaction 9) k_1 and the mass transfer coefficient of water $k_{1L,a}$, which both show a decreasing trend along time. In the beginning of the hydrolysis, the transfer of water from the aqueous phase to the oil phase accelerates the reacting process. As the reaction progresses, the main contributors are the kinetic parameters related to (Reaction 10) and (Reaction 11). In the case of n_{DG}, k_1, and $k_{1L,a}$, they contribute greatly to the variance at 0.5 h, where they lose their relevance as the reaction progresses. Then, the most influential parameters are the kinetic related to (Reaction 10). Their significance have an appreciable change during the reaction as seen in Figure A.2. In regards to n_{MG}, the parameters associated with the consumption and generation of n_{MG} in (Reaction 10), (Reaction 11), and (Reaction 12) present the largest variations because n_{MG} participates in more reactions of the system than all the other components. As previously mentioned, the reactions are consecutive and reversible. Hence, it is possible that every group of parameters might affect the equations which govern the model differently. When it comes to n_{FA} in Figure 5.7, the main contributors to the sensitivity, at the beginning, are rate constant for forward

(Reaction 9) and the mass transfer coefficient of water. The later is understood by the diffusion of water through the oil film to the oil phase bulk where the reaction takes place. Then, kinetic parameters related to (Reaction 9), (Reaction 10), and (Reaction 11) contribute greatly, which is explained by the fact that the mole balances involving FA do not have a mass transfer component since the generated products are assumed to remain in the oil phase, where they were generated.

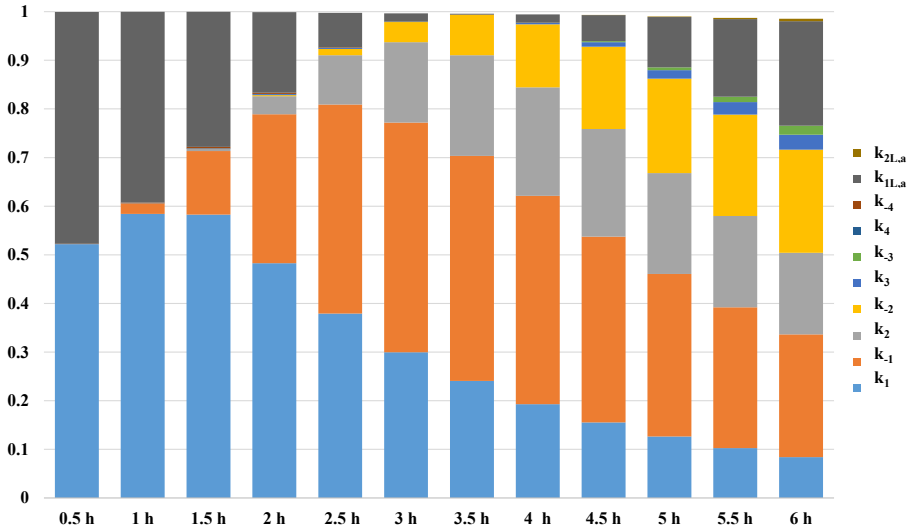

Figure 5.6: Contribution to the variations in the model output n_{TG} over time by using Sobol's sensitivity indices for the hydrolysis at 180°C - 1:27.5 oil-to-water molar ratio - 600 rpm.

A closer look to the 10 estimated parameters shows that the mass transfer phenomena ($k_{1L,a}$ and $k_{2L,a}$) and the three reaction pathways (k_1 and k_{-1} (Reaction 9), k_2 and k_{-2} (Reaction 10), k_3 and k_{-3} (Reaction 11)), are the parameters which have a relatively significant effect on all the four model outputs. The non-influential parameters indicate that at the given experimental conditions, they do not affect the measured outputs. Therefore such information can be used as input to prioritize the research areas, for example, in improving the design of experiments to estimate those parameters or in simplifying the model. This is relevant in particular when reparametrizing and recalibrating the model for different feedstock with different initial composition (e.g. palm fatty acid distillate) or operating conditions (use of catalyst).

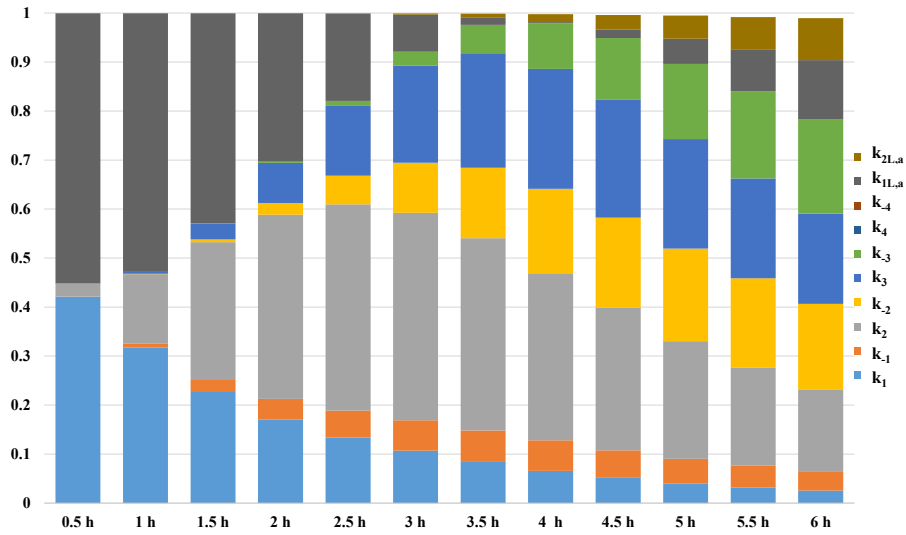

Figure 5.7: Contribution to the variations in the model output n_{FA} over time by using Sobol's sensitivity indices for the hydrolysis at 180°C - 1:27.5 oil-to-water molar ratio - 600 rpm.

The results from the uncertainty analysis showed that the parameter estimates are trustworthy given the narrow working bounds obtained in the model outputs, which is of great interest for predictive purposes. It should be mentioned that the mass transfer coefficients can change during the reaction given the change of the component fractions in the consumed and generated phases. Hence, the values for these are deemed as average. In this regard, uncertainty analysis helped to validate the assumption that the estimated parameters are constant during the reaction. For process development, these analysis are useful when choosing type and finding optimal configurations in reactors. For example the use of batch data to predict reactor configuration residence times and conversions are easy to apply and fast to use. This analysis is therefore of considerable interest to improve the understanding of design and operating variables that increase the feasibility of vegetable oil utilization. It is because they provide information that could be used to compare different modeling approaches under different operating conditions.

5.5.4 Analysis of residuals

The residuals are calculated based on the validation set (hydrolysis at 180°C, 1:27.5 oil-to-water mol ratio and 600 rpm) and are presented in Figure 5.8. The errors for n_{TG}, n_{DG}, n_{MG}, and n_{FA} stay within -0.02 and 0.02 moles. If the residuals follow a standard normal distribution and are uncorrelated, the use of the model does not yield to errors in the evaluations. The Gaussian probability plots in Figure 5.8 shows the distance of the residuals to a standard distribution. The third plot in Figure 5.8 determines if there is any information in the residuals that is not obtained when the model is evaluated. It can be seen that there are spikes in almost all plots, however, they are not significant because they do not exceed the limit set by the confidence intervals.

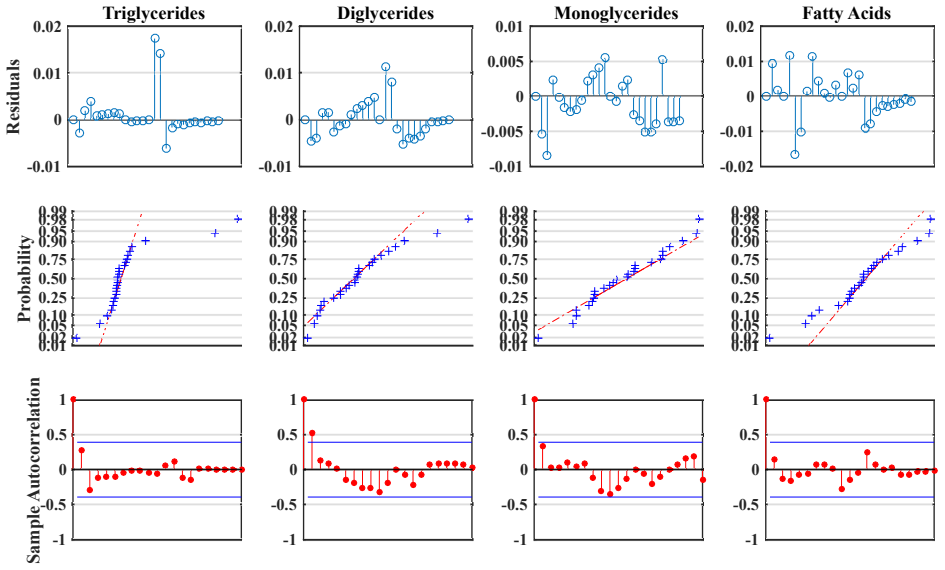

Figure 5.8: Residual analysis for the validation set (hydrolysis at 180°C, 1:27.5 oil-to-water mol ratio and 600 rpm).

5.6 Conclusions

A model describing the batch hydrolysis of rapeseed oil which includes kinetics and mass transfer at subcritical conditions is presented in this chapter. The primary objective for developing this model is to analyze experimental data collected from typical batch tests and to estimate model parameters. The

developed model was further investigated by using Monte Carlo simulations to statistically quantify the changes in the outputs obtained with the model by the action of uncertainties in the parameter estimates. To understand which parameters in the model contribute to the uncertainty, a sensitivity analysis method was used (Polynomial chaos expansions based Sobol sensitivity indices). The results from the sensitivity analysis helped to identify what parameters in the model are influential, giving insight into the robustness and predictive potential of the developed model which form the grounds for any simplification or model-based decision making for detailed process characterization, design, optimization, and operation of the hydrolysis of rapeseed oil.

CHAPTER 6

Simulation of a rapeseed oil processing plant

An important subject in chemical engineering calculations is the validation of models which accurately defines the behavior of a system. This task depends strongly upon selecting accurate estimation and simulation methods. Missing or insufficient physical properties and operating parameters can weaken the accuracy of a model or even prevent one from simulating it (Frutiger et al. 2018).

Hence, it is decisive to an effective design to find and use good values for such parameters and properties. In this way, simulation of chemical processes is a relevant validation strategy for improving property and process modeling as well as designing and optimizing the reaction and recovery of high value added products.

For design purposes, such as determining the size of reaction units or the cost of the entire separation of components, the results of a simulation should show that the estimates are trustworthy given the tight confidence intervals defined by experiments and models. This makes simulation a powerful set of tools to validate the assumptions and phenomena involved in a chemical process. An effective process simulation in the oleochemical industry must ensure:

- Upward flexibility so as to increase or decrease production capacity in order to keep pace with demand.

- Excellence in process and engineering solutions by designing and specifying the most suitable key components.

- Highly effective design using the best engineering criteria and materials.

- High yields and accurate process control.

In this chapter, the simulation of the hydrolysis of rapeseed oil is presented by using the Colgate-Emery process (Barnebey and Brown 1948). SimSci PRO/II process simulator from AVEVA Software was used to carry out this task. The objective of these simulations is to compare the production of fatty acids in subcritical medium on different flowsheet configurations by using the simplified kinetic and mass transfer model presented in chapter 4 with a base case where conversions in reactions are defined. These simulations allow the identification of the key points for the economic evaluation of each production alternative and the assessment of the economic viability of each of the technologies in different scenarios.

6.1 Preliminary considerations

A series of steps must be followed before one can proceed with the simulations. First, the chemical components which are part of the simulations need to be defined as well as the most appropriate thermodynamic method to represent the systems involved. Then, the conditions and inlet flows of the process streams are defined. Finally, calculations are performed for sizing the process equipment. The development of these steps are presented in the following sections.

6.1.1 Chemical components

Rapeseed oil and its fatty acids were treated as pseudo-components (West, Posarac, and Ellis 2008). Its boiling point and other critical properties were estimated using the group contribution method of Constantinou and Gani 1994. Such properties are compiled in the *CAPEC Lipids Database* (Diaz-Tovar, Gani, and Sarup 2011). In addition to the oil and fatty compounds mentioned, glycerol and water are present in the simulations. Both components were available in the PRO/II SimSci Bank database, hence it was not necessary to estimate any of their properties to perform this work. In the simulations, catalysts or cosolvents were not used.

The values for the critical properties, boiling point, and acentric factor for the components are shown in Table 6.1 (Diaz-Tovar, Gani, and Sarup 2011).

Property	Rapeseed oil	Fatty acids	Glycerol	Water
T_c (K)	976.675	796.760	850	647.13
P_c (kPa)	648.416	1419.857	7500	22055
V_c $\left(\frac{m^3}{kmol}\right)$	3.195	1.033	0.264	0.055948
T_b (K)	835.981	625.481	561.7	373.15
ω	0.416	0.813	0.512	0.3448
MW $\left(\frac{g}{mol}\right)$	874.822	278.826	92.093	18.015

Table 6.1: Properties of components used in simulation.

6.1.2 Thermodynamic models for simulation

Thermodynamic methods available in SimSci PRO/II were used in the simulations. This software includes a specific database for oleochemicals, with several relevant compounds such as mono-, di- and triglycerides and fatty acids. In the same way, thermodynamic models and parameters had been customized for systems which involved lipids by several authors (Diaz-Tovar, Gani, and Sarup 2011; Cunico et al. 2014).

Due to the presence of strongly polar compounds (water and glycerol), Zhang et al. 2003 recommend the use of excess Gibbs free energy methods such as Non-Random Two Liquid (NRTL) or Universal Quasi-Chemical Functional-group Activity Coefficients (UNIFAC). Moreover, these methods are recommended for systems involving high pressures and temperatures, especially under subcritical and supercritical conditions. In all the calculations the liquid-liquid equilibrium was calculated by using the modified UNIFAC-Dortmund to take into account the biphasic characteristic of the process. The calculation algorithm used in the distillation columns was *Chemdist*, which is highly useful for the distillation of strongly non-ideal mixtures (Byrne and Baird 1985).

6.1.3 Plant capacity and definition of streams

In all simulations carried out in this chapter, there were only two input streams: vegetable oil and water. These streams were fed at 25°C and 101.3 kPa. The main input stream is the feed of vegetable oil into the plant. In this work, the presence of suspended solids, metals, moisture and other compounds present in small amounts in vegetable oils was not considered. The oil stream consists only of triglycerides and fatty acids. According to Hammond et al. 2005, the fatty acids content in crude rapeseed oil usually varies between 0.3% and 0.7%

by mass (Hammond et al. 2005). Hence, an average value of 0.5% of free fatty acids for crude rapeseed oil was adopted.

In this work, a processing capacity of 12625 $\frac{kg}{h}$ of fatty acids was established, which corresponds to the average value of a mid-range oleochemical processing facility in June 2016 (BCC Research 2016). Moreover, reaction conditions of 40:1 water-to-oil molar ratio, temperature of 250°C and pressure of 4000 kPa were used in the simulations.

6.1.4 Reaction kinetics

For the reaction in the base case, as most studies in the literature indicate, a conversion of 95% of the triglycerides was considered. This is a conservative value, due to the real possibility of achieving almost-complete conversion to products. This value is an intermediate between the values adopted in other studies by A. Johnson et al. 1975 and J. King, R. Holliday, and G. List 1999.

The kinetic and mass transfer model used for simulating and comparing the process with the base case comprises three control mechanisms within the overall reaction: an initial mass transfer regime followed by irreversible pseudo second order and finally a reversible second order equilibrium reaction. Due to its heterogeneous nature, the hydrolysis of vegetable oil is affected not only by the chemical kinetics but also by the rate of mass transfer between the oil and water. This simple model, does not require complex computation of the kinetic constants, resulting in less computational time in the process simulator. Detailed information on parameters and assumptions can be found in chapter 4.

6.2 Flow-sheets and simulations

Flowsheets of the simulations for the production of fatty acids under subcritical conditions are shown in Figures 6.1 to 6.3. In this study, three scenarios were simulated. "Scenario 1" is the basic design of the plant, which does not involve heat integration, glycerol treatment or oil recycling. "Scenario 2" is the same as in the first case except for the inclusion of heat exchange systems, and "Scenario 3" involves both the heat exchanging system and the recycle of residual oil and production of technical grade glycerol. Each of these scenarios and their simulations are described below.

6.2.1 Scenario 1

Figure 6.1 shows the flowchart for the first scenario. The physical conditions and composition of all process streams can be seen in Table 6.2 and 6.3. Firstly, it is desired to place the raw materials at the temperature and pressure conditions of the reaction. The pumping of the raw materials must be done before heating to avoid cavitation in the pumps. Therefore, the vegetable oil stream feeds the pump PUMP1, which raises its pressure to the required 4000 kPa. The water feed meets the water recycle in the mixer MIX1 and its pressure is then raised to 4000 kPa by the pump PUMP2.

The stationary controller C1 is used to regulate the water inlet so as to ensure the 40:1 water-to-oil molar ratio in the reactor. The streams are then mixed in the mixer MIX2 and are heated in the heat exchanger HX1. All mixers used in this work operate adiabatically and without pressure drop. They do not necessarily have physical representation in the plant, where it only serves as a simulation feature.

In the heat exchanger HX1, the feed temperature is raised to 250°C with the aid of superheated steam. Then, the stream passes to the subcritical reactor, which operates at 250°C and 4000kPa. A reaction procedure with the kinetic equations presented in a previous session were used to calculate the overall conversion of triglycerides. The reaction products are transported to the heat exchanger HX2, where it is cooled to 80°C.

The products of reaction then pass to the distillation column COL1. One peculiarity of this column is that it can operate at atmospheric pressure due to the flow of water into the system is large. The column consists of five stages, total condenser and reflux ratio equal to 2. At the top, 99.9% of the water is recovered at a mass fraction of approximately 91%. The water is recycled to the mixer MIX1, where it meets the feed stream.

The bottom product of the column is cooled to 35°C in the heat exchanger HX3 and moves to the decanter where the crude glycerol is recovered in a purity of 86-88%. The raffinate goes to the distillation column COL2, where it is desired to place the fatty acids within the highest purity. This column was simulated with five stages, partial condenser and reflux ratio equal to 2. The column operates under vacuum so that the degradation temperature of the fatty acids is not reached at the top of the column.

Two products are formed in the column condenser. In the vapor phase, the effluent 109 is composed of water and fatty acids. In the liquid phase

the fatty acids are obtained within the specifications defined by the desired quality. The bottom stream, effluent 110, consists mostly of unreacted oil. This stream, due to the high flow rate, needs specific treatment.

6.2.2 Scenario 2

Figure 6.2 shows the flowchart for the second scenario. The physical conditions and composition of all process streams can be seen in Table 6.4 to 6.5. The only difference from this scenario with the previous is the inclusion of two additional heat exchangers, HX1A and HX1-B. In the heat exchanger HX1-A, the hot stream, which leaves the reactor in a subcritical state, is used to heat the stream of vegetable oil that feeds the plant. The specification on this heat exchanger is that minimum approach temperatures of 10°C are maintained. Therefore, the oil stream is heated to 240°C. Stream 104B, which temperature is now around 190°C, is used to heat the water stream in the HX1-B exchanger. By maintaining again the specification with respect to approach temperatures, the water stream leaves the exchanger at about 180°C. The water and oil streams are mixed in the mixer MIX2 and are heated to 250°C in the heat exchanger HX1, where they then proceed to the reactor. The product stream, already cooled, goes to the water recovery column COL1. The rest of the process is identical to the Scenario 1.

6.2.3 Scenario 3

Figure 6.3 shows the flowchart for the third scenario. The physical conditions and composition of all process streams can be seen in Table 6.6 to 6.7. The idea of this scenario is to take advantage of the benefits brought by recycling the non-consumed oil and the treatment of crude glycerol. The treatment of glycerol allows the commercialization of this as technical grade glycerol, which has a higher added value than crude glycerol. In order to recycle the oil, it is only necessary to reestablish the current pressure since the distillation column COL1 is operated under vacuum. To do this, pump PUMP3 is used. The recycled oil stream joins the vegetable oil feed in mixer MIX3. For the treatment of the glycerol after separation in the decanter a flash vessel with vacuum is used (30 kPa) at 80°C.

Stream		**Crude-oil**	**Water**	**101**	**102**	**103**
Phase		Liquid	Liquid	Liquid	Liquid	Vapor
Temperature	°C	25.0	25.0	36.9	73.3	250.0
Pressure	kPa	101.3	101.3	4000	4000	4000
Mass flow	$\frac{kg}{h}$	12636.44	2067.14	12636.44	41605.07	41605.07
Mass fraction						
Rapeseed oil		0.9950	0	0.9950	0.3022	0.3022
Free fatty acids		0.0050	0	0.0050	0.0015	0.0015
Glycerol		0	0	0	0	0
Water		0	1	0	0.6963	0.6963
Stream		**104**	**105**	**106**	**107**	**108**
Phase		Vapor	Liquid	Liquid	Liquid	Liquid
Temperature	°C	250.0	80.0	104.8	35.0	35.0
Pressure	kPa	4000	4000	111.3	111.3	111.3
Mass flow	$\frac{kg}{h}$	41605.16	41605.16	14703.69	14703.69	13286.5
Mass fraction						
Rapeseed oil		0.0151	0.0151	0.0428	0.0428	0.0473
Free fatty acids		0.3038	0.3038	0.8597	0.8597	0.9514
Glycerol		0.0301	0.0301	0.0851	0.0851	0.0001
Water		0.651	0.651	0.0125	0.0125	0.0012
Stream		**109**	**110**	**201**	**202**	**203**
Phase		Vapor	Liquid	Liquid	Liquid	Liquid
Temperature	°C	121.8	104.0	78.2	74.7	83.2
Pressure	kPa	10.0	20.0	101.3	101.3	4000
Mass flow	$\frac{kg}{h}$	4.39	657.12	26901.47	28968.63	28968.63
Mass fraction						
Rapeseed oil		0	0.9567	0	0	0
Free fatty acids		0.0153	0.0433	0	0	0
Glycerol		0.0031	0	0	0	0
Water		0.9816	0	1	1	1
Stream		**Glycerol**	**Fatty acids**			
Phase		Liquid	Liquid			
Temperature	°C	35	121.8			
Pressure	kPa	111	13			
Mass flow	$\frac{kg}{h}$	1417.18	12625			
Mass fraction						
Rapeseed oil		0	0			
Free fatty acids		0	0.9990			
Glycerol		0.8814	0.0001			
Water		0.1186	0.0009			

Table 6.2: Information of process streams for Scenario 1 - **Base case**.

Stream		**Crude-oil**	**Water**	**101**	**102**	**103**
Phase		Liquid	Liquid	Liquid	Liquid	Vapor
Temperature	°C	25.0	25.0	37.6	74.3	250.0
Pressure	kPa	101.3	101.3	4000	4000	4000
Mass flow	$\frac{kg}{h}$	12594.36	2141.89	12594.36	42717.84	42717.84
Mass fraction						
Rapeseed oil		0.9950	0	0.9950	0.2801	0.2801
Free fatty acids		0.0050	0	0.0050	0.0147	0.0147
Glycerol		0	0	0	0	0
Water		0	1	0	0.7052	0.7052
Stream		**104**	**105**	**106**	**107**	**108**
Phase		Vapor	Liquid	Liquid	Liquid	Liquid
Temperature	°C	250.0	80.0	104.8	35.0	35.0
Pressure	kPa	4000	4000	111.3	111.3	111.3
Mass flow	$\frac{kg}{h}$	42717.19	42717.19	14736.18	14736.18	13307.81
Mass fraction						
Rapeseed oil		0.014	0.014	0.0406	0.0406	0.045
Free fatty acids		0.2968	0.2968	0.8604	0.8604	0.9527
Glycerol		0.0289	0.0289	0.0837	0.0837	0.005
Water		0.6604	0.6604	0.0153	0.0153	0.0018
Stream		**109**	**110**	**201**	**202**	**203**
Phase		Vapor	Liquid	Liquid	Liquid	Liquid
Temperature	°C	185.2	104.0	78.5	75.1	83.3
Pressure	kPa	10.0	20.0	101.3	101.3	4000
Mass flow	$\frac{kg}{h}$	65.96	616.85	27981.61	30123.48	30123.48
Mass fraction						
Rapeseed oil		0	0.9698	0	0	0
Free fatty acids		0.5876	0.0302	0	0	0
Glycerol		0.0693	0	0	0	0
Water		0.3431	0	1	1	1
Stream		**Glycerol**	**Fatty acids**			
Phase		Liquid	Liquid			
Temperature	°C	34.8	181.6			
Pressure	kPa	110.3	12.0			
Mass flow	$\frac{kg}{h}$	1428.37	12625			
Mass fraction						
Rapeseed oil		0	0			
Free fatty acids		0.0001	0.9997			
Glycerol		0.8581	0.0002			
Water		0.1418	0.0001			

Table 6.3: Information of process streams for Scenario 1 - **Kinetic/Mass transfer model**.

Stream		**Crude-oil**	**Water**	**101**	**101B**	**102**
Phase		Liquid	Liquid	Liquid	Liquid	Vapor
Temperature	°C	25.0	25.0	36.9	240	213.9
Pressure	kPa	101.3	101.3	4000	4000	4000
Mass flow	$\frac{kg}{h}$	12636.44	2066.64	12636.44	12636.44	23667.47
Mass fraction						
Rapeseed oil		0.9950	0	0.9950	0.9950	0.5312
Free fatty acids		0.0050	0	0.0050	0.0050	0.0027
Glycerol		0	0	0	0	0
Water		0	1	0	0	0.4661
Stream		**103**	**104**	**104B**	**105**	**106**
Phase		Vapor	Vapor	Liquid	Liquid	Liquid
Temperature	°C	250.0	250.0	190.8	119	104.8
Pressure	kPa	4000	4000	4000	4000	111.3
Mass flow	$\frac{kg}{h}$	41607.29	41607.38	41607.33	41607.33	14703.66
Mass fraction						
Rapeseed oil		0.3022	0.0151	0.0151	0.0151	0.0428
Free fatty acids		0.0015	0.3038	0.3038	0.3038	0.8597
Glycerol		0	0.0301	0.0301	0.0301	0.0851
Water		0.6966	0.6511	0.6511	0.6511	0.0125
Stream		**107**	**108**	**109**	**110**	**201**
Phase		Liquid	Liquid	Vapor	Liquid	Liquid
Temperature	°C	35	35	121.8	104.0	78.2
Pressure	kPa	111.3	111.3	10	20	101.3
Mass flow	$\frac{kg}{h}$	14703.66	13286.5	4.39	657.2	26903.68
Mass fraction						
Rapeseed oil		0.0428	0.0473	0	0.9567	0
Free fatty acids		0.8597	0.9514	0.0153	0.0433	0
Glycerol		0.0851	0.0001	0.0031	0	0
Water		0.0125	0.0012	0.9816	0	1
Stream		**202**	**203**	**203B**	**Glycerol**	**Fatty acids**
Phase		Liquid	Liquid	Liquid	Liquid	Liquid
Temperature	°C	74.8	83.2	280.8	35	121.8
Pressure	kPa	101.3	4000	4000	111.3	10
Mass flow	$\frac{kg}{h}$	28790.85	28790.85	28790.85	1417.15	12625
Mass fraction						
Rapeseed oil		0	0	0	0	0
Free fatty acids		0	0	0	0	0.999
Glycerol		0	0	0	0.8814	0.0001
Water		1	1	1	0.1186	0.009

Table 6.4: Information of process streams for Scenario 2 - **Base case**.

Stream		**Crude-oil**	**Water**	**101**	**101B**	**102**
Phase		Liquid	Liquid	Liquid	Liquid	Mixed
Temperature	°C	25.0	25.0	37.6	240	212.1
Pressure	kPa	101.3	101.3	4000	4000	4000
Mass flow	$\frac{kg}{h}$	12594.36	2141.56	12594.36	12594.36	26717.96
Mass fraction						
Rapeseed oil		0.9950	0	0.9950	0.9950	0.4652
Free fatty acids		0.0050	0	0.0050	0.0050	0
Glycerol		0	0	0	0	0
Water		0	1	0	0	0.5348
Stream		**103**	**104**	**104B**	**105**	**106**
Phase		Vapor	Vapor	Liquid	Liquid	Liquid
Temperature	°C	250.0	250.0	188.7	144.2	90.9
Pressure	kPa	4000	4000	4000	4000	111.3
Mass flow	$\frac{kg}{h}$	42722.08	42722.04	42722.12	42722.12	14736.23
Mass fraction						
Rapeseed oil		0.2801	0.014	0.014	0.014	0.0406
Free fatty acids		0	0.2968	0.2968	0.2968	0.8604
Glycerol		0	0.0289	0.0289	0.0289	0.0837
Water		0.7052	0.6603	0.6603	0.6603	0.0154
Stream		**107**	**108**	**109**	**110**	**201**
Phase		Liquid	Liquid	Vapor	Liquid	Liquid
Temperature	°C	35	35	185.2	104.0	78.5
Pressure	kPa	111.3	111.3	10	20	101.3
Mass flow	$\frac{kg}{h}$	14736.23	13307.81	65.96	616.85	27985.89
Mass fraction						
Rapeseed oil		0.0406	0.0450	0	0.9698	0
Free fatty acids		0.8604	0.9527	0.5875	0.0302	0
Glycerol		0.0837	0.0005	0.0693	0	0
Water		0.0154	0.0018	0.3432	0	1
Stream		**202**	**203**	**203B**	**Glycerol**	**Fatty acids**
Phase		Liquid	Liquid	Liquid	Liquid	Liquid
Temperature	°C	75.1	83.3	248.8	35	185.2
Pressure	kPa	101.3	4000	4000	111.3	10
Mass flow	$\frac{kg}{h}$	30127.72	30127.72	30127.72	1428.42	12625
Mass fraction						
Rapeseed oil		0	0	0	0	0
Free fatty acids		0	0	0	0.0001	0.9997
Glycerol		0	0	0	0.8581	0.0002
Water		1	1	1	0.1418	0.0001

Table 6.5: Information of process streams for Scenario 2 - **Kinetic/Mass transfer model**.

Stream		**Crude-Oil**	**Water**	**101**	**101B**	**102**
Phase		Liquid	Liquid	Liquid	Liquid	Mixed
Temperature	°C	25	25	63.2	240	217.6
Pressure	kPa	101.3	101.3	4000	4000	4000
Mass flow	$\frac{kg}{h}$	11980.90	2062.49	12636.72	12636.72	25212.14
Mass fraction						
Rapeseed oil		0.995	0	0.993	0.993	0.4977
Free fatty acids		0.005	0	0.0069	0.0069	0.0035
Glycerol		0	0	0	0	0
Water		0	1	0	0	0.4988
Stream		**103**	**104**	**104B**	**105**	**106**
Phase		Vapor	Vapor	Liquid	Liquid	Liquid
Temperature	°C	250	250	194.6	119.4	104.8
Pressure	kPa	4000	4000	4000	4000	111.3
Mass flow	$\frac{kg}{h}$	41550.47	41550.56	41550.35	41550.35	14699.29
Mass fraction						
Rapeseed oil		0.302	0.0151	0.0151	0.0151	0.0427
Free fatty acids		0.0021	0.3042	0.3042	0.3042	0.8599
Glycerol		0	0.03	0.03	0.03	0.0849
Water		0.6959	0.6506	0.6506	0.6506	0.0125
Stream		**107**	**108**	**109**	**110**	**110B**
Phase		Liquid	Liquid	Vapor	Liquid	Liquid
Temperature	°C	35	35	121.8	200	200
Pressure	kPa	111.3	111.3	10	20	101.3
Mass flow	$\frac{kg}{h}$	14699.29	13285.2	4.38	655.82	655.82
Mass fraction						
Rapeseed oil		0.0427	0.0472	0	0.9567	0
Free fatty acids		0.8599	0.9515	0.0153	0.0433	0
Glycerol		0.0849	0.0001	0.0031	0	0
Water		0.0125	0.0012	0.9816	0	1
Stream		**110C**	**111**	**201**	**202**	**203**
Phase		Liquid	Vapor	Vapor	Liquid	Liquid
Temperature	°C	51.9	80	78.2	74.8	83.2
Pressure	kPa	101.3	30	101.3	101.3	4000
Mass flow	$\frac{kg}{h}$	12636.72	166	26851.06	26913.76	26913.76
Mass fraction						
Rapeseed oil		0.993	0	0	0	0
Free fatty acids		0.0069	0	0	0	0
Glycerol		0	0.0009	0	0	0
Water		0	0.9991	1	1	1
Stream		**203B**	**Crude-Gly**	**Glycerol**	**Fatty acids**	
Phase		Liquid	Liquid	Liquid	Liquid	
Temperature	°C	184.6	35	80	121.8	
Pressure	kPa	4000	111.3	30	10	
Mass flow	$\frac{kg}{h}$	28913.76	1414.09	1248.09	12625	
Mass fraction						
Rapeseed oil		0	0	0	0	
Free fatty acids		0	0	0	0.999	
Glycerol		0	0.8816	0.9987	0.0001	
Water		1	0.1184	0.0013	0.0009	

Table 6.6: Information of process streams for Scenario 3 - **Base case**.

Stream		**Crude-Oil**	**Water**	**101**	**101B**	**102**
Phase		Liquid	Liquid	Liquid	Liquid	Mixed
Temperature	°C	25	25	62.4	240	213.9
Pressure	kPa	101.3	101.3	4000	4000	4000
Mass flow	$\frac{kg}{h}$	11979.92	2139.45	12597.55	12597.55	26501.4
Mass fraction						
Rapeseed oil		0.995	0	0.951	0.951	0.452
Free fatty acids		0.005	0	0.049	0.049	0.0233
Glycerol		0	0	0	0	0
Water		0	1	0	0	0.541
Stream		**103**	**104**	**104B**	**105**	**106**
Phase		Vapor	Vapor	Liquid	Liquid	Liquid
Temperature	°C	250	250	192.1	144.3	91.1
Pressure	kPa	4000	4000	4000	4000	111.3
Mass flow	$\frac{kg}{h}$	42760.07	42760.02	42760.06	42760.06	14736.34
Mass fraction						
Rapeseed oil		0.2802	0.014	0.014	0.014	0.0406
Free fatty acids		0.0004	0.2965	0.2965	0.2965	0.8604
Glycerol		0	0.0289	0.0289	0.0289	0.0838
Water		0.7054	0.6606	0.6606	0.6606	0.0152
Stream		**107**	**108**	**109**	**110**	**110B**
Phase		Liquid	Liquid	Vapor	Liquid	Liquid
Temperature	°C	35	35	185.3	200	200
Pressure	kPa	111.3	111.3	10	20	101.3
Mass flow	$\frac{kg}{h}$	14736.34	13308.58	65.95	617.63	617.63
Mass fraction						
Rapeseed oil		0.0406	0.045	0	0.9698	0.9698
Free fatty acids		0.8604	0.9527	0.5888	0.0302	0.0302
Glycerol		0.0838	0.0005	0.0697	0	0
Water		0.0152	0.0018	0.3422	0	0
Stream		**110C**	**111**	**201**	**202**	**203**
Phase		Liquid	Vapor	Vapor	Liquid	Liquid
Temperature	°C	50.3	80	78.5	75.1	83.3
Pressure	kPa	101.3	30	101.3	101.3	4000
Mass flow	$\frac{kg}{h}$	12597.55	199.71	28023.71	30162.51	30162.51
Mass fraction						
Rapeseed oil		0.951	0	0	0	0
Free fatty acids		0.049	0	0	0	0
Glycerol		0	0	0	0	0
Water		0	1	1	1	1
Stream		**203B**	**Crude-Gly**	**Glycerol**	**Fatty acids**	
Phase		Liquid	Liquid	Liquid	Liquid	
Temperature	°C	182.1	35	80	185.3	
Pressure	kPa	4000	111.3	30	10	
Mass flow	$\frac{kg}{h}$	30162.51	1427.76	1228.05	12625	
Mass fraction						
Rapeseed oil		0	0	0	0	
Free fatty acids		0	0.0001	0	0.9997	
Glycerol		0	0.8595	0.9982	0.0002	
Water		1	0.1404	0.0008	0.0001	

Table 6.7: Information of process streams for Scenario 3 - **Kinetic/Mass transfer model**.

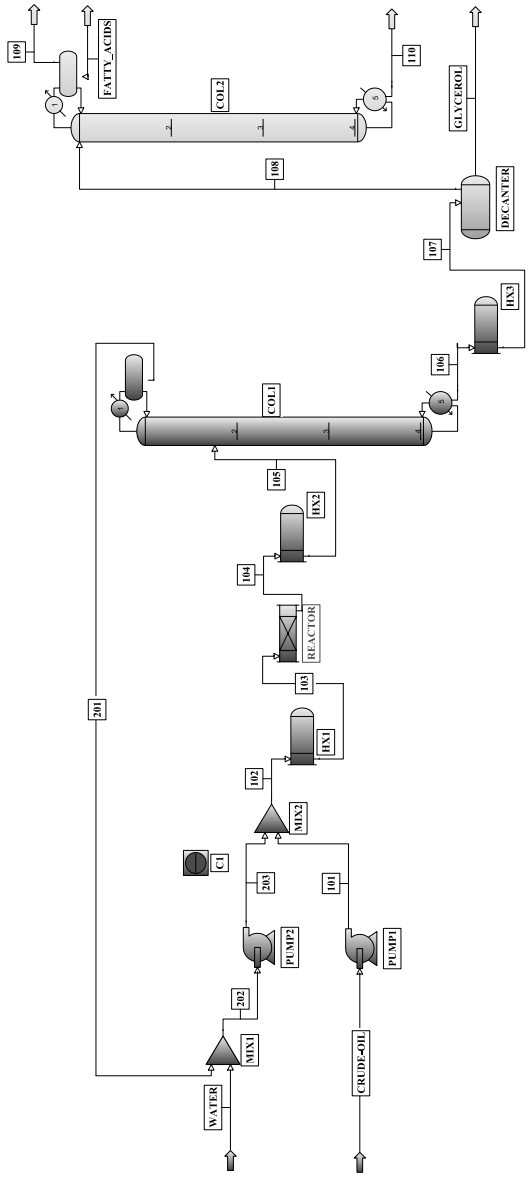

Figure 6.1: Flowsheet of Scenario 1 for the production of fatty acids.

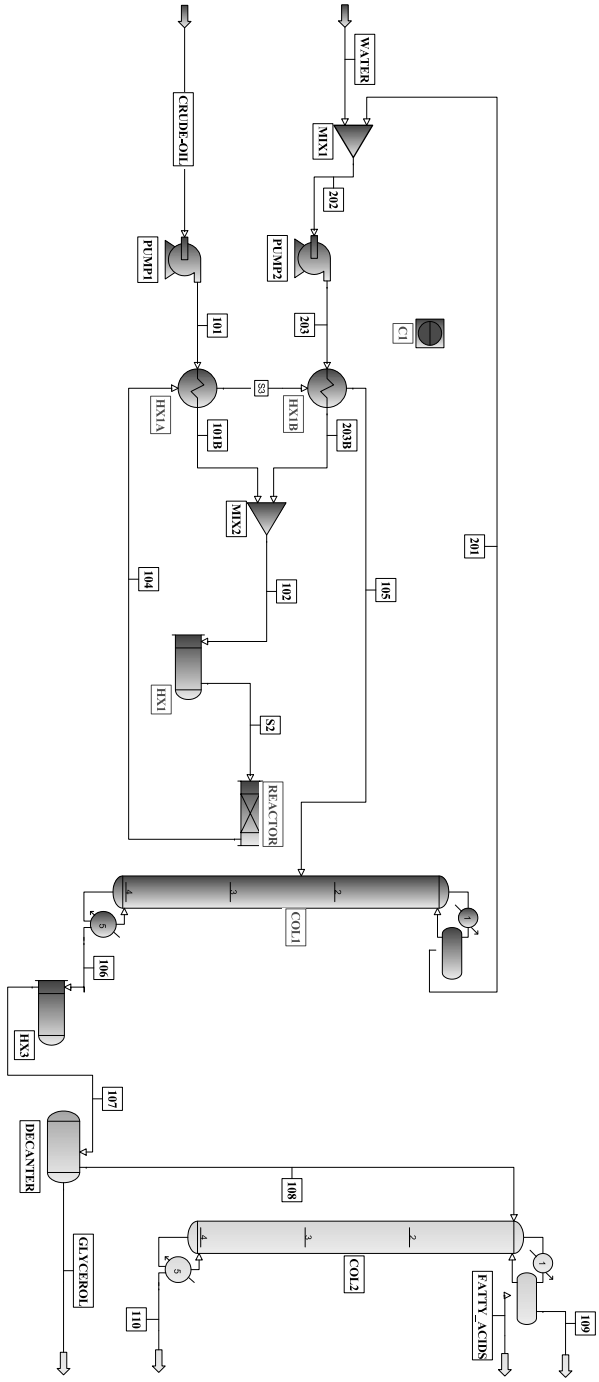

Figure 6.2: Flowsheet of Scenario 2 for the production of fatty acids.

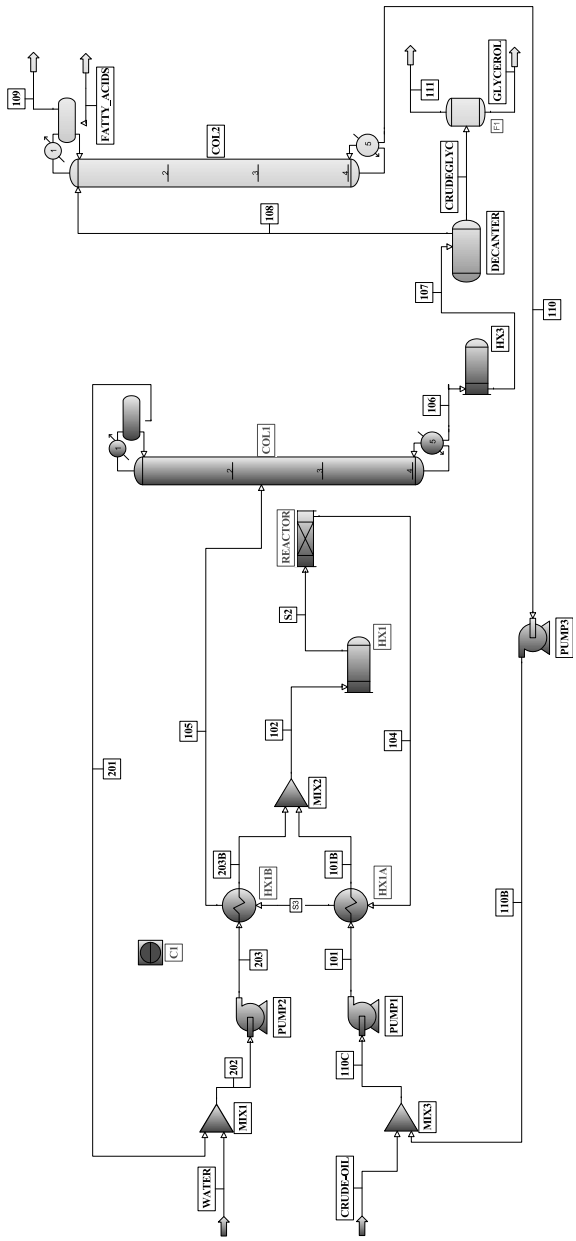

Figure 6.3: Flowsheet of Scenario 3 for the production of fatty acids.

6.3 Sizing of equipment

6.3.1 Reactors

In order to size a reactor it is necessary to know the conversion attained or the kinetics of reaction. Rate equations in the form of power laws with different reaction orders and the same rate constant can result in reactors of very different volumes. Hence, a conversion of 95% for the base case and a simplified kinetic and mass transfer model (discussed in chapter 4) were implemented in SimSci Pro/II for every scenario (Forero-Hernandez et al. 2017).

The subcritical reactor was simulated as a PFR (Plug Flow Reactor). As discussed in the literature, tubular reactors are widely used for reactions in subcritical and supercritical media. For the sizing of this type of reactor, a molar balance for the triglycerides is given by Equation (6.1):

$$F_{TG0} - (F_{TG0} + \mathrm{d}F_{TG}) - r_{TG}\mathrm{d}V = 0 \tag{6.1}$$

Where F_{TG} is the mole flow rate of triglycerides $\left(\frac{mole}{min}\right)$, F_{TG0} is the initial mole flow rate of triglycerides $\left(\frac{mole}{min}\right)$, r_{TG} is the reaction rate of triglycerides $\left(\frac{mole}{L \cdot min}\right)$ and V is the volume (L).

Equation (6.1) can be simplified as:

$$-\mathrm{d}F_{TG} = -r_{TG}\mathrm{d}V \tag{6.2}$$

The molar flow rate of triglycerides at a given time can be determined from the initial molar flow and conversion:

$$-\mathrm{d}F_{TG} = -F_{TG0}\mathrm{d}X_{TG} = -\upsilon C_{TG0}\mathrm{d}X_{TG} \tag{6.3}$$

Where X_{TG} is the conversion of triglycerides, C_{TG0} the initial concentration of triglycerides $\left(\frac{mole}{L}\right)$ and υ the volumetric flow rate in the reactor $\left(\frac{L}{min}\right)$.

Replacing Equation (6.3) in (6.2):

$$\mathrm{d}V = \frac{\upsilon\ C_{TG0}\ \mathrm{d}X_{TG}}{-r_{TG}} \tag{6.4}$$

If one uses the kinetic expression for the consumption of triglycerides presented in chapter 4, the term $-r_{TG}$ takes the form of Equation :

$$\begin{aligned} -r_{TG} =& k_{1La}\left(1 - X_{TG}\right) - k_{\text{pseudo}} C_{TG0}\left(1 - X_{TG}\right)^2 \\ &+ k_1 C_{TG0}\left(1 - X_{TG}\right)\left(\frac{C_{TG0}}{C_{W0}} - 3X_{TG}\right) - 3k_2 C_{TG0} X_{TG}^2 \end{aligned} \tag{6.5}$$

When one substitutes Equation (6.5) into Equation (6.4) and integrate it over the entire length of the reactor, it is possible to obtain an expression for the volume of reaction. The volume of the reactor can then be calculated from the value established by the kinetics, from the value obtained in the simulator to the volumetric flow rate and the value obtained in the literature for the kinetic constant.

For the hydrolysis of rapeseed oil, knowing that the volumetric flow obtained in SimSci PRO/II was equal to 2041.46 $\left(\frac{L}{min}\right)$ and using the values obtained for the kinetic and mass transfer parameters, it is possible to calculate a volume of $61.15m^3$ in the base case using a fixed value for the conversion and $48.5m^3$ for the simulations using the developed model.

For the hydrolysis of rapeseed oil, when it is known that the volumetric flow obtained in SimSci PRO/II was equal to 2041.46 $\left(\frac{L}{min}\right)$ and when the values obtained for the kinetic and mass transfer parameters are used, it is possible to calculate a volume of $61.15m^3$ in the base case. The aforementioned is possible by using a fixed value for the conversion and $48.5m^3$ for the simulations, through the use of the developed model.

The reactor was designed as a horizontal vessel with a length to diameter ratio of 3:1. 316 stainless steel was used for the reactor walls, due to the high temperatures and operating pressures (West, Posarac, and Ellis 2008). Due to the high flow rates, the horizontal character of the flow and the subcritical state of the reaction medium, the presence of mixers was not considered necessary. All reactors are accompanied by a stainless steel coil for temperature control.

6.3.2 Distillation columns

All distillation columns were designed as packed columns. For water separation columns (COL1) and for fatty acids purification (COL2), packing is

required because of the high viscosity of the components involved in the process. These columns were designed with 2-in Pall rings because they were wide and contained a small number of theoretical stages. Leva's method was used for the calculation of the diameter of the columns, which is the same used by West, Posarac, and Ellis 2008. The column diameter can be estimated empirically from the flooding velocity, as shown in Equation (6.6).

$$D = \sqrt{\frac{4G}{fU_f \pi \rho_G}} \tag{6.6}$$

Where G is the mass flow rate of vapor $\left(\frac{kg}{s}\right)$, f an empiric factor equal to 0.7, U_f the flooding rate $\left(\frac{ft}{s}\right)$ and (ρ_G) the density of the vapor phase $\left(\frac{kg}{ft^3}\right)$.

The correlation of Leva to calculate the flooding velocity is given by Equations (6.7)–(6.11):

$$Y = \exp\left(3.7121 - 1.0371\left(\ln F_{LG}\right) - 0.1501\left(\ln F_{LG}\right)^2 - 0.007544\left(\ln F_{LG}\right)^3\right) \tag{6.7}$$

$$F_{LG} = \frac{L}{G}\left(\frac{\rho_G}{\rho_L}\right)^{\frac{1}{2}} \tag{6.8}$$

$$Y = \frac{U_f^2\, F_P}{g}\rho_G f\left(\rho_L\right) f\left(\mu_L\right) \tag{6.9}$$

$$f\left(\rho_L\right) = -0.8787 + 2.6776\left(\frac{1}{\rho_L}\right) - 0.6313\left(\frac{1}{\rho_L}\right)^2 \tag{6.10}$$

$$f\left(\mu_L\right) = 0.96\mu_L^{0.19} \tag{6.11}$$

Where L is the liquid mass rate $\left(\frac{kg}{s}\right)$, ρ_L the liquid phase density $\left(\frac{kg}{ft^3}\right)$, μ_L the liquid phase viscosity (cP), g the gravity $\left(g = 32.2\frac{ft}{s^2}\right)$ and F_P is the packing factor, relative to the type of packing $\left(\frac{ft}{ft^3}\right)$

For 1-in metal Pall rings, the packing factor is equal to 56 $\frac{ft}{ft^3}$. For 2-in metal Pall rings, the packing factor is 27 $\frac{ft}{ft^3}$. The values for the mass flow rates of the liquid phase and the vapor phase, as well as density and viscosity, were obtained directly from the simulator. All values obtained were within the validity range of the formulas used (Seader, Seider, and Lewin 2004).

Ideally, the diameter of a distillation column should be calculated for each stage. However, because the work has only a preliminary estimate of costs, it was decided to express the diameter of the columns as the mean of the top, middle and bottom diameters, and only information on three or four theoretical plates.

In order to determine the height of the distillation columns, the theoretical plate equivalent height (HETP) was used. All columns are designed by assuming 50% efficiency at all stages, except the condenser and the boiler. To obtain the HETP value for the two types of packing, the empirical formulas presented by Seader, Seider, and Lewin 2004 were used. For distillation column COL1 which works with more viscous fluids and for column COL2 which operates under vacuum, Equation (6.12) was used.

$$\text{HETP} = 1.5D_P + 0.5 \tag{6.12}$$

Where HETP is the height equivalent to a theoretical plate (ft) and D_P is the nominal diameter of the packing used (in).

The height of the packed volume is obtained by multiplying the HETP by the number of equilibrium stages, except condenser and reboiler. The total height of the columns was obtained by adding the height of the packed volume to three quarters of the diameter for the condenser and an entire diameter for the boiler.

6.3.3 Flash columns

The flash vessel FLASH1 was calculated according to the methodology presented by Towler and Sinnott 2012. According to the authors, the vessel diameter should be large enough so as the velocity of the gas phase is reduced below the rate of separation of the liquid droplets. The calculation of the diameter can be done with Equation (6.13).

$$D = \sqrt{\frac{4G}{\pi u_s}} \tag{6.13}$$

Where G is the volumetric flow rate $\left(\frac{m^3}{s}\right)$, u_s is the separation velocity of the liquid droplets $(\frac{m}{s})$.

The separation velocity of the liquid droplets can be obtained by Equation (6.14).

$$u_s = 0.07 \left(\frac{\rho_L - \rho_G}{\rho_G}\right)^2 \tag{6.14}$$

Where ρ_L and ρ_G are the liquid and vapor densities respectively $\left(\frac{kg}{m^3}\right)$.

Once the diameter is determined, sufficient height should be provided above the vessel entrance so that the liquid droplets can separate. Towler and Sinnott 2012 recommend to use a height equal to the diameter with a minimum of one meter. The vessel entrance should be situated at a height of half a diameter above the liquid level with a minimum of 60 cm. The authors also recommend a time of 10 minutes for holdup of liquid in the vessel (Towler and Sinnott 2012). From this time and by knowing the vessel diameter and the liquid outlet flow obtained in the simulator, it is possible to calculate the height of the liquid phase in the vessel. FLASH1 is set to be built with carbon steel because there is no presence of highly corrosive materials.

6.3.4 Decanter

The decanter is designed in carbon steel and horizontal configuration with a length to diameter ratio of 4:1. The decanting area of the decanters is calculated to provide 1 ft^2 for each 5 $\frac{gal}{min}$ of feed which follows the instructions of Seader, Seider, and Lewin 2004, and it is taken into consideration that the liquid phase occupies half the volume of the vessel (Seader, Seider, and Lewin 2004).

6.3.5 Heat exchangers

Heat exchanger with a heat exchange area greater than 200 ft were designed as floating head, shell and tube. The heat exchangers with an area below 200

ft were designed as tube-in-tube exchangers (Seader, Seider, and Lewin 2004). Condensers and column distillation columns were considered as common heat exchangers which follow the same type of approach for their initial design. As for flash vessels and reactors, stainless steel coils were used to provide heat. For a preliminary estimate of the sizing of the exchangers, the only required dimension was the area of thermal exchange which can easily be obtained by Equation (6.15).

$$Q = U A_\tau \Delta T_{LM} \tag{6.15}$$

Where Q is the heat transfer rate, U is the overall heat transfer coefficient, A_τ the area of heat exchange and ΔT_{LM} the logarithmic mean temperature difference.

The heat transfer rate was obtained directly from the process simulator. The global heat transfer coefficient, which depends heavily on the equipment and materials involved in the thermal exchange, must be obtained in practice or, for a preliminary design, values from the literature. The values used in this work were extracted from Seader, Seider, and Lewin 2004, who made a collection of experimental data published by several authors (Seader, Seider, and Lewin 2004). The values used in flash vessels, reactors, condensers and reboilers can be seen in Table 6.8.

Equipment	**Operation**	**Material**	**U** $\left(\frac{BTU}{^\circ F\ hr\ ft^2}\right)$
Reactor			
Subcritical	Heat	Fatty acids	60
Flash vessel			
FLASH1	Heat	Organic mixture	50
Condensers			
COL1	Cold	Water vapor	20
COL2	Cold	Fatty acids	100
COL3	Cold	Water vapor	100
Reboilers			
COL1	Heat	Fatty acids	200
COL2	Heat	Rapeseed oil	200
COL3	Heat	Aqueous mixture	250

Table 6.8: Overall heat transfer coefficients in equipment.

As for the utilities, for the heating of all the equipment, except the subcritical reactor and the column COL2 column, saturated steam at 400 psi was

used in which temperature is approximately 229.2°C. In these conditions, the enthalpy of vaporization is approximately 1.816 $\frac{kJ}{kg}$.

For cooling, common water was used entering at 25°C and exiting at 35°C. Heat exchangers are commonly constructed solely of carbon steel.

6.4 Economic evaluation

The economic evaluation proposed in this work consists of the calculation of the investment necessary for the construction of the plants for the given scenarios, the production costs associated with the production of fatty acids, the revenue from a given economic scenario and comparison of the different plants from certain economic criteria.

This approach can be called a *study estimate* (Lemmens 2016). This analysis depends on the construction of a flow chart for the analyzed process, the solution of the mass and energy balances involved and the prior design of the equipment. However, this is not an accurate method of economic evaluation. It is only a preliminary step, but it may well be used to compare different processes (Turton et al. 2008).

As explained before, the production plants were simulated with a production capacity of 12625 $\frac{kg}{h}$, which is corresponding to the average mass capacity of a middle range oleochemical processing plant. All costs were estimated based on an operating factor of 7920 $\frac{h}{year}$, which corresponds to 330 working days (about 90% of the days of the year).

The economic scenarios considered in this work allows a real comparison between the study cases. All prices for reactants, products and utilities were found in open literature and are summarized in Table 6.9.

Raw materials and Products	**Price**	**Utilities**	**Price**
Rapeseed oil	0.879	Superheated steam	0.01
Water	0.00103	Vapor 400 psi	0.0015
Fatty acids	1.15	Cooling water	0.00103
Glycerol (>98%)	0.79	Electricity (US$/KWh)	0.1375
Crude glycerol	0.33	Waste treatment	0.15

Table 6.9: Prices of the components involved in the processes (US$/kg).

6.4.1 Investment

The method used in this work to estimate the total investment required for the construction of a new fatty acids production plant was the Lang method. According to Seader, Seider, and Lewin 2004, the method has a degree of uncertainty of ±35%. The first step is to obtain the purchase price of each equipment. This can be obtained, for a *study estimate*, from empirical formulas available in the literature. As these formulas were produced for a certain year, it is necessary to update the prices of the equipment for the current reality. This can be done through the application of the Chemical Engineering Plant Cost Index (Hameed, Lai, and Chin 2009; Garrett 2012).

When one adds all the purchase prices together, it is possible to obtain the total purchase price of the equipment. The total value is multiplied by 1.05 to take into account the transport of the equipment to the plant site. Then, the result is multiplied by the Lang factor (f_L) to obtain the fixed investment. Equation (6.16) summarizes each of these steps.

$$I_F = 1.05 f_L \sum_i \left(\frac{PCI}{PCI_b} \right) C_i \tag{6.16}$$

Where f_L is the Lang factor, PCI the Plant Cost Index for the selected year, PCI_b Plant Cost Index for the reference year and C_i the purchasing of equipment i.

The Lang factor is used to take into account installation, instrumentation and control costs, plumbing, power grid, OSBL (Outside Battery Limits), land acquisition, construction and engineering costs, and fees involved. For a plant that operates only with liquids, the Lang factor is equal to 4.8. To reach the total investment, the fixed investment is added to the working capital,which is estimated at 15% of the total investment.

All equipment acquisition prices were extracted from Seader, Seider, and Lewin 2004 and refer to the middle of the year 2004 ($\text{PCI}_b = 394$) Seader, Seider, and Lewin 2004. The authors made a collection of a series of works available in the literature and created empirical formulas of price estimate of these equipment by interpolation of the data found. The formulas used to estimate the cost of equipment in this work are shown in the following sections. All values were updated for the first half of 2018 through the application of a PCI equal to 571.5.

More details on the sizing and costing of equipment can be found in the Supporting Information.

6.4.2 Production costs

The total cost of production is the cost related to the day-to-day operation of a plant. This cost can be divided into three categories: direct costs, indirect costs and overhead costs (Turton et al. 2008). Direct costs of production include the cost of raw material, operating labor cost, technical supervision, utilities, disposal of effluents, maintenance, operational suppliers, and royalties for patents and innovations. The costs for the raw materials are obtained from the flows used in the plants and the price of each material, according to Table 6.9.

The cost of raw materials is calculated from the reactor volume and the density of the feed stream. The multiplication of these values is an approximation of the mass of material inside the reactor, according to Equation (6.17).

$$m = \rho V \tag{6.17}$$

Where m is the mass of both reactants and products in the reactor (kg), ρ is the density of inlet streams to the reactor $\left(\frac{kg}{m^3}\right)$, and V is the reactor volume (m^3).

The operating labor cost can be obtained from an estimate of the number of workers required in the plant, in turn, which in turn can be done through Equation (6.17).

$$N_{OP} = \left(6.29 + 31.7P^2 + 0.23N_{NP}\right)^{0.5} \tag{6.18}$$

In this equation, P is the number of processes which involves transport, distribution, removal or control of solids formation. Furthermore, N_{NP} is the number of equipment that does not involve the handling of particulate solids, which includes columns, reactors and heat exchangers. Pumps and vessels generally do not enter this count (Turton et al. 2008). The operating labor cost is obtained by multiplying the number of workers per shift by the factor of operation and by the wage of each worker, which in this work was considered equal to US$5 per hour. The other direct costs are calculated as shown in Tables 6.10 and 6.11.

Indirect production costs include packaging and storage of materials, payment of local taxes and interest. The costs in this category are independent of the production level of the plant. The last category, general expenses, refers to administrative costs, distribution and sale of products, research and development. Both indirect and overhead costs are calculated from other costs, as will be shown in Tables 6.10 and 6.11.

6.4.3 Economic evaluation

The economic evaluation criteria used in this work were total investment in the plant, production costs, total revenue related to one year of operation, annual net profit and the equilibrium price of fatty acids. The first two were described in the previous sections. The total revenue was obtained from the flows of each product, multiplied by the respective price of the product. The evaluated products are fatty acids and, depending on the scenario, crude glycerol or technical grade glycerol. The yearly net profit is obtained by subtracting the total revenue by the total cost of production, which is also calculated for one year of operation. The equilibrium price of fatty acids was obtained for each case by varying the price of fatty acids until the annual revenue equaled the total cost of production.

6.5 Results - Sizing of equipment

Table 6.10 shows the dimensions and costs of the main equipment involved in the production of fatty acids in subcritical media by using a fixed conversion. While, Table 6.11 shows the results obtained for the production of fatty acids by using an simplified kinetic and mass transfer model for the hydrolysis of rapeseed oil. The costs of reactors and flash vessels include the costs of the coils used for heating or cooling. The cost of the columns include the costs of the condenser and the reboiler. A more detailed presentation of the costs and properties of each equipment, as well as the costs related to pumps and heat exchangers is given in the Supporting Information (**??**).

As seen in the tables, the fact that the reaction rate is higher for the kinetic and mass transfer model resulted in a lower volume reactor and, consequently, lower cost in relation to the reactor by using the simplified case. The reactor for the production of fatty acids by using the extended model costs about 75.5% of the price of a reactor for the production of the simplified model. There was no major difference in the dimensions and cost of the COL1 col-

umn between models. However, the COL2 column of the extended model is significantly lower than the COL2 column of the base case. This difference occurred at the level of mass flow of liquid and gas inside the column, which implied larger diameters for the base case. In the other equipment, the differences were small.

As explained before, the difference between simple and integrated cases occurs only in relation to the raw material heating system and the cooling of the reaction products. There is no change in the mass balances involved in the system. The costs of the reactors, columns and separators are roughly the same for all the scenarios and cases.

6.6 Economic analysis of different scenarios

Table 6.12 shows the results of the economic analysis performed on the different scenarios for the production of fatty acids by using a fixed conversion and Table 6.13 shows the results of the different scenarios by using a kinetic model for reaction.

Equipment		**Scenario 1**	**Scenario 2**	**Scenario 3**
Reactor	Subcritical reactor			
	Dimension (DxL) [m]	2.96 x 8.88	2.96 x 8.88	2.95 x 8.88
	Cost US$ x 10^3	2847.83	2847.83	2846.7
Columns	COL1			
	Dimension (DxH) [m]	2.73 x 12.24	2.73 x 12.24	2.7 x 12.18
	Cost US$ x 10^3	357.8	357.8	353.71
	COL2			
	Dimension (DxH) [m]	2.76 x 13.37	2.76 x 13.37	2.76 x 13.37
	Cost US$ x 10^3	316.65	316.65	316.61
Separators	Decanter			
	Dimension (DxL) [m]	0.58 x 2.33	0.56 x 2.32	0.58 x 2.33
	Cost US$ x 10^3	13.27	13.27	13.26
	Flash vessel			
	Dimension (DxH) [m]			0.60 x 2.19
	Cost US$ x 10^3			42.06

Table 6.10: Dimensions of the main equipment - **Base case**.

Equipment		Scenario 1	Scenario 2	Scenario 3
Reactor	Subcritical reactor			
	Dimension (DxL) [m]	2.74 x 8.22	2.74 x 8.22	2.74 x 8.22
	Cost US$ x 10^3	2152.45	2152.45	2147.94
Columns	COL1			
	Dimension (DxH) [m]	2.75 x 12.29	2.75 x 12.29	2.73 x 12.25
	Cost US$ x 10^3	367.93	367.93	364.94
	COL2			
	Dimension (DxH) [m]	2.46 x 12.85	2.46 x 12.85	2.46 x 12.85
	Cost US$ x 10^3	248.45	248.45	248.36
Separators	Decanter			
	Dimension (DxL) [m]	0.59 x 2.36	0.59 x 2.36	0.59 x 2.36
	Cost US$ x 10^3	13.38	13.38	13.38
	Flash vessel			
	Dimension (DxH) [m]			0.66 x 2.08
	Cost US$ x 10^3			45.79

Table 6.11: Dimensions of the main equipment - **Kinetic/Mass transfer model**.

It can be seen, by comparing technologies, that when one uses a fixed value for the conversion in the reactor, it requires a much greater investment. This result is a reflection of the aspects discussed in the previous section, since the use of a kinetic expression allows one to calculate the generation or production of all the species. Additionally, when one uses a kinetic expression in the Scenario 3, it is possible to obtain a positive net annual profit after taxes.

According to the results presented in Table 6.12 and 6.13, the investment plant more than doubles when installing the energy reuse system of the reactor effluent. These are two large stainless steel exchangers with a reinforcement of pressure. The largest of these exchangers, HX1-B, which is responsible for heating the water stream, can cost almost twice as much as the reactor. This factor must be taken into account when choosing the energy reuse system. The advantage will come in cost of production.

In regards to the raw materials, they account for 75-76% of direct costs and 63-64% of total production costs. Therefore, the final price of fatty acids is greatly influenced by the prices of raw materials, which in turn are strongly influenced by economic, social and climatic issues. Therefore, in order to

		Sc. 1	Sc. 2	Sc.3
Investment				
Total cost of equipment		4.55	9.67	9.78
Fixed investment C_{FC}		22.97	48.75	49.3
Working capital $C_{WC} = 0.15C_{FC}$		3.44	7.31	7.39
Total investment $C_{TC} = C_{FC} + C_{WC}$		26.41	56.06	56.69
Direct costs				
Raw material				
	Rapeseed oil	87.97	87.97	83.4
	Water	0.01671	0.01156	0.01682
Operating labor C_{OL}		0.19	0.19	0.19
Technical supervision $C_{SC} = 0.15C_{OL}$		0.02	0.02	0.02
Utilities				
	Superheated steam	22.15	13.46	13.31
	HP steam	0.5	0.5	0.46
	Cooling water	2.3	1.94	1.94
	Electricity	0.37	0.37	0.38
Waste treatment		0.78	0.78	0.2
Maintenance and repairs, $C_{MR} = 0.06C_{FC}$		1.37	2.92	2.95
Supplies $C_S = 0.15C_{MR}$		0.2	0.43	0.44
Laboratory analysis $C_L = 0.15C_{OL}$		0.02	0.02	0.02
Patents and royalties		4.72	4.51	4.32
Subtotal		119.90	113.12	107.64
Indirect costs				
Packaging and storage $C_{OPS} = 0.6(C_{OL} + C_{SC} + C_{MR})$		0.96	1.89	1.91
Local taxes $LT = 0.015C_{FC}$		0.34	0.73	0.73
Legal aid $IN = 0.005C_{FC}$		0.11	0.24	0.24
Subtotal		1.42	2.86	2.89
General expenses				
Administrative costs $C_{AD} = 0.25C_{OPS}$		0.24	0.47	0.47
Distribution and sales $CDS = 0.10C_{TP}$		15.73	15.05	14.41
R&D $C_{RD} = 0.05C_{TP}$		7.86	7.52	7.2
Subtotal		23.84	23.05	22.09
Total production cost C_{TP}		143.74	136.17	129.73
Income				
Annual sales of fatty acids		114.98	114.98	114.98
Annual sales of glycerol		3.7	3.7	11.05
Total income		118.68	118.68	126.484
Annual net profit		-25.06	-17.49	-3.246
Equilibrium price of fatty acids (US$/kg)		1.43	1.36	1.29

Table 6.12: Economic evaluation for base case (USx10^6$).

		Sc. 1	Sc. 2	Sc.3
Investment				
Total cost of equipment		3.84	7.78	7.91
Fixed investment C_{FC}		19.36	39.23	39.87
Working capital $C_{WC} = 0.15C_{FC}$		2.90	5.88	5.98
Total investment $C_{TC} = C_{FC} + C_{WC}$		22.26	45.11	45.85
Direct costs				
Raw material				
	Rapeseed oil	87.67	87.67	83.4
	Water	0.01746	0.01746	0.01745
Labor cost C_{OL}		0.19	0.19	0.19
Technical supervision $C_{SC} = 0.15C_{OL}$		0.02	0.02	0.02
Utilities				
	Superheated steam	20.07	10.78	10.62
	HP steam	0.55	0.55	0.52
	Cooling water	2.36	1.97	1.98
	Electricity	0.38	0.38	0.39
Waste treatment		0.81	0.81	0.31
Maintenance and repairs, $C_{MR} = 0.06C_{FC}$		1.16	2.35	2.39
Supplies $C_S = 0.15C_{MR}$		0.17	0.35	0.35
Laboratory analysis $C_L = 0.15C_{OL}$		0.02	0.02	0.02
Patents and royalties		4.6	4.34	4.16
Subtotal		118.01	109.79	104.36
Indirect costs				
Packaging and storage $C_{OPS} = 0.6(C_{OL} + C_{SC} + C_{MR})$		0.83	1.54	1.57
Local taxes $LT = 0.015C_{FC}$		0.29	0.58	0.59
Legal aid $IN = 0.005C_{FC}$		0.09	0.19	0.19
Subtotal		1.21	2.33	2.36
General expenses				
Administrative costs $C_{AD} = 0.25C_{OPS}$		0.2	0.38	0.39
Distribution and sales $CDS = 0.10C_{TP}$		15.33	14.48	13.89
RD $C_{RD} = 0.05C_{TP}$		7.66	7.24	6.94
Subtotal		23.21	22.1	21.23
Total production cost C_{TP}		141.22	131.89	125.59
Income				
Annual sales of fatty acids		114.98	114.98	114.98
Annual sales of glycerol		3.73	3.73	10.79
Total income		118.71	118.71	125.768
Annual net profit		-22.51	-13.18	+0.178
Equilibrium price of fatty acids (US$/kg)		1.41	1.32	–

Table 6.13: Economic evaluation for kinetic model (US$$x10^6$).

reduce the final price of fatty acids, rate reduction policies and subsidies in general should be focused on the acquisition of raw materials.

Despite more than doubling the investment needed to build the plant, the implementation of the energy integration system generated savings of 4-6% in production costs. The tables show that utility costs can be quite high, as expected. This is mainly due to the large amount of superheated steam needed to heat the raw materials to 250°C. Besides the economic benefit, the economy with utilities contributes with greater autonomy and sustainability for the process, since it would stop the consumption of fuel in order to obtain it.

The recycling of residual oil was responsible for a saving of 4% with a 5% saving on vegetable oil. This result is compatible with a conversion of 95% of the oil to the reactor.

According to the values presented in Tables 6.12 and 6.13, for the process to be profitable the price of fatty acids should be at least 12% higher for a simulation which uses a conversion reaction and 14% for a simulation which uses a kinetic model. However, this increase is still possible within the reality of the oleochemical market (BCC Research 2016).

In regards to vegetable oil, for a conversion reactor process to become profitable it would be necessary to purchase rapeseed oil at a maximum value of 0.531 ($\frac{US\$}{kg}$, which corresponds to reductions of 40% in prices. It is considered that such reduction in prices can be achieved through public policies and direct negotiation between oil producer and fatty acids producers.

6.6.1 Sensitivity analysis

The sensitivity of the total cost of production, the annual net profit and the equilibrium price of fatty acids (dependent variables) in relation to the prices of fatty acids, vegetable oil and water (independent variables) were evaluated. For this, a positive perturbation of 1% was made in each of the independent variables and the effect of these disturbances on each of the dependent variables was measured. The results can be seen in Table 6.14.

As can be seen, in Table 6.14 the most important variable is the price of vegetable oil. For a variation of 1% in the price of vegetable oil, the net profit of the company can vary up to 2.52% in the case of a fixed conversion and 2.85% in the case of a simulation which uses a kinetic model for the reaction.

	Fatty acids		**Rapeseed oil**		**Water**	
	Base case	Model	Base case	Model	Base case	Model
Total production cost			0.71%	0.72%	0.1%	0.1%
Annual net profit	2.38%	2.72%	-2.52%	-2.85%	-0.41%	-0.09%
Equilibrium price			0.75%	0.77%	0.1%	0.11%

Table 6.14: Sensitivity analysis.

The price of water was, among the analyzed variables, the one that had the least effect on the economic results of the plants. This is due to the fact that, in all cases, the largest portion of water is consumed and the remaining in the process is recycled, which reduces the need for material acquisition.

The price of fatty acids had similar weight to the price of vegetable oil on the annual net profit in both. This is because the amount of fatty acids produced is similar to the amount of fatty material which enters the plants, i.e., the mass gain relative to the assimilation of water by the oil molecules is small (about 5%). In addition, the base price for fatty acids in the assessed scenarios was relatively close to the price of rapeseed oils, thus the size of the disturbance was also high.

6.7 Conclusions

In the present chapter, SimSci Pro/II was used in the simulation of the production of fatty acids with water from rapeseed oil in subcritical medium by using a fixed value of conversion and a model-based approach for the reaction section of the plant. The implantation of an energy recovery system and the recycling of the residual oil in the proposed scenarios were also evaluated, so as to verify how much these alternatives would contribute in the valorization of the process. The mass and energy balances were solved with the simulator and the data were used for the equipment sizing and for a comparative economic evaluation between the approaches and the technologies. Then, sensitivity on prices of raw materials and equilibrium price of products analyzes were performed. In all the scenarios, raw materials accounted for a large share of total production costs. It was found that the final price of fatty acids is strongly influenced by the prices of these two inputs. This relationship was clear in the sensitivity analysis. A 1% variation in the price of vegetable oil can cause variations of around 0.75% in the price of fatty acids. Despite the large investment needed to install the energy recovery system, it was able to

generate savings of 4–6% in production costs. In the same way, recycling the residual oil was responsible for savings of around 4%. The highest annual net profit was obtained by simulating the reaction with a kinetic expression, despite the higher investment and the consequent longer return time. It has been shown in this chapter that the economic viability of each of the technologies analyzed depends heavily on the current economic scenario as well as the accuracy of the models used to represent a process as new research is conducted to optimize the models and the conditions of the process.

CHAPTER 7

An analysis of fluid flow behavior in an industrial scale spray column – a coupled CFD and kinetics study

7.1 Process description

As described by A. Johnson et al. 1975 and as shown in Figure 7.1, the continuous hydrolysis of fats is performed in a spray column reactor by feeding water between 180°C–270°C and 25–40 bar pressure through sprays in the top of the column and the fat mixed with live steam at the bottom. Droplets of water pass down the column and come in contact with the partially hydrolyzed fat which ascends from the base of the column. A small amount of water dissolves in the fat phase and there it reacts chemically. In this way, it produces glycerine and the corresponding fatty acids.

The hydrolysis of triglycerides is generally considered a three-step set of consecutive and reversible reactions in which one mole of triglyceride is generated and consumed in each step. As a result of its heterogeneous nature, the hydrolysis reaction is affected, not only, by the chemical kinetics but also by the rate of mass transfer between the oil and water, as well as, another observable variables with the process such as temperature, pressure, density, viscosity, and geometry of reactor (Forero-Hernandez et al. 2017).

However, the behavior of such variables inside a reactor is difficult to observe due to the relative harsh conditions in which this process takes place. In this way, Computational Fluid Dynamics Analysis becomes a relevant alternative in order to simulate and get a better understanding of the phenomena which occurs inside the column, since it allows one to model and visualize the fluid behavior of all reaction components in the the reactor.

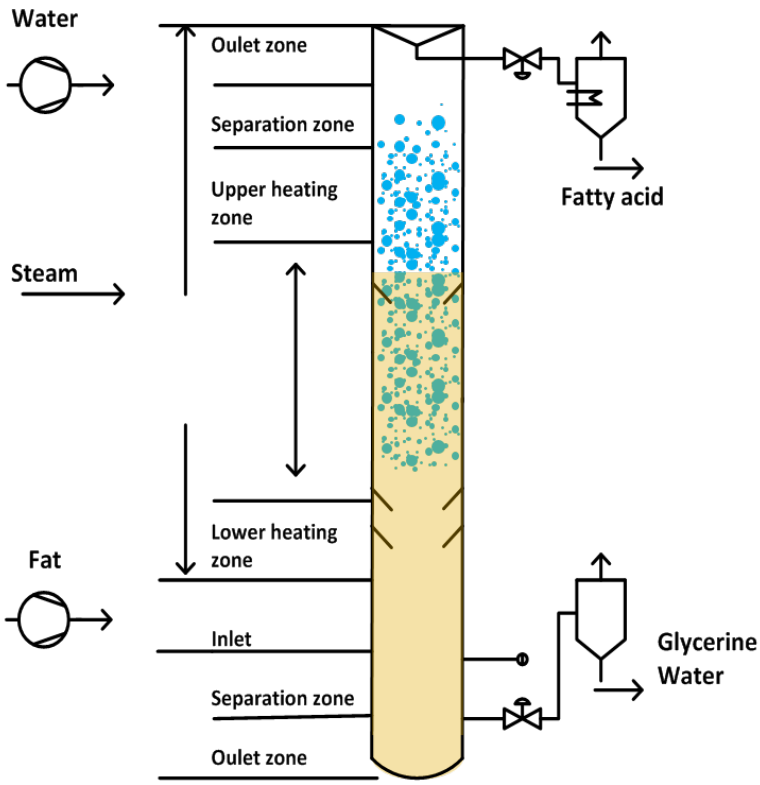

Figure 7.1: Process flow diagram of an hydrolysis spray reactor.

7.2 Computational Fluid Dynamics

The solution of a fluid dynamics problem is performed by configuring boundary conditions, domains, and setting initial conditions, as well as, defining multiphase, multicomponent, turbulence, reaction, and buoyancy models.

The regions of fluid flow in fluid dynamics are called domains. A domain requires the following: a region where the flow is defined, the physical conditions of the flow which determine the modeling of specific characteristics (such as heat transfer or buoyancy,) and the physicochemical properties of the compounds in the region.

The software used in numerical simulations was *Ansys CFX 17.1*. In this software the continuity and momentum equations are solved by using the finite volume method. This software enables the modeling of fluid mixtures with their corresponding properties (Ansari and Kim 2009). For this purpose, *Ansys CFX* calculates the properties of the mixtures from the properties of the components and their amounts in the mixture (Ansys 2011).

The equations used by *Ansys CFX* are based on the macroscopic scale of fluids. The behavior of these fluids in any geometry is described by the conservation of mass, energy and momentum, assuming that the fluid is continuous. Thus, the steady-state transport equations described by the equation of continuity (Equation (7.1)) and the Navier-Stokes equations (Equation (7.2)) were used in the simulations, and are presented as follows (Temam 2001):

$$\nabla \left(\rho U\right) = 0 \tag{7.1}$$

$$\rho \left[\left(U \cdot \nabla\right) U\right] = -\nabla p + \mu \nabla^2 \cdot U + \rho g \tag{7.2}$$

Where ρ is the density $\left(\frac{kg}{m^3}\right)$, U the vector of velocities $\left(\frac{m}{s}\right)$, and p the pressure $\left(\frac{kg}{m\ s^2}\right)$. μ is the dynamic viscosity $\left(\frac{kg}{m\ s}\right)$ and g is the gravity $\left(\frac{m}{s^2}\right)$. In Equation (7.2), the term in the left represents the spatial acceleration of the fluid, while the terms in the left represent the pressure gradient, the viscous stresses, and the contributions of gravity, electric fields or magnetic fields. The conservation of the mass for the chemical species i is expressed by:

$$\rho \left(U \cdot \nabla Y_i\right) = \rho D_i \nabla^2 Y_i + S_i \tag{7.3}$$

Where Y_i is the mass fraction of the species i, D_i is the kinematic diffusion coefficient of species i, and S_i is the mass source of species i due to the action of chemical reactions (Santana, Júnior, and Taranto 2015). In Equation (7.3), the term on the left side represents the spatial variations of the mass fraction,

while the terms on the right side represent the mass diffusive transport and the mass source. This mass source is modeled according to Equation (7.4):

$$S_i = MW_i \left(\sum_{r_r}^{n_r} \upsilon_i'' r_r - \sum_{r_r}^{n_r} \upsilon_i' r_r \right) \tag{7.4}$$

Where MW_i is the molecular weight of the chemical species i, $''$ and $'$ are the stoichiometric coefficients of the species as products or as reactants, respectively. In the chemical reaction, r and r_r are the rate of reaction r. This reaction rate depends on several factors, such as the type of oil and kinetic model considered. Since the triglyceride reaction rate is expressed in the form of r_{TG}, the mass conservation for the components vegetable oil (triglycerides), water, glycerol, and fatty acids are expressed as:

$$\rho \left(U \cdot \nabla Y_{TG} \right) = \rho D_{TG} \nabla^2 Y_{TG} + MW_{TG} \left(-r_{TG} \right) \tag{7.5}$$

$$\rho \left(U \cdot \nabla Y_{FA} \right) = \rho D_{FA} \nabla^2 Y_{FA} + MW_{FA} \left(3 r_{TG} \right) \tag{7.6}$$

$$\rho \left(U \cdot \nabla Y_{Gly} \right) = \rho D_{Gly} \nabla^2 Y_{Gly} + MW_{Gly} \left(r_{TG} \right) \tag{7.7}$$

$$\rho \left(U \cdot \nabla Y_{W} \right) = \rho D_{W} \nabla^2 Y_{W} + MW_{W} \left(-3 r_{TG} \right) \tag{7.8}$$

Where MW_{TG}, MW_W, MW_{Gly}, and MW_{FA} are the molecular weights of vegetable oil (triglyceride), water, glycerol, and fatty acids in $\frac{kg}{kmol}$, respectively. The diffusion coefficient of water in the oil was calculated by using the Wilke-Chang equation and was equal to $1.2x10^{-9} \frac{m^2}{s}$ (Temam 2001). For the other chemical species, dynamic viscosity values of the medium were used in the calculation of the diffusion coefficient.

7.2.1 Geometry

A geometry consists of the representation developed in a CAD software (*Computer Aided Design*) of the physical system and its boundary conditions (walls, inputs, outputs, and objects). The modeling of reactors is complex because they usually have static parts, such as walls and baffles, and moving parts,

impellers or nozzles. In this regard, it is important to build a geometry which is as close to reality as possible in order to obtain more accurate results.

Figure 7.2 shows the geometries used for the simulations. The flow domain of the spray column reactor was developed in *SolidWorks 2017* by extruding a sketch with 0.66 m of internal diameter and 35 m of height. Additionally, a nozzle with 4.2 cm of internal radius was drawn in order to include the inlet of sprayed water to the system. These geometries mimic roughly the setup presented by Attarakih et al. 2012.

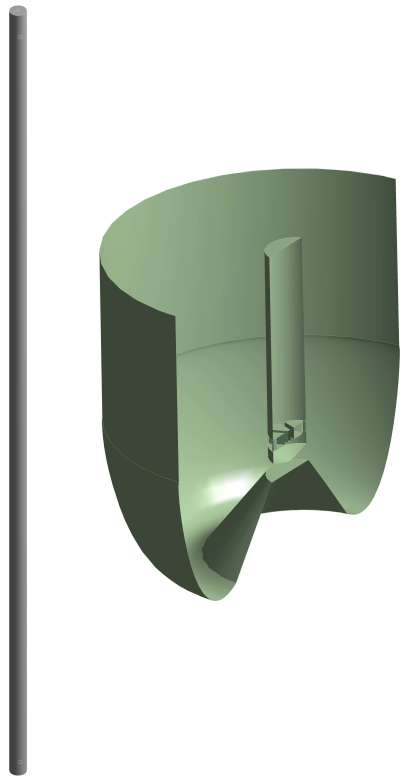

Figure 7.2: Left: Spray column reactor. Right: spray nozzle.

7.2.2 Mesh

Discretization methods such as finite differences (FDA), finite volumes (FVA), or finite elements (FEM) allow the linearization of the equations which model

the phenomenon into a set of algebraic equations which are solved by the different numerical methods. To solve the problems in computational fluid dynamics, the finite volume method is most often used (Anderson, Tannehill, and Pletcher 2016).

The finite volume method was developed by B. H. McDonald and Wexler 1972 and MacCormack and Paullay 1972 and was initially employed in solving two-dimensional problems. Every finite volume method basically seeks to obtain approximate equations by dividing the domain into elementary volumes, while it is satisfying the conservation of transport properties for each volume.

The approximate equations are obtained by integrating, in space and time, the equations of mass, energy, and momentum in their divergent form. When the previous equations are integrated in all the elementary volumes, an algebraic equation is obtained for each element. Therefore, the values of all the properties involved are obtained in discrete points along the domain (Istok 1989).

To divide the physical domain of the problem into finite volumes, a computational mesh is required. This mesh can contain elements of various shapes and sizes. This flexibility eases the discretization of equipment with complex geometries. The elements used are: hexahedrons, tetrahedrons, prisms, and pyramids. In practice the main types of meshes are hexahedral and tetrahedral. Hexahedral meshes are often classified as structured and tetrahedral as unstructured.

The structure of the mesh is not related to the shape of the element, but rather to how each element is connected to each other within the linear system. Thus, it is possible to have tetrahedral structured meshes and hexahedral unstructured meshes. In the case of a geometry with curved surfaces such as the spray column reactor, the generation of fully structured hexahedral meshes is much more complex.

A three dimensional structured mesh of the flow domain was developed by using the meshing tool included in *Ansys Workbench 17.1*. Due to time limitations, a more structured mesh study was not developed. However, it is understood by the author that further refinement of the mesh could provide an increase in the speed and accuracy of the solution of the study case. The obtained mesh consisted of

7.3 Simulation settings

Ansys CFX-Pre is used to define the simulations. The analyzes, which consist of flow physics, boundary conditions, initial values, and solver parameters, were also specified. A range of boundary conditions which included inputs, outputs, and wall, along with, contour conditions for heat transfer models and periodicity were used.

The CFD simulation was carried out by using *Ansys CFX 17.1* and it was configured to solve chemical kinetics, and the governing equations of continuity, momentum, and energy. The system was simulated as a continuous reactor with an initial load of rapeseed oil of 7.5 m^3 where water was continually introduced by a nozzle on top at a rate of 2291 $\frac{kg}{hr}$ with a droplet diameter of 0.5 μm and oil from the bottom at a rate of 4651 $\frac{kg}{hr}$ at 523.15 K and 41 bar. The settings used in the definition of the multiphase simulation were compiled from sources found in literature, and are presented in Table 7.1 and 7.2 (Attarakih et al. 2012; Wang et al. 2013).

Morphology - Oil	Continuous fluid
Morphology - Water	Dispersed fluid
Free surface model	Standard
Turbulence	k-Epsilon
Heat transfer	Thermal Energy
Fluid buoyancy model	Density difference
Temperature (K)	523.15
Turbulence eddy dissipation (m^2/S^3)	100
Turbulence kinetic energy (m^2/S^2)	1

Table 7.1: Simulation settings.

Fluid pair model	**Interface transfer**	**Momentum transfer (Drag force)**
Triglyceride to Water	Mixture model	Drag coefficient = 0.44
Triglyceride to FA	Particle model	Schiller Naumann
Fatty acids to Water	Particle model	Schiller Naumann
Glycerol to Water	Particle model	Schiller Naumann

Table 7.2: Simulation settings (Wang et al. 2013).

Necessary physicochemical properties shown in Table 7.3 were calculated by using polynomial fittings of experimental data versus temperature for the

desired temperature. Correlation parameters for these polynomials have been obtained from the *CAPEC Lipids Database* Diaz-Tovar, Gani, and Sarup 2011.

Properties	Triglyceride	Fatty Acids	Water	Glycerol
Molar mass (g/mol)	878	282	18	92
Density (g/cm^3)	0.753	0.734	0.8	1.092
Cp (J/mole K)	2023.55	826.7	87.38	258.4
Dynamic viscosity (N s/m^2)	0.00021	0.00053	0.00011	0.00061
Thermal conductivity	0.16	0.08	0.62	0.32
Thermal expansivity	0.002	0.001	0.0002	0.0009

Table 7.3: Physicochemical properties of components.

Kinetic and mass transfer were calculated by using the simplified model presented in a previous chapter (Forero-Hernandez et al. 2017).

In the simulations of this chapter a multicomponent multiphasic system was adopted with isothermal condition and incompressible laminar flow. A physical timescale of 90 minutes was chosen, so as to mimic the normal reaction time in a spray column for the hydrolysis of oil.

For the numerical methods, high resolution schemes were used to solve the advective terms, which are reserved for the transport of velocity with the velocity itself. An RMS (Root Mean Square) convergence criterion of 1×10^{-5} was used. The simulations were solved in parallel processing by using a Intel(R) Xeon(R) CPU ES-1620 @ 3.60GHz processors and 64GB RAM.

The analysis of the mixture focused on evaluation of the state of the system and the compositions of the components at the specified reaction time. However, as part of a future work, and in order to achieve a more realistic model, rigorous conditions of meshing and mass transfer constraints need to be applied.

7.4 Results

The simulation of the hydrolysis of triglycerides at subcritical conditions was carried out with the aid of the kinetic model developed in *Ansys CFX* by the authors (Forero-Hernandez et al. 2017). The numerical results of the consumption of oil are shown in Figure 7.4 and data on the generation of fatty acids and glycerol in Figures 7.5 and 7.6. Moreover, these values of

concentration as a function of height along the central axis of the reactor are also shown in Figures 7.4, 7.5, and 7.6 .

Water was fed into the upper part of the reactor by means of the nozzle and moved at a relative high speed to the lower part of the column due to buoyancy as shown in Figure 7.3. Consequently, the sprayed water mixed with the triglyceride bulk located in the lower part of the column where it forms a two-phase system due to low solubility. Once the reactants were mixed, the reaction among them began. Triglycerides were consumed mainly in the middle section of the column, as seen in Figure 7.4. This performance is at least partly due to the fact that the reactants have been introduced separately, which makes the contact between the reagents ideal.

Figure 7.5 shows the fatty acids concentration distribution throughout the reactor at different reaction times. It can be seen that their formation occurs at the middle section of the reactor reaching their maximum concentration. Fatty acids are the less dense components in the mixture, hence they accumulate at the top of the column at the outlet. On the other hand, it can be seen in Figure 7.6 that glycerol was generated and was diluted to the bottom of the column. This behavior is expected given the difference in densities and the biphasic nature of the generated mixture. In this particular case, water flowing from the top drags down the glycerol, where it forms an aqueous phase called sweet-water due to the good solubility between these components. In industry, this mixture can be separated by evaporation or distillation.

The evolution of triglycerides and fatty acids during the course of the simulation is illustrated in Figure 7.7, where data is provided in terms of concentration. Visually speaking the behavior of the system resembles the traditional concentration profiles one can find for such reacting system. Additionally, one can see that triglycerides were not entirely consumed in the final stages of the simulation. Simulation mismatches with the reality may be due to process phenomena and conditions not taken into account and for errors when setting up the system. As the chemical reactions were implemented, the reaction rates are expected to vary as the flow occurs. The formation and consumption of the components of the system is obtained exactly as expected. It shows that the kinetic model can actually be applied to the case. In this regard, data obtained in a real set-up could be used to validate these simulations.

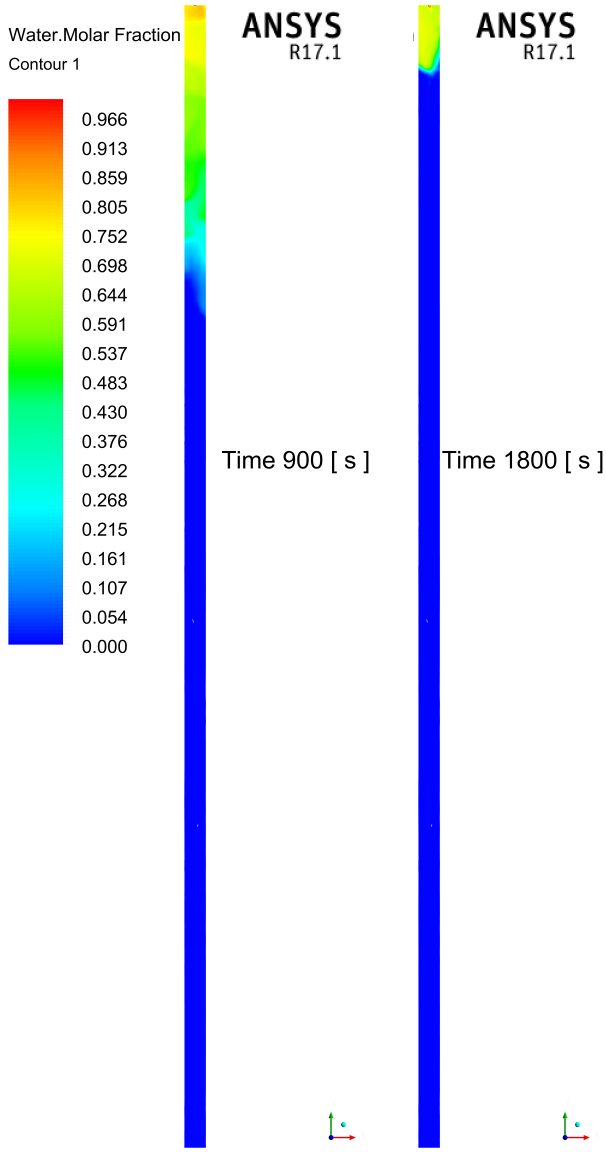

Figure 7.3: Molar fraction of water introduced in the column.

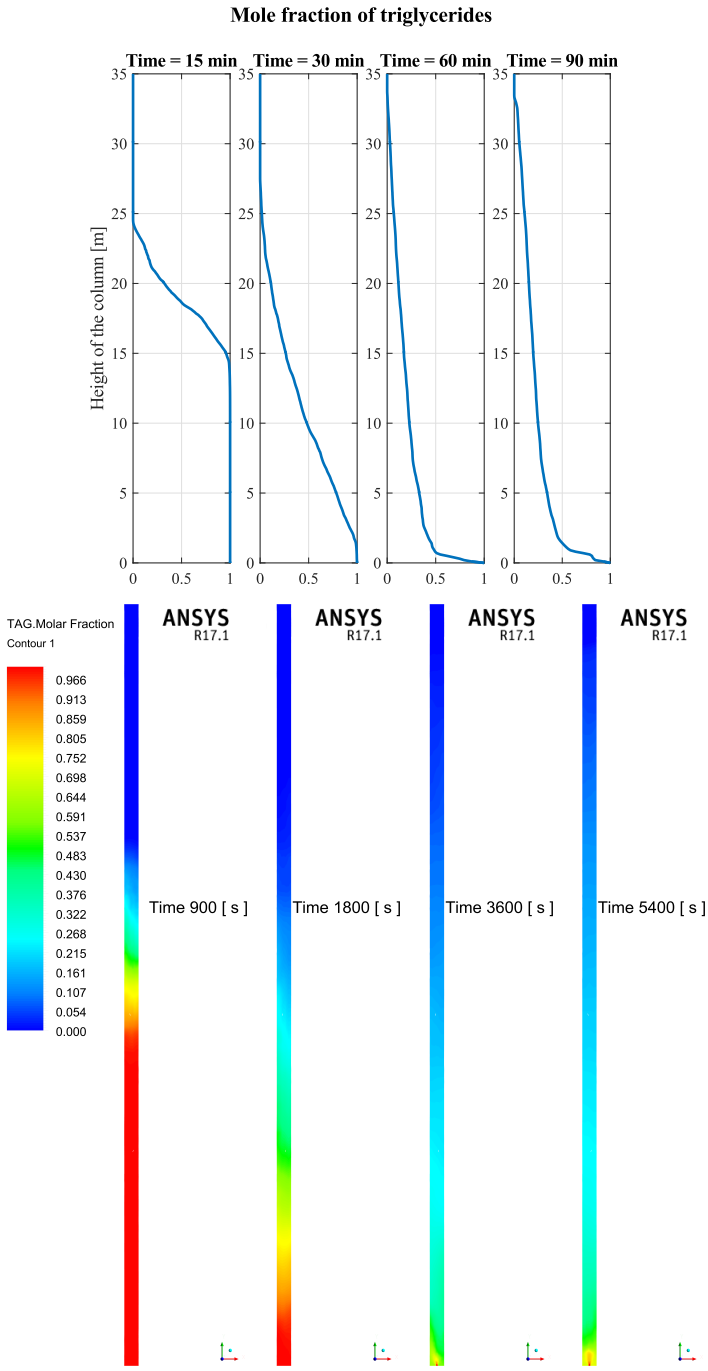

Figure 7.4: Molar fraction and concentration of triglycerides in the column at different times.

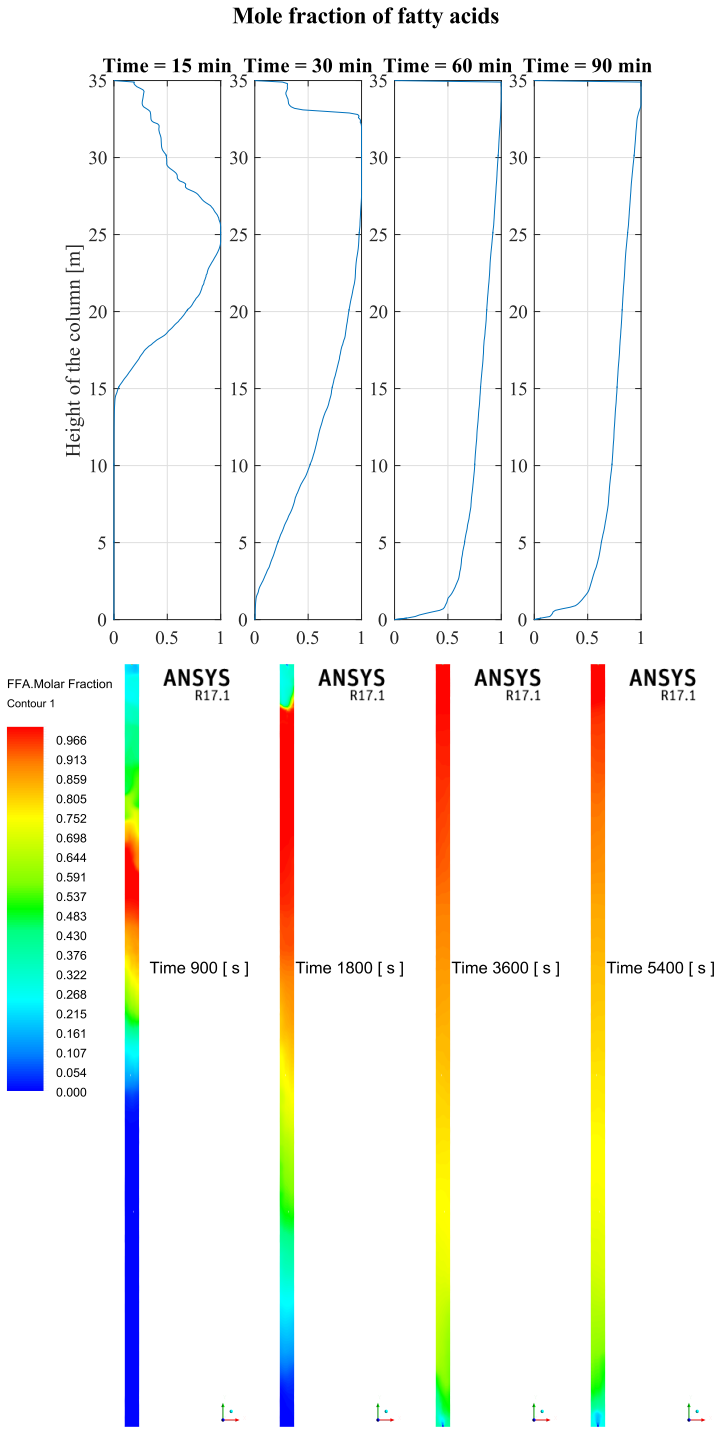

Figure 7.5: Molar fraction and concentration of fatty acids in the column at different times.

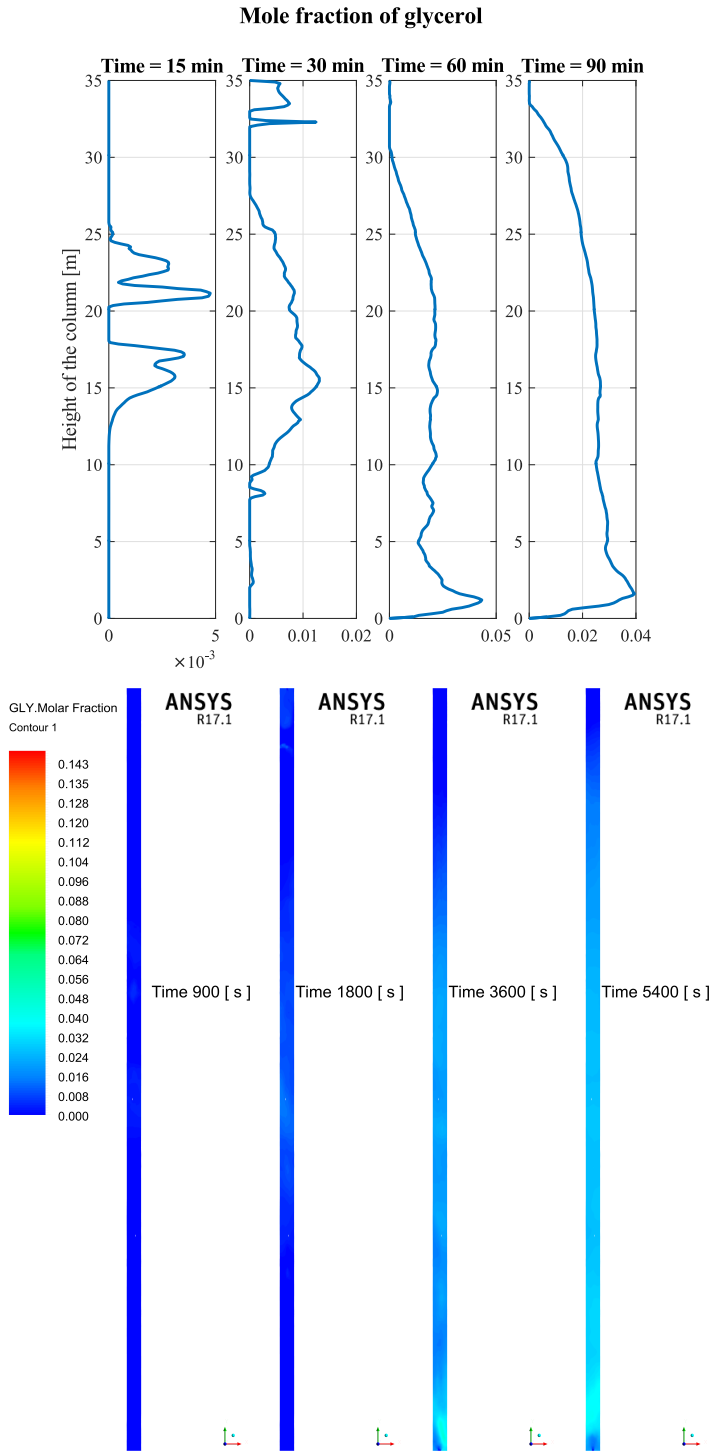

Figure 7.6: Molar fraction and concentration of glycerol in the column at different times.

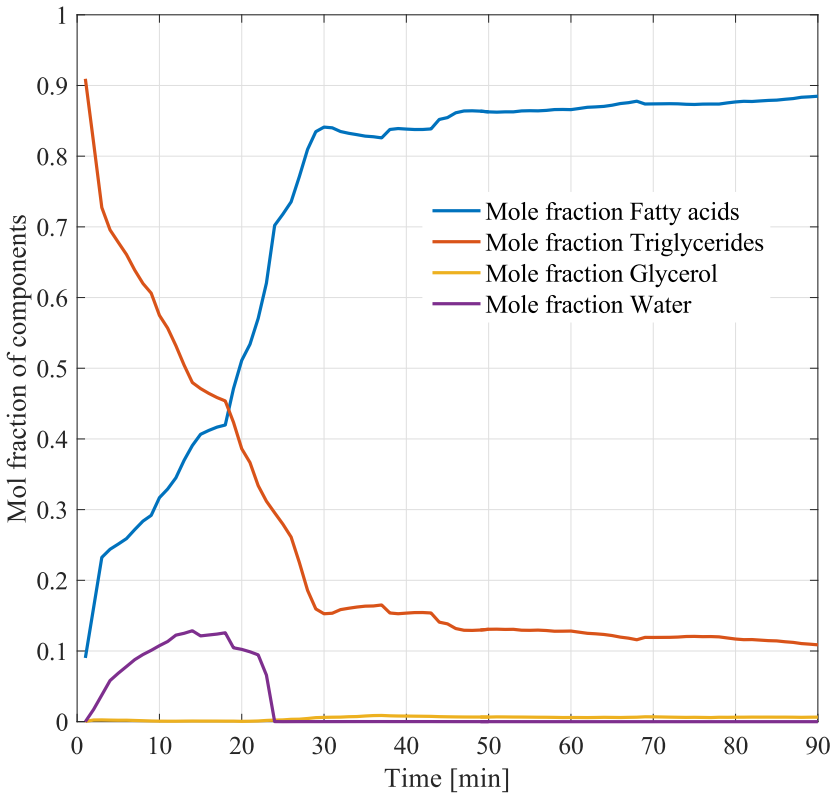

Figure 7.7: Average value of mole fractions of components in the reactor.

7.5 Conclusions

For process understanding purposes, such as to determine when and how the hydrolysis is favoured, mixing times, and for tracking the entire flowing mixture, the results show that CFD analysis have great potential in the areas of interest. It should be noted that given the reaction mixture changes during the reaction (e.g. viscosity, density, presence of emulsifying agents, and distribution of liquid phases), a reliable simulation tool can be used to simulate and evaluate such changes as well as other reactor configurations. Therefore, this analysis is of considerable interest to improve the understanding of design and operating variables which increase the feasibility of vegetable oil utilization because it provides information which could be used to compare different modeling approaches under different operating conditions.

CHAPTER 8

Conclusions and future work

The main objective of this project was to study the hydrolysis of rapeseed oil under subcritical conditions to produce fatty acids. To fulfill this purpose, experiments were performed in a batch reactor in order to obtain high yields of fatty acids. To estimate the most favorable operating conditions for fatty acids production, it was necessary to carry out several tests in a stirred reactor based on an experimental design, and ANOVA and RSM analyses. In this regard, the use of the experimental design allowed a careful analysis of the process variables with a small number of experiments and how they affect the yield to fatty acids. The results showed that by carrying out the reaction together with the optimized conditions allows one to reach yields of fatty acids of up to 93.83%. This analysis provided a powerful tool to optimize the hydrolysis conditions which constitutes an important improvement in the yield obtained in the experiments. Obtaining such information contributes to future studies in industrial scale as well as to compare the efficiency of processing vegetable oils.

As such, this study provided additional insights about the thermodynamic behavior of the hydrolysis of vegetable oils. Although the literature contains some information about the process and its kinetic features, there is little information on the thermodynamic behavior of the process. The thermodynamic analysis adopted in this work, through the minimization of energy Gibbs using thermodynamic models for the calculation of activities is able to predict the chemical and phase equilibrium robustly. In real experiments and industrial plants the conversion of reactants is associated with its kinetic features mechanisms. However, the reaction conversion and the distribution of the products at the equilibrium, from a thermodynamic point of view allows a better understanding of the influence of the process parameters, such as system temperature, pressure and initial amount of reactants. In general, the

thermodynamic analysis of the chemical and phase equilibrium of the hydrolysis of vegetable oils allows better understanding of the behavior of the products and phases formed at equilibrium. In addition, this work may contribute to the development of a hydrolysis process where the experimental yields reach levels similar to the ones obtained from the theory.

This work also presented a combined modeling approach to investigate the kinetics and mass transfer effects on the hydrolysis of rapeseed oil. The primary purpose of the developed simplified and extended model is to interpret experimental data collected from typical batch tests and to estimate parameters for the proposed model. Due to its heterogeneous nature, the hydrolysis reaction is affected not only by the chemical kinetics but also by the rate of mass transfer between the oil and water as well as their specific contact area in this two phase emulsion.

The developed models included the mass transfer coefficient as a function of operation and process variables, e.g. agitation speed, temperature, pressure, density, and viscosity. Thereafter, a Monte Carlo based uncertainty analysis was performed to find the accuracy of estimated parameters, the mean and standard deviations of the model outputs from experimental data. This method was then successfully applied to calculate the accuracy of the estimated parameters as well as their confidence intervals. The results showed that the presented models were able to predict accurately the experimental data with narrow confidence intervals.

To understand which parameters in the model are responsible for the output uncertainty, a sensitivity analysis method was used (Polynomial chaos expansions based Sobol sensitivity indices). The performed sensitivity analysis detected the influential and non-influential parameters to the model outputs, which allows one to validate the model and assumptions proposed.

These analyses provided insights on the relative importance of parameters and their changes as the reaction progresses, where the parameters related to the mass transfer and the first steps of the reacting system linked to the consumption of triglycerides are the most important. Since the lack of experimental data is a crucial issue in the hydrolysis of rapeseed oil, it was found that this model-based analysis of experimental data has great potential as a tool for the design and optimization of production systems, which help to save time and resources required for experimental testing.

In conventional chemical processes, researchers and industry professionals

routinely use modeling and simulation techniques to develop and optimize industrial equipment and processes. Therefore, the model developed together with the methodologies involved showed great potential as tools for the design and optimization of production systems, helping to save time and resources required for experimental testing.

In this study, simulations of the production of fatty acids were performed in a commercial process simulator by using one of the kinetic models for the hydrolysis of rapeseed oil. This analysis involved the evaluation of reactions, separations, product generation, co-products, utility consumption, and economic viability analysis. In this stage, the implementation of modifications to the conventional production flowsheet such as an energy recovery system and the recycling of the residual oil in the proposed scenarios was evaluated so as to verify, how much these alternatives would contribute for improvements in the economy of the process. The mass and energy balances were solved with the simulator and the data was used to size the necessary equipment and to perform a comparative economic evaluation between the approaches and the technologies. Then, sensitivity on prices of raw materials and equilibrium price of products analyzes were performed. In all the scenarios, raw materials accounted for a large share of the total production costs. It was found that the final price of fatty acids is strongly influenced by the prices of these two inputs. It was identified that the economic viability of each of the technologies analyzed depends heavily on the current economic scenario as well as the accuracy of the models used to represent a process, as new research is conducted to optimize the models and the conditions of the process.

From this perspective, it is necessary to study the operation of this type of reactor in order to allow for further optimization of the process, which involves reactor design and operation. This is the case because the experimental methods for investigating flow behavior and chemical reactions are expensive. Hence, for simulation and process understanding purposes, a computational fluid dynamics (CFD) model of flow in a spray column reactor was developed alongside the simplified kinetic model so as to study the behavior of the hydrolysis of oil in an industrial scale. The methodology used in the development of this process has practically not been explored by researchers of the area, a fact that can be verified by the scarcity of works in the literature which uses this approach. The distribution of concentrations over time obtained for the components of the mixture by means of simulation describe satisfactorily the behavior reported in the literature. It is the literature from which the kinetic model and assumptions were obtained and the distribution of the mass

fractions of the substances in the reactor indicated efficient mixing. However, more exact results for validation can be achieved by employing data obtained in an industrial set-up.

The following suggestions for future work may be considered:

- Development of control strategies of the operating units as well as studies of plant initialization (start-up). This would allow decision making for optimization according to the dynamic behavior of the process.
- Investigation of the dependence of kinetic data on the raw material under varying composition, since a deeper knowledge of it it would bring the developed models closer to reality of industrial processing.
- Analysis of alternative raw materials, such as soybean oil, palm oil or lard to validate the proposed models. The use of the simulation in these cases can help in the planning of experiments in the laboratory stage.
- Analysis of heat transfer and mixing in the reactor by evaluating the effect of steam on the reacting system.
- Further validation of the CFD simulation with literature or industrial data by comparing experimental and simulated data.

CHAPTER 9

Supporting Information

Liquid-Liquid Equilibrium Calculations

Modified UNIFAC (Dortmund)

The modified UNIFAC (Dortmund) model has a combinatorial contribution ($\ln \gamma_i^C$) to the activity coefficient, which is directly related to differences in size and shape of the molecules, and a residual contribution ($\ln \gamma_i^R$) to define the energetic interactions between the molecules as presented by Gmehling et al Lohmann and Jürgen Gmehling 2001; Juergen Gmehling, J. Li, and Schiller 1993; Jürgen Gmehling, Lohmann, et al. 1998; Jürgen Gmehling, Wittig, et al. 2002; Jakob et al. 2006.

$$\ln \gamma_i = \ln \gamma_i^C + \ln \gamma_i^R \tag{A.1}$$

The combinatorial part is given by:

$$\ln \gamma_i^{'} = 1 - V_i^{'} + \ln V_i^{'} - 5q_i \left[1 - \frac{V_i}{F_i} + \ln\left(\frac{V_i}{F_i}\right)\right] \tag{A.2}$$

The pure-component parameters r_i and q_i are respectively, related to molecular van der Waals volume and molecular surface area. They are calculated as the sum of the group volume and group parameters, R_K and Q_K.

The mole fraction of component j in the mixture is denoted as z_j. Thus:

$$r_i = \sum_k v_k^{(i)} R_K \qquad q_i = \sum_k v_k^{(i)} Q_K \tag{A.3}$$

Where v_k^i, always an integer, is the number of groups of type k in the molecule i. The group parameters R_K and Q_K are normally obtained from van der Waals group volumes and surface areas.

The residual part is given by:

$$\ln \gamma_i^R = \sum_k v_k^{(i)} \left[\ln \Gamma_k - \ln \Gamma_k^{(i)} \right] \tag{A.4}$$

Γ_k is the group residual activity coefficient, and $\Gamma_k^{(i)}$ is the residual activity coefficient of group k in a reference solution containing only molecules of type i.

$$\ln \Gamma_k = Q_k \left[1 - \ln \left(\sum_m \theta_m \psi_{mk} \right) - \sum_m \frac{(\theta_m \psi_{mk})}{\sum\limits_n \theta_n \psi_{nk}} \right] \tag{A.5}$$

$$\theta_m = \frac{Q_m X_m}{\sum\limits_n Q_n X_n} \qquad X_m = \frac{\sum\limits_i v_m^{(i)} x_i}{\sum\limits_i \sum\limits_m v_k^{(i)} x_i} \tag{A.6}$$

The surface area fraction of group m in the mixture is represented by θ_m and X_m is the mole fraction of group m in the mixture. The group interaction parameter ψ_{nm} characterizes the interaction between groups m and n at temperature T through parameters a, b and c.

$$\Psi_{nm} = \exp \left(-\frac{a_{nm} + b_{nm} T + c_{nm} T^2}{T} \right) \tag{A.7}$$

Liquid-Liquid Equilibrium Algorithm

The equilibrium for a liquid – liquid system is defined by the equation:

$$\gamma_i^\alpha z_i^\alpha = \gamma_i^\beta z_i^\beta \qquad i = 1, 2, 3..., Component \tag{A.8}$$

Where γ_i, the activity coefficient of component i in phase (α or β), is predicted using the modified UNIFAC (Dortmund) model. z_i^α and z_i^β represent the mole fraction of component i in phase α and β respectively.

The algorithm is summarized as a flow diagram in Figure A.1 as proposed and presented by O'Connell and Haile O'Connell and Haile 2005. If the system

temperature and pressure are known (as they usually are for liquid-liquid equilibrium situations), then the problem can be posed as an analogy to isothermal flash calculations. In such an approach, the known quantities are temperature T, pressure P and the set of overall system mole fractions z. The following relation can be defined:

$$z_i = \frac{n_i}{n_{Total}} = \frac{n_i^\alpha + n_i^\beta}{n_{Total}^\alpha + n_{Total}^\beta} \tag{A.9}$$

Then the quantities to be computed would be the mole fractions in each phase, z^α and z^β, and the fraction of total material in one phase, $R = \frac{n_i^\beta}{n_{Total}}$.

Distributions coefficients for each component m_i are defined by $m_i = \frac{z_i^\beta}{z_i^\alpha}$. In order to calculate the required mole fractions, a gamma-gamma formulation for the phase equilibrium equations needs to be expressed in terms of the distribution coefficients as:

$$m_i = \frac{z_i^\beta}{z_i^\alpha} = \frac{\gamma_i^\alpha}{\gamma_i^\beta} \qquad i = 1, 2, \ldots, Component \tag{A.10}$$

For each component i in the liquid-liquid system, a material balance is written as:

$$z_i^\alpha (1 - R) + z_i^\beta R = z_i \tag{A.11}$$

Where $R = \frac{n_i^\beta}{n_{Total}}$. Then, by using Equation (A.10) for the distribution coefficients, it is possible to eliminate z_i^β in favor of z_i^α:

$$z_i^\alpha (1 - R) + z_i^\alpha m_i R = z_i \tag{A.12}$$

Solving for z_i^α and z_i^β:

$$z_i^\alpha = \frac{z_i}{1 + R(m_i - 1)} \qquad z_i^\beta = \frac{z_i m_i}{1 + R(m_i - 1)} \tag{A.13}$$

However, the mole fractions in each phase must sum to unity, therefore, a Rachford-Rice type function F must be defined as Rachford and Rice 1952:

$$F \equiv \sum_{i}^{m} z_i^{\beta} - \sum_{i}^{m} z_i^{\alpha} = \sum_{i}^{m} \frac{z_i \left(m_i - 1\right)}{1 + R \left(m_i - 1\right)} = 0 \tag{A.14}$$

This Rachford-Rice type function is one equation in the unknown R, independent of the number of components present, which readily lends itself to a solution by Newton's method. A flow diagram for solving this problem is shown in Figure A.1.

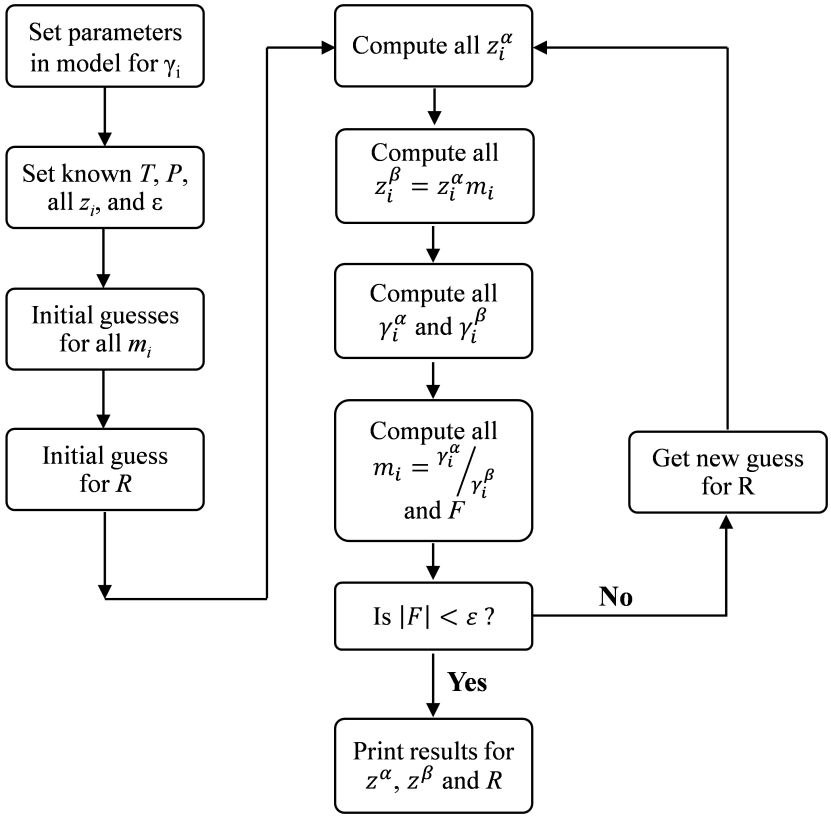

Figure A.1: Rachford-Rice algorithm applied to the gamma-gamma method for solving multicomponent liquid-liquid equilibrium problems (adapted from O'Connel et al. O'Connell and Haile 2005).

Results of the Sobol' sensitivity analysis

In this section (Tables A.1 to A.4), we provide original numerical values coming out from the sensitivity analysis. Values from Tables A.1 to A.4 were used to produce plots for triglycerides and fatty acids in the main text, and Figure A.2 and A.3; which were also used to discuss the results of the sensitivity analysis.

First order Sobol' sensitivity indices												
	0.5 h	**1 h**	**1.5 h**	**2 h**	**2.5 h**	**3 h**	**3.5 h**	**4 h**	**4.5 h**	**5 h**	**5.5 h**	**6 h**
k_1	0.522	0.584	0.583	0.483	0.379	0.300	0.241	0.193	0.155	0.126	0.102	0.084
k_{-1}	0.001	0.022	0.131	0.306	0.430	0.472	0.463	0.428	0.382	0.334	0.290	0.253
k_2	0.000	0.000	0.004	0.037	0.101	0.165	0.207	0.223	0.221	0.207	0.188	0.168
k_{-2}	0.000	0.000	0.000	0.002	0.013	0.041	0.084	0.130	0.169	0.195	0.208	0.212
k_3	0.000	0.000	0.001	0.002	0.002	0.001	0.000	0.003	0.009	0.018	0.026	0.031
k_{-3}	0.000	0.000	0.000	0.000	0.000	0.000	0.000	0.000	0.002	0.005	0.011	0.019
k_4	0.000	0.000	0.001	0.001	0.000	0.000	0.000	0.000	0.000	0.000	0.000	0.000
k_{-4}	0.000	0.001	0.003	0.003	0.001	0.000	0.000	0.000	0.000	0.000	0.000	0.000
$k_{1L,a}$	0.477	0.392	0.278	0.166	0.071	0.017	0.001	0.017	0.054	0.104	0.160	0.215
$k_{2L,a}$	0.000	0.000	0.000	0.000	0.000	0.000	0.000	0.000	0.000	0.001	0.003	0.005
$\sum S_i$	1.000	1.000	1.000	0.999	0.998	0.997	0.996	0.994	0.993	0.990	0.987	0.985

Total Sobol' sensitivity indices												
	0.5 h	**1 h**	**1.5 h**	**2 h**	**2.5 h**	**3 h**	**3.5 h**	**4 h**	**4.5 h**	**5 h**	**5.5 h**	**6 h**
k_1	0.523	0.584	0.583	0.483	0.380	0.301	0.242	0.195	0.158	0.129	0.105	0.086
k_{-1}	0.001	0.022	0.131	0.307	0.432	0.475	0.466	0.433	0.387	0.341	0.297	0.260
k_2	0.000	0.000	0.005	0.038	0.102	0.167	0.209	0.226	0.224	0.211	0.192	0.172
k_{-2}	0.000	0.000	0.000	0.002	0.013	0.042	0.084	0.131	0.171	0.198	0.213	0.218
k_3	0.000	0.000	0.001	0.002	0.002	0.001	0.000	0.003	0.010	0.018	0.027	0.032
k_{-3}	0.000	0.000	0.000	0.000	0.000	0.000	0.000	0.000	0.002	0.006	0.012	0.020
k_4	0.000	0.000	0.001	0.001	0.000	0.000	0.000	0.000	0.000	0.000	0.000	0.000
k_{-4}	0.000	0.001	0.003	0.003	0.001	0.000	0.000	0.000	0.000	0.000	0.000	0.000
$k_{1L,a}$	0.477	0.393	0.278	0.166	0.071	0.017	0.002	0.017	0.055	0.107	0.164	0.221
$k_{2L,a}$	0.000	0.000	0.000	0.000	0.000	0.000	0.000	0.000	0.000	0.001	0.003	0.006
$\sum S_{Ti}$	1.000	1.000	1.001	1.001	1.002	1.003	1.004	1.006	1.007	1.010	1.013	1.015

Table A.1: First order and total Sobol sensitivity indices of the model outputs n_{TG} for the hydrolysis at 180°C - 1:27.5 oil-to-water molar ratio - 600 rpm.

First order Sobol' sensitivity indices												
	0.5 h	**1 h**	**1.5 h**	**2 h**	**2.5 h**	**3 h**	**3.5 h**	**4 h**	**4.5 h**	**5 h**	**5.5 h**	**6 h**
k_1	0.607	0.249	0.006	0.003	0.012	0.014	0.013	0.012	0.009	0.008	0.006	0.005
k_{-1}	0.001	0.020	0.022	0.015	0.006	0.002	0.000	0.000	0.000	0.001	0.000	0.000
k_2	0.071	0.708	0.788	0.749	0.714	0.657	0.584	0.509	0.439	0.376	0.325	0.274
k_{-2}	0.000	0.003	0.021	0.070	0.157	0.261	0.351	0.409	0.437	0.443	0.433	0.415
k_3	0.000	0.000	0.001	0.002	0.007	0.017	0.033	0.051	0.068	0.082	0.090	0.096
k_{-3}	0.000	0.000	0.000	0.000	0.000	0.002	0.005	0.013	0.026	0.042	0.059	0.081
k_4	0.000	0.001	0.001	0.001	0.000	0.000	0.000	0.000	0.000	0.000	0.000	0.000
k_{-4}	0.001	0.008	0.005	0.003	0.001	0.001	0.000	0.000	0.000	0.000	0.000	0.000
$k_{1L,a}$	0.320	0.009	0.155	0.157	0.101	0.045	0.010	0.001	0.011	0.032	0.057	0.086
$k_{2L,a}$	0.000	0.000	0.000	0.000	0.000	0.000	0.001	0.002	0.005	0.011	0.020	0.031
$\sum S_i$	0.999	0.998	0.999	0.999	0.999	0.999	0.998	0.997	0.996	0.994	0.991	0.989

Total Sobol' sensitivity indices												
	0.5 h	**1 h**	**1.5 h**	**2 h**	**2.5 h**	**3 h**	**3.5 h**	**4 h**	**4.5 h**	**5 h**	**5.5 h**	**6 h**
k_1	0.608	0.250	0.007	0.004	0.012	0.014	0.013	0.012	0.009	0.008	0.006	0.005
k_{-1}	0.001	0.020	0.022	0.015	0.006	0.002	0.000	0.000	0.001	0.001	0.001	0.001
k_2	0.071	0.709	0.789	0.750	0.715	0.658	0.585	0.510	0.440	0.378	0.327	0.277
k_{-2}	0.000	0.003	0.021	0.070	0.158	0.262	0.353	0.412	0.441	0.448	0.439	0.422
k_3	0.000	0.000	0.001	0.002	0.007	0.018	0.034	0.052	0.070	0.084	0.093	0.099
k_{-3}	0.000	0.000	0.000	0.000	0.000	0.002	0.006	0.014	0.027	0.044	0.062	0.086
k_4	0.000	0.001	0.001	0.001	0.000	0.000	0.000	0.000	0.000	0.000	0.000	0.000
k_{-4}	0.001	0.008	0.006	0.003	0.001	0.001	0.000	0.000	0.000	0.000	0.000	0.000
$k_{1L,a}$	0.321	0.010	0.156	0.157	0.101	0.046	0.010	0.001	0.011	0.032	0.059	0.088
$k_{2L,a}$	0.000	0.000	0.000	0.000	0.000	0.000	0.001	0.002	0.006	0.012	0.022	0.034
$\sum S_{Ti}$	1.001	1.002	1.001	1.001	1.001	1.001	1.002	1.003	1.005	1.006	1.009	1.011

Table A.2: First order and total Sobol sensitivity indices of the model outputs n_{DG} for the hydrolysis at 180°C - 1:27.5 oil-to-water molar ratio - 600 rpm.

First order Sobol' sensitivity indices												
	0.5 h	**1 h**	**1.5 h**	**2 h**	**2.5 h**	**3 h**	**3.5 h**	**4 h**	**4.5 h**	**5 h**	**5.5 h**	**6 h**
k_1	0.138	0.142	0.110	0.034	0.003	0.000	0.002	0.003	0.003	0.003	0.003	0.003
k_{-1}	0.000	0.002	0.010	0.018	0.014	0.008	0.004	0.002	0.001	0.000	0.000	0.000
k_2	0.351	0.455	0.466	0.224	0.056	0.008	0.000	0.002	0.005	0.007	0.007	0.008
k_{-2}	0.000	0.002	0.020	0.047	0.052	0.044	0.032	0.022	0.013	0.009	0.005	0.003
k_3	0.003	0.049	0.290	0.652	0.780	0.768	0.713	0.625	0.535	0.449	0.374	0.317
k_{-3}	0.000	0.000	0.003	0.020	0.060	0.122	0.196	0.281	0.345	0.386	0.410	0.415
k_4	0.000	0.000	0.000	0.000	0.000	0.000	0.000	0.000	0.000	0.000	0.000	0.000
k_{-4}	0.001	0.001	0.001	0.000	0.000	0.000	0.000	0.000	0.000	0.000	0.000	0.000
$k_{1L,a}$	0.504	0.349	0.098	0.002	0.030	0.038	0.022	0.007	0.001	0.003	0.009	0.016
$k_{2L,a}$	0.000	0.000	0.000	0.001	0.003	0.011	0.027	0.052	0.086	0.129	0.175	0.217
$\sum S_i$	0.997	0.999	0.998	0.997	0.999	0.998	0.996	0.993	0.990	0.986	0.982	0.978

Total Sobol' sensitivity indices												
	0.5 h	**1 h**	**1.5 h**	**2 h**	**2.5 h**	**3 h**	**3.5 h**	**4 h**	**4.5 h**	**5 h**	**5.5 h**	**6 h**
k_1	0.139	0.142	0.111	0.035	0.004	0.000	0.002	0.003	0.004	0.003	0.003	0.003
k_{-1}	0.000	0.002	0.010	0.018	0.014	0.008	0.005	0.002	0.001	0.000	0.000	0.000
k_2	0.354	0.455	0.467	0.225	0.057	0.008	0.001	0.003	0.006	0.008	0.008	0.008
k_{-2}	0.000	0.002	0.020	0.048	0.052	0.044	0.033	0.023	0.015	0.010	0.006	0.004
k_3	0.003	0.049	0.292	0.654	0.780	0.768	0.713	0.626	0.535	0.450	0.375	0.318
k_{-3}	0.000	0.000	0.003	0.020	0.061	0.123	0.199	0.286	0.355	0.399	0.426	0.436
k_4	0.000	0.000	0.000	0.000	0.000	0.000	0.000	0.000	0.000	0.000	0.000	0.000
k_{-4}	0.001	0.001	0.001	0.000	0.000	0.000	0.000	0.000	0.000	0.000	0.000	0.000
$k_{1L,a}$	0.507	0.349	0.099	0.003	0.031	0.038	0.023	0.007	0.001	0.003	0.009	0.017
$k_{2L,a}$	0.000	0.000	0.000	0.001	0.004	0.012	0.030	0.058	0.095	0.141	0.191	0.237
$\sum S_{Ti}$	1.003	1.001	1.002	1.003	1.001	1.002	1.004	1.007	1.010	1.014	1.018	1.022

Table A.3: First order and total Sobol sensitivity indices of the model outputs n_{MG} for the hydrolysis at 180°C - 1:27.5 oil-to-water molar ratio - 600 rpm.

First order Sobol' sensivitity indices												
	0.5 h	**1 h**	**1.5 h**	**2 h**	**2.5 h**	**3 h**	**3.5 h**	**4 h**	**4.5 h**	**5 h**	**5.5 h**	**6 h**
k_1	0.421	0.318	0.229	0.171	0.134	0.107	0.084	0.066	0.052	0.040	0.032	0.026
k_{-1}	0.001	0.008	0.024	0.042	0.055	0.062	0.064	0.062	0.056	0.051	0.044	0.039
k_2	0.027	0.142	0.279	0.376	0.421	0.423	0.392	0.341	0.291	0.240	0.201	0.167
k_{-2}	0.000	0.001	0.006	0.024	0.058	0.102	0.144	0.172	0.184	0.189	0.182	0.174
k_3	0.000	0.006	0.032	0.082	0.143	0.198	0.234	0.245	0.240	0.223	0.204	0.185
k_{-3}	0.000	0.000	0.000	0.002	0.010	0.028	0.058	0.093	0.126	0.153	0.177	0.192
k_4	0.000	0.000	0.000	0.000	0.000	0.000	0.000	0.000	0.000	0.000	0.000	0.000
k_{-4}	0.000	0.000	0.000	0.000	0.000	0.000	0.000	0.000	0.000	0.000	0.000	0.000
$k_{1L,a}$	0.551	0.526	0.429	0.303	0.178	0.075	0.016	0.002	0.017	0.052	0.086	0.121
$k_{2L,a}$	0.000	0.000	0.000	0.000	0.001	0.003	0.007	0.016	0.030	0.047	0.066	0.085
$\sum S_i$	0.999	0.999	1.000	1.000	0.999	0.999	0.999	0.998	0.996	0.995	0.992	0.989

Total Sobol' sensitivity indices												
	0.5 h	**1 h**	**1.5 h**	**2 h**	**2.5 h**	**3 h**	**3.5 h**	**4 h**	**4.5 h**	**5 h**	**5.5 h**	**6 h**
k_1	0.422	0.318	0.229	0.171	0.134	0.107	0.084	0.066	0.052	0.040	0.032	0.026
k_{-1}	0.001	0.008	0.024	0.042	0.055	0.063	0.065	0.062	0.056	0.051	0.045	0.040
k_2	0.027	0.143	0.280	0.376	0.421	0.424	0.392	0.341	0.291	0.240	0.201	0.168
k_{-2}	0.000	0.001	0.006	0.024	0.059	0.103	0.144	0.173	0.185	0.190	0.183	0.176
k_3	0.000	0.006	0.032	0.082	0.143	0.198	0.234	0.245	0.241	0.224	0.205	0.185
k_{-3}	0.000	0.000	0.000	0.002	0.010	0.029	0.059	0.095	0.129	0.157	0.184	0.200
k_4	0.000	0.000	0.000	0.000	0.000	0.000	0.000	0.000	0.000	0.000	0.000	0.000
k_{-4}	0.000	0.000	0.000	0.000	0.000	0.000	0.000	0.000	0.000	0.000	0.000	0.000
$k_{1L,a}$	0.551	0.526	0.429	0.303	0.178	0.076	0.016	0.003	0.018	0.052	0.087	0.123
$k_{2L,a}$	0.000	0.000	0.000	0.000	0.001	0.003	0.008	0.018	0.032	0.051	0.072	0.093
$\sum S_{Ti}$	1.001	1.001	1.000	1.000	1.001	1.001	1.001	1.002	1.004	1.005	1.008	1.011

Table A.4: First order and total Sobol sensitivity indices of the model outputs n_{FA} for the hydrolysis at 180°C - 1:27.5 oil-to-water molar ratio - 600 rpm.

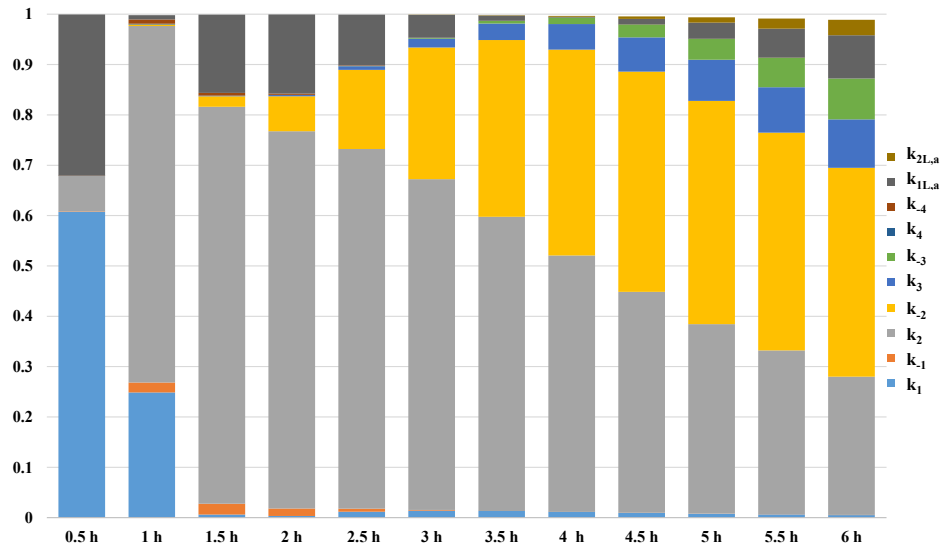

Figure A.2: Contribution to the variations in the model output n_{DG} over time using Sobol sensitivity indices for the hydrolysis at 180°C - 1:27.5 oil-to-water molar ratio - 600 rpm.

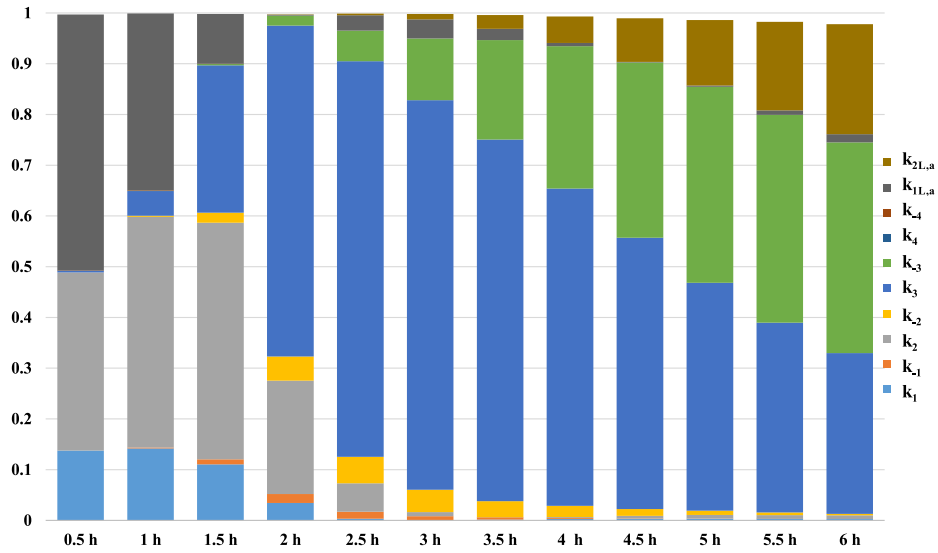

Figure A.3: Contribution to the variations in the model output n_{MG} over time using Sobol sensitivity indices for the hydrolysis at 180°C - 1:27.5 oil-to-water molar ratio - 600 rpm.

Sizing and costing of selected equipment

9.0.1 Pumps

In this work, pumps PUMP1 and PUMP2 were designed as positive displacement pumps of stainless steel, due to the high power required to reach the 4000 kPa. For the other pumps, the simplest option was chosen between centrifugal pumps and external gear pumps, all made of carbon steel. All other pumps were designed as external gear pumps.

The cost of centrifugal pumps can be obtained from Equation (A.15).

$$C_P = F_T F_M C_B \tag{A.15}$$

The F_T factor is relative to the type of pump, which can be considered equal to 1 for one stage pumps with vertical orientation and 3600 rpm. F_M is a material factor. For carbon steel pumps, it equals to 1.35. C_B is given by Equation (A.16). This equation depends on S, which is the pump size factor. It is a function of the flow Q which is passing through the pump $\left(\frac{gallon}{min}\right)$ and the manometric head H (ft), as presented in Equation (A.17).

$$C_B = \exp\left(9.2951 - 0.6019\ln(S) + 0.0519\left(\ln(S)\right)^2\right) \tag{A.16}$$

$$S = QH^0.5 \tag{A.17}$$

For an external gear pump, the cost can be obtained by Equations (A.18) and (A.19). The cost depends on the flow Q which the pump processes in $\left(\frac{gallon}{min}\right)$ and the same material factor as the cost of the centrifugal pump.

$$C_P = F_M C_B \tag{A.18}$$

$$C_B = \exp\left(7.2744 + 0.1986\ln(Q) + 0.0291\left(\ln(Q)\right)^2\right) \tag{A.19}$$

Equation (A.18) also applies to positive displacement pumps. However, C_B takes the form of Equation (A.20), which is a function of the power consumed by the motor coupled to the pump. The material factor for stainless steel

positive displacement pumps is 2.2. A 90% efficiency was assumed for these pumps.

$$C_B = \exp\left(7.3883 - 0.26986\ln(P_C) + 0.06718\left(\ln(P_C)\right)^2\right) \tag{A.20}$$

9.0.2 Electric motors

To operate, a pump depends on an electric motor, the cost of which is not included in Equations (A.15) and (A.18). The cost of the electric motors for pumping systems is described by Equation (A.21).

$$C_M = F_T C_B \tag{A.21}$$

The F_T factor depends on the type of motor. For the present case, it is recommended to use explosion proof motors whose F_T value is 1.8. In addition, the cost of the motors will depend on the power consumed, according to Equation (A.22).

$$\begin{aligned} C_B = &\exp(5.48663 + 0.13141\ln(P_C) + 0.053255\left(\ln(P_C)\right)^2 \\ &+ 0.028628\left(\ln(P_C)\right)^3 - 0.0035548\left(\ln(P_C)\right)^4) \end{aligned} \tag{A.22}$$

To estimate the power consumed by the motor, Equation (A.22) can be used:

$$P_C = \frac{QH_\rho}{33000\eta_P\eta M} \tag{A.23}$$

In this equation, Q is the flow through the pump $\left(\frac{gallon}{min}\right)$, H is the manometric height (ft) and ρ is the density of the liquid $\left(\frac{gallon}{min}\right)$. η_P and η_M are given by Equations (A.24) and (A.25).

$$\eta_P = -0.316 + 0.2401\ln(Q) - 0.01199\left(\ln(Q)\right)^2 \tag{A.24}$$

$$\eta_M = 0.8 + \left(\ln\left(\frac{QH_\rho}{33000\eta_P}\right)\right) - 0.00182\left(\ln\left(\frac{QH_\rho}{33000\eta_P}\right)\right)^2 \tag{A.25}$$

9.0.3 Heat exchangers

The cost of shell and tube heat exchangers can be obtained by Equations (A.26) and (A.27). In them, A_T represents the area of thermal exchange, or more precisely, the outer area of the tubes.

$$C_{TC} = F_P F_M F_L C_B \tag{A.26}$$

$$C_B = \exp(11.667 - 0.8709 \ln(A_T) + 0.09005 (\ln(A_T))^2 \tag{A.27}$$

The F_M factor is related to the construction materials of the exchangers and is given by Equation (A.28).

$$F_M = a + \left(\frac{A}{100}\right)^2 \tag{A.28}$$

Most plant heat exchangers are constructed solely of carbon steel. In this case, both a and b are equal to zero. The HX1, HX1-A and HX1-B exchanger must be constructed entirely of stainless steel, due to the high corrosive power of the materials. In this case, a is equal to 2.7 and b is equal to 0.07.

The F_P factor is a cost correction factor for a pressure reinforcement on the side of the shell. The HX1, HX1-A and HX1-B exchangers must take this factor into account due to the high pressures of the streams or utilities involved. To determine F_P, Equation (A.30) is used, which is a function of the pressure on the side of the shell (psig).

$$F_P = 0.9803 + 0.018 \left(\frac{P}{100}\right) + 0.0017 \left(\frac{P}{100}\right)^2 \tag{A.29}$$

The F_L factor is a pipe length correction. All heat exchangers were designed with a length of 8 ft, for which F_L is equal to 1.25.

The coils, used in the temperature control of the reactors and flash vessels, had their purchase cost estimated by Equation (A.31).

$$C_{\text{coil}} = \exp(7.8375 + 0.4343 \ln(A_T) + 0.03812 (\ln(A_T))^2 \tag{A.30}$$

9.0.4 Distillation columns

The cost of the distillation columns was obtained through Equation (A.31).C_V is the cost of the vessel, which depends on its weight W (lb) according to Equation (A.32). The weight of the vessel can be obtained by Equation (A.33). In this equation, D is the internal diameter of the column, L is the height of the column, t_s is the wall thickness of the column and ρ_S is the density of carbon steel, which can be taken equal to 0.284 $\frac{lb}{in^3}$ for a preliminary design.

$$C_{DC} = F_M C_V + C_{PL} \tag{A.31}$$

$$C_V = \exp(7.0374 + 0.18255 \ln(W) + 0.02297 (\ln(W))^2 \tag{A.32}$$

$$W = \pi (D + t_s) (L + 0.8D) t_s \rho_s \tag{A.33}$$

C_{PL} is the cost related to the installation of platforms and ladders and is given by Equation (A.34).

$$C_{PL} = 237.1 D^{0.6331} L^{0.80161} \tag{A.34}$$

Wall thickness of the column depends on whether it operates at atmospheric pressure or under vacuum. For the columns at atmospheric pressure (COL1), the thickness is calculated by Equation (A.35)

$$t_s = \frac{10D}{2SE - 12} \tag{A.35}$$

.

In this equation, D is the inner diameter of the column. S is the maximum stress allowed for column construction material at operating temperature. For the cases present in this work, the value of 13.750 psi was adopted. The term E corresponds to the soldering efficiency. The value of 0.85 was adopted due to the walls of the columns were not very thick.

The thickness calculated by Equation (A.35) does not necessarily correspond to the final thickness. For the sake of structural safety, a minimum thickness is required for each column diameter. These specifications are given in Table A.5.

Vessel diameter (ft)	Minimum thickness (in)
To 4	1/4
4-6	5/16
6-8	3/8
8-10	7/16
10-12	1/2

Table A.5: Minimum diameters for the wall of vertical vessels.

After the thickness is obtained by Equation (A.35) or Table A.5, $\frac{1}{4}$ in should be added to the column wall to deal with the corrosion of the material. The F_M factor depends on the type of material. All columns were designed in carbon steel, hence the value of F_M was always equal to 1. For vacuum columns, Equation (A.36) should be used to determine the thickness of the walls.

$$t_s = 1.3 D_0 \left(\frac{PL}{E_M D_0} \right)^{0.4} \tag{A.36}$$

In this equation, D_0 is the outer diameter of the column (in), P is the lowest operating pressure (psig), L is the height of the column (in), and E_M is the elasticity modulus of the building material (psi) which is obtained in the highest operating temperature (°F) according to Equation (A.37). The following situation was obtained by linear interpolation of the data presented by Seader et al (Seader, Seider, and Lewin 2004).

$$E_M = (30.4342 - 0.00629T)\, x10^6 \tag{A.37}$$

The vacuum columns must also be equipped with vacuum apparatus. Their cost can be obtained by Equation (A.38).

$$C_{\text{vacuum}} = 1.8x1.33x \left(\frac{G}{P} \right)^{0.41} \tag{A.38}$$

In this expression, G is the mass vapor flow at the vacuum generation point $\left(\frac{lb}{h}\right)$ and P is the desired pressure (torr).

In addition to the costs related to the vessel, the cost of the vessels also involves the purchase price of the vessel. 1 in Metal Pall rings cost around 39 $\frac{US\$}{ft^3}$ and 2-in metal Pall rings cost around 25 $\frac{US\$}{ft^3}$. The required filling volume

can be obtained from the inner diameter of the column and the height of the column except for condenser and reboilers.

9.0.5 Reactors

The calculation of the cost of the reactors is similar to the cost calculation of the distillation columns given by Equation (A.31). However, the expression for the cost estimate of the vessel is different. The reactors were designed as horizontal vessels, whose cost can be estimated by Equation (A.39).

$$C_V = \exp(8.717 - 0.233\ln(W) + 0.04333\,(\ln(W))^2 \tag{A.39}$$

The weight of the vessels is also obtained by Equation (A.33) and the wall thickness is obtained by Equation (A.35), with the same corrections made to the distillation column. The cost with the installation of platforms and ladders must be obtained by Equation (A.40) for the horizontal vessel and by Equation (A.41) for the vertical vessel, where D is the inner diameter of the vessel (ft) and L is the height (ft).

$$C_{PL} = 1580D^{0.20294} \tag{A.40}$$

$$C_{PL} = 285.1D^{0.20294}L^{0.70684} \tag{A.41}$$

For reactors which are operating at high temperature and pressure, made of stainless steel, the cost of the vessel should be multiplied by a material factor of 2.1.

9.0.6 Decanter

The decanter, used for the separation of glycerol, was sized as a horizontal vessel. To determine its purchase cost, Equations (A.31) and (A.39) were used.

9.0.7 Flash vessels

Flash vessels are vertical vessels equipped with a vacuum system. To determine their cost, Equation (A.39) is used. Equation (A.38) is used to determine the cost of the vacuum apparatus.

Heat exchangers			
HX1		**HX3**	
Heat exchanged (MJ/hr)	44.737	Heat exchanged (MJ/hr)	39.831
Heat exchange area (m^2)	172.734	Heat exchange area (m^2)	261.388
HE coeff. (KJ/°C m^2 hr)	1227.451	HE coeff. (KJ/°C m^2 hr)	1022.876
Utilities flow (kg/hr)	140991.1	Utilities flow (kg/hr)	952794.1
Cost (US$)	208310.4	Cost (US$)	709694.4
HX3			
Heat exchanged (MJ/hr)	2.058		
Heat exchange area (m^2)	65.405		
HE coeff. (KJ/°C m^2 hr)	1022.876		
Utilities flow (kg/hr)	42943.11		
Cost (US$)	33628.8		
Pumps			
PUMP1		**PUMP2**	
Volumetric flow (m^3/hr)	13.85	Volumetric flow (m^3/hr)	38.372
Pressure added (kPa)	19898.7	Pressure added (kPa)	19898.7
Power (HP)	125.318	Power (HP)	342.284
Electricity (KW)	93.487	Electricity (KW)	255.344
Cost (US$)	21476.18	Cost (US$)	49951.67
Reactor			
Temperature °C	250		
Pressure (kPa)	4007		
Height/Diameter (m)	8.88/2.96		
Utilities flow (kg/hr)	17552.61		
Cost of cooling coil (US$)	297160.5		
Cost (US$)	2847831		
Decanter			
Length/Diameter (m)	2.33/0.58		
Cost (US$)	13265.65		
Distillation columns			
COL1		**COL2**	
Temp. - Top/Bottom (°C)	78.2/104.78	Temp. - Top/Bottom (°C)	121.75/400
Press.- Top/Bottom (kPa)	101.3/111.3	Press. - Top/Bottom (kPa)	10/20
Height/Diameter (m)	12.24/2.73	Height/Diameter (m)	13.37/2.76
Heat in condenser (kJ/hr)	78.67	Heat in condenser (kJ/hr)	21.7
Heat in reboiler (kJ/hr)	76.45	Heat in reboiler (kJ/hr)	24.47
Utilities-Condenser (kg/hr)	3786675	Utilities-Condenser (kg/hr)	1044609.81
Utilities-Reboiler (kg/hr)	42103.13	Utilities-Reboiler (kg/hr)	121130.43
Theoretical stages	5	Theoretical stages	5
Reflux ratio (molar)	2	Reflux ratio (molar)	2
Cost (US$)	234830.6	Cost (US$)	212206.9
Cost of condenser (US$)	88664.38	Cost of condenser (US$)	69914.73
Cost of reboiler (US$)	34308.92	Cost of reboiler (US$)	34527.24

Table A.6: Equipment for Scenario 1 - **Base case**.

Heat exchangers			
HX1A		**HX1B**	
Heat exchanged (MJ/hr)	9.753	Heat exchanged (MJ/hr)	25.038
Heat exchange area (m^2)	316.046	Heat exchange area (m^2)	3026.36
HE coeff. (KJ/°C m^2 hr)	409.15	HE coeff. (KJ/°C m^2 hr)	409.15
Utilities flow (kg/hr)	0	Utilities flow (kg/hr)	0
Cost (US$)	795185	Cost (US$)	5080255
HX1		**HX3**	
Heat exchanged (MJ/hr)	9.951	Heat exchanged (MJ/hr)	2.058
Heat exchange area (m^2)	92.03	Heat exchange area (m^2)	65.406
HE coeff. (KJ/°C m^2 hr)	1227.451	HE coeff. (KJ/°C m^2 hr)	1022.876
Utilities flow (kg/hr)	31362.36	Utilities flow (kg/hr)	49245.09
Cost (US$)	156940.3	Cost (US$)	33628.94
Pumps			
PUMP1		**PUMP2**	
Volumetric flow (m^3/hr)	13.85	Volumetric flow (m^3/hr)	38.372
Pressure added (kPa)	19898.7	Pressure added (kPa)	19898.7
Power (HP)	125.318	Power (HP)	342.284
Electricity (KW)	93.487	Electricity (KW)	255.344
Cost (US$)	21476.18	Cost (US$)	49951.67
Reactor			
Temperature °C	250		
Pressure (kPa)	4007		
Height/Diameter (m)	8.88/2.96		
Utilities flow (kg/hr)	17552.61		
Cost of cooling coil (US$)	297160.5		
Cost (US$)	2847831		
Decanter			
Length/Diameter (m)	2.33/0.58		
Cost (US$)	13265.64		
Distillation columns			
COL1		**COL2**	
Temp. - Top/Bottom (°C)	78.2/104.78	Temp. - Top/Bottom (°C)	121.75/400
Press.- Top/Bottom (kPa)	101.3/111.3	Press. - Top/Bottom (kPa)	10/20
Height/Diameter (m)	12.24/2.73	Height/Diameter (m)	13.37/2.76
Heat in condenser (kJ/hr)	78.67	Heat in condenser (kJ/hr)	21.7
Heat in reboiler (kJ/hr)	76.45	Heat in reboiler (kJ/hr)	24.47
Utilities-Condenser (kg/hr)	3786674.88	Utilities-Condenser (kg/hr)	1044609.81
Utilities-Reboiler (kg/hr)	42103.13	Utilities-Reboiler (kg/hr)	121130.43
Theoretical stages	5	Theoretical stages	5
Reflux ratio (molar)	2	Reflux ratio (molar)	2
Cost (US$)	234830.6	Cost (US$)	212206.9
Cost of condenser (US$)	88664.38	Cost of condenser (US$)	69914.73
Cost of reboiler (US$)	34308.92	Cost of reboiler (US$)	34527.24

Table A.7: Equipment for Scenario 2 - **Base case**.

Heat exchangers			
HX1A		**HX1B**	
Heat exchanged (MJ/hr)	9.118	Heat exchanged (MJ/hr)	25.56
Heat exchange area (m^2)	316.227	Heat exchange area (m^2)	3067.14
HE coeff. (KJ/°C m^2 hr)	409.15	HE coeff. (KJ/°C m^2 hr)	409.15
Utilities flow (kg/hr)	0	Utilities flow (kg/hr)	0
Cost (US$)	795465.9	Cost (US$)	5150560
HX1		**HX3**	
Heat exchanged (MJ/hr)	9.36	Heat exchanged (MJ/hr)	2.059
Heat exchange area (m^2)	89.529	Heat exchange area (m^2)	65.404
HE coeff. (KJ/°C m^2 hr)	1227.451	HE coeff. (KJ/°C m^2 hr)	1022.876
Utilities flow (kg/hr)	29499.37	Utilities flow (kg/hr)	49270.26
Cost (US$)	155261.9	Cost (US$)	33628.57
Pumps			
PUMP1		**PUMP2**	
Volumetric flow (m^3/hr)	14.011	Volumetric flow (m^3/hr)	38.299
Pressure added (kPa)	19898.7	Pressure added (kPa)	19898.7
Power (HP)	126.749	Power (HP)	341.637
Electricity (KW)	94.555	Electricity (KW)	254.861
Cost (US$)	21682.97	Cost (US$)	49877.68
PUMP3			
Volumetric flow (m^3/hr)	0.9202		
Pressure added (kPa)	81.3		
Power (HP)	0.0518		
Electricity (KW)	0.0386		
Cost (US$)	4195.92		
Reactor		**Flash vessel FLASH1**	
Temperature °C	250	Temperature °C	80
Pressure (kPa)	4007	Pressure (kPa)	30
Height/Diameter (m)	8.88/2.96	Height/Diameter (m)	2.19/0.6
Utilities flow (kg/hr)	17504.3	Utilities flow (kg/hr)	298.57
Cost of cooling coil (US$)	296378.1	Cost of cooling coil (US$)	20454.24
Cost (US$)	2846697	Cost (US$)	42061.52
Decanter			
Length/Diameter (m)	2.33/0.58		
Cost (US$)	13264.52		
Distillation columns			
COL1		**COL2**	
Temp. - Top/Bottom (°C)	78.21/104.84	Temp. - Top/Bottom (°C)	121.79/400
Press.- Top/Bottom (kPa)	101.3/111.3	Press. - Top/Bottom (kPa)	10/20
Height/Diameter (m)	12.18/2.73	Height/Diameter (m)	13.37/2.76
Heat in condenser (kJ/hr)	78.53	Heat in condenser (kJ/hr)	21.7
Heat in reboiler (kJ/hr)	71.22	Heat in reboiler (kJ/hr)	24.47
Utilities-Condenser (kg/hr)	3780156.72	Utilities-Condenser (kg/hr)	1044469.52
Utilities-Reboiler (kg/hr)	39226.13	Utilities-Reboiler (kg/hr)	121114.62
Theoretical stages	5	Theoretical stages	5
Reflux ratio (molar)	2	Reflux ratio (molar)	2
Cost (US$)	231932.8	Cost (US$)	212192.8
Cost of condenser (US$)	88547.61	Cost of condenser (US$)	69889.14
Cost of reboiler (US$)	33233.06	Cost of reboiler (US$)	34525.15

Table A.8: Equipment for Scenario 3 - **Base case**.

Heat exchangers			
HX1		**HX3**	
Heat exchanged (MJ/hr)	48.843	Heat exchanged (MJ/hr)	42.381
Heat exchange area (m^2)	188.936	Heat exchange area (m^2)	278.124
HE coeff. (KJ/°C m^2 hr)	1227.451	HE coeff. (KJ/°C m^2 hr)	1022.876
Utilities flow (kg/hr)	153930.8	Utilities flow (kg/hr)	1013801
Cost (US$)	218152.1	Cost (US$)	736045
HX3			
Heat exchanged (MJ/hr)	1.586		
Heat exchange area (m^2)	58.138		
HE coeff. (KJ/°C m^2 hr)	1022.876		
Utilities flow (kg/hr)	37955.83		
Cost (US$)	32463.72		
Pumps			
PUMP1		**PUMP2**	
Volumetric flow (m^3/hr)	14.09	Volumetric flow (m^3/hr)	39.452
Pressure added (kPa)	19898.7	Pressure added (kPa)	19898.7
Power (HP)	127.454	Power (HP)	351.802
Electricity (KW)	95.08	Electricity (KW)	262.445
Cost (US$)	21784.71	Cost (US$)	51030.59
Reactor			
Temperature °C	250		
Pressure (kPa)	4007		
Height/Diameter (m)	8.22/2.74		
Utilities flow (kg/hr)	7907.221		
Cost of cooling coil (US$)	141979.5		
Cost (US$)	2152452		
Decanter			
Length/Diameter (m)	2.36/0.59		
Cost (US$)	13380.51		
Distillation columns			
COL1		**COL2**	
Temp. - Top/Bottom (°C)	78.5/90.94	Temp. - Top/Bottom (°C)	185.2/400
Press.- Top/Bottom (kPa)	101.3/111.3	Press. - Top/Bottom (kPa)	10/20
Height/Diameter (m)	12.29/2.75	Height/Diameter (m)	12.85/2.46
Heat in condenser (kJ/hr)	88.2	Heat in condenser (kJ/hr)	14.07
Heat in reboiler (kJ/hr)	88.18	Heat in reboiler (kJ/hr)	18.52
Utilities-Condenser (kg/hr)	4245318.1	Utilities-Condenser (kg/hr)	67718.03
Utilities-Reboiler (kg/hr)	46912.39	Utilities-Reboiler (kg/hr)	91686.1
Theoretical stages	5	Theoretical stages	5
Reflux ratio (molar)	2	Reflux ratio (molar)	2
Cost (US$)	237201.7	Cost (US$)	179183.4
Cost of condenser (US$)	96373.86	Cost of condenser (US$)	38699.66
Cost of reboiler (US$)	34351.45	Cost of reboiler (US$)	30562.61

Table A.9: Equipment for Scenario 1 - **Kinetic/Mass transfer model**.

Heat exchangers			
HX1A		**HX1B**	
Heat exchanged (MJ/hr)	10.509	Heat exchanged (MJ/hr)	26.74
Heat exchange area (m^2)	343.4381	Heat exchange area (m^2)	2320.3
HE coeff. (KJ/°C m^2 hr)	409.15	HE coeff. (KJ/°C m^2 hr)	409.15
Utilities flow (kg/hr)	0	Utilities flow (kg/hr)	0
Cost (US$)	837497	Cost (US$)	3893512
HX1		**HX3**	
Heat exchanged (MJ/hr)	11.603	Heat exchanged (MJ/hr)	1.586
Heat exchange area (m^2)	105.712	Heat exchange area (m^2)	58.137
HE coeff. (KJ/°C m^2 hr)	1227.451	HE coeff. (KJ/°C m^2 hr)	1022.876
Utilities flow (kg/hr)	36568.97	Utilities flow (kg/hr)	37954.06
Cost (US$)	166088	Cost (US$)	32463.59
Pumps			
PUMP1		**PUMP2**	
Volumetric flow (m^3/hr)	14.09	Volumetric flow (m^3/hr)	39.452
Pressure added (kPa)	19898.7	Pressure added (kPa)	19898.7
Power (HP)	127.454	Power (HP)	351.802
Electricity (KW)	95.08	Electricity (KW)	262.444
Cost (US$)	21784.71	Cost (US$)	51030.59
Reactor			
Temperature °C	250		
Pressure (kPa)	4007		
Height/Diameter (m)	8.22/2.74		
Utilities flow (kg/hr)	7907.221		
Cost of cooling coil (US$)	141979.5		
Cost (US$)	2152452		
Decanter			
Length/Diameter (m)	2.36/0.59		
Cost (US$)	13380.52		
Distillation columns			
COL1		**COL2**	
Temp. - Top/Bottom (°C)	78.5/90.94	Temp. - Top/Bottom (°C)	185.2/400
Press.- Top/Bottom (kPa)	101.3/111.3	Press. - Top/Bottom (kPa)	10/20
Height/Diameter (m)	12.29/2.75	Height/Diameter (m)	12.85/2.46
Heat in condenser (kJ/hr)	88.2	Heat in condenser (kJ/hr)	14.07
Heat in reboiler (kJ/hr)	85.18	Heat in reboiler (kJ/hr)	18.52
Utilities-Condenser (kg/hr)	4245318.1	Utilities-Condenser (kg/hr)	677108.03
Utilities-Reboiler (kg/hr)	46912.39	Utilities-Reboiler (kg/hr)	91686.1
Theoretical stages	5	Theoretical stages	5
Reflux ratio (molar)	2	Reflux ratio (molar)	2
Cost (US$)	237201.7	Cost (US$)	179183.4
Cost of condenser (US$)	96373.86	Cost of condenser (US$)	38699.66
Cost of reboiler (US$)	34351.45	Cost of reboiler (US$)	30562.61

Table A.10: Equipment for Scenario 2 - **Kinetic/Mass transfer model**.

Heat exchangers			
HX1A		**HX1B**	
Heat exchanged (MJ/hr)	9.938	Heat exchanged (MJ/hr)	27.328
Heat exchange area (m^2)	346.517	Heat exchange area (m^2)	2368.83
HE coeff. (KJ/°C m^2 hr)	409.15	HE coeff. (KJ/°C m^2 hr)	409.15
Utilities flow (kg/hr)	0	Utilities flow (kg/hr)	0
Cost (US$)	842235.9	Cost (US$)	3973202
HX1		**HX3**	
Heat exchanged (MJ/hr)	11.056	Heat exchanged (MJ/hr)	1.59
Heat exchange area (m^2)	104.872	Heat exchange area (m^2)	58.183
HE coeff. (KJ/°C m^2 hr)	1227.451	HE coeff. (KJ/°C m^2 hr)	1022.876
Utilities flow (kg/hr)	34845.13	Utilities flow (kg/hr)	38035.7
Cost (US$)	165456.5	Cost (US$)	32470.88
Pumps			
PUMP1		**PUMP2**	
Volumetric flow (m^3/hr)	14.285	Volumetric flow (m^3/hr)	39.504
Pressure added (kPa)	19898.7	Pressure added (kPa)	19898.7
Power (HP)	129.188	Power (HP)	352.255
Electricity (KW)	96.374	Electricity (KW)	262.782
Cost (US$)	22035.09	Cost (US$)	51081.59
PUMP3			
Volumetric flow (m^3/hr)	0.9731		
Pressure added (kPa)	81.3		
Power (HP)	0.05458		
Electricity (KW)	0.0407		
Cost (US$)	4270.64		
Reactor		**Flash vessel FLASH1**	
Temperature °C	250	Temperature °C	80
Pressure (kPa)	4007	Pressure (kPa)	30
Height/Diameter (m)	8.22/2.74	Height/Diameter (m)	2.08/0.66
Utilities flow (kg/hr)	7713.86	Utilities flow (kg/hr)	345.7106
Cost of cooling coil (US$)	138868.6	Cost of cooling coil (US$)	22723.15
Cost (US$)	2147939	Cost (US$)	45792.92
Decanter			
Length/Diameter (m)	2.36/0.59		
Cost (US$)	13880.49		
Distillation columns			
COL1		**COL2**	
Temp. - Top/Bottom (°C)	78.5/91.05	Temp. - Top/Bottom (°C)	185.31/400
Press.- Top/Bottom (kPa)	101.3/111.3	Press. - Top/Bottom (kPa)	10/20
Height/Diameter (m)	12.25/2.73	Height/Diameter (m)	12.85/2.46
Heat in condenser (kJ/hr)	88.33	Heat in condenser (kJ/hr)	14.06
Heat in reboiler (kJ/hr)	80.15	Heat in reboiler (kJ/hr)	18.51
Utilities-Condenser (kg/hr)	4251693.12	Utilities-Condenser (kg/hr)	676571.72
Utilities-Reboiler (kg/hr)	44142.66	Utilities-Reboiler (kg/hr)	91650.55
Theoretical stages	5	Theoretical stages	5
Reflux ratio (molar)	2	Reflux ratio (molar)	2
Cost (US$)	235029.3	Cost (US$)	179133.5
Cost of condenser (US$)	96486.85	Cost of condenser (US$)	38668.16
Cost of reboiler (US$)	33426.88	Cost of reboiler (US$)	30557.71

Table A.11: Equipment for Scenario 3 - **Kinetic/Mass transfer model**.

Bibliography

Abdelmoez, Wael, NA Mostafa, and Ahmad Mustafa (2013). "Utilization of oleochemical industry residues as substrates for lipase production for enzymatic sunflower oil hydrolysis". In: *Journal of cleaner production* 59, pp. 290–297 (cit. on p. 6).

Aguieiras, Erika CG et al. (2014). "Biodiesel production from Acrocomia aculeata acid oil by (enzyme/enzyme) hydroesterification process: use of vegetable lipase and fermented solid as low-cost biocatalysts". In: *Fuel* 135, pp. 315–321 (cit. on p. 10).

Al, Resul et al. (2019). "Meta-modeling based efficient global sensitivity analysis for wastewater treatment plants – An application to the BSM2 model". In: *Manuscript submitted for publication to Computers and Chemical Engineering* (cit. on p. 82).

Alenezi, R. et al. (2009). "Hydrolysis kinetics of sunflower oil under subcritical water conditions". In: *Chemical Engineering Research and Design* 87.6, pp. 867–873. ISSN: 02638762. DOI: 10.1016/j.cherd.2008.12.009 (cit. on pp. 14, 64, 70).

Alves, Melquizedeque B et al. (2014). "Cadmium and tin magnetic nanocatalysts useful for biodiesel production". In: *Journal of the Brazilian Chemical Society* 25.12, pp. 2304–2313 (cit. on p. 10).

Anderson, Dale, John C Tannehill, and Richard H Pletcher (2016). *Computational fluid mechanics and heat transfer*. CRC Press (cit. on p. 132).

Aniya, Vineet K et al. (2015). "Modeling and simulation of batch kinetics of non-edible karanja oil for biodiesel production: a mass transfer study". In: *Fuel* 161, pp. 137–145 (cit. on p. 60).

Ansari, Mubashshir Ahmad and Kwang-Yong Kim (2009). "A numerical study of mixing in a microchannel with circular mixing chambers". In: *AIChE Journal* 55.9, pp. 2217–2225 (cit. on p. 129).

Ansys, Inc (2011). "ANSYS FLUENT theory guide". In: *Ansys Fluent user guide*, p. 794 (cit. on p. 129).

AOCS (2017). "Acid Value - Official Method Cd 3d-63". In: *Sampling and Analysis of commercial fats and oils* (cit. on p. 18).

Archuleta, Richard Charles (1991). "Non-catalytic steam hydrolysis of fats and oils". PhD thesis, pp. 1–79 (cit. on p. 14).

Astarita, G. (1967). *Mass transfer with chemical reaction* (cit. on p. 72).

Attarakih, Menwer et al. (2012). "Mathematical modeling of high-pressure oil-splitting reactor using a reduced population balance model". In: *Chemical Engineering Science* 84, pp. 276–291. ISSN: 00092509. DOI: 10.1016/j.ces.2012.08.046 (cit. on pp. 72, 131, 133).

Awadallak, Jamal A et al. (2013). "Enzymatic catalyzed palm oil hydrolysis under ultrasound irradiation: diacylglycerol synthesis". In: *Ultrasonics sonochemistry* 20.4, pp. 1002–1007 (cit. on p. 1).

Azim, Nur Husna, Atiqah Subki, and Zetty Norhana Balia Yusof (2018). *Abiotic stresses induce total phenolic, total flavonoid and antioxidant properties in Malaysian indigenous microalgae and cyanobacterium*. DOI: 10.1017/CBO9781107415324.004 (cit. on p. 83).

Bailey, Alton Edward and Fereidoon Shahidi (2005). *Bailey's industrial oil and fat products*. John Wiley & Sons. ISBN: 9780471384601 (cit. on p. 6).

Balcao, Victor M and F Xavier Malcata (1998). "Lipase catalyzed modification of milkfat". In: *Biotechnology advances* 16.2, pp. 309–341 (cit. on p. 1).

Barnebey, HL and AC Brown (1948). "Continuous fat splitting plants using the colgate-emery process". In: *Journal of the American Oil Chemists' Society* 25.3, pp. 95–99 (cit. on p. 96).

BCC Research (2016). *Global Markets for Oleochemical Fatty Acids Use*. Tech. rep. BCC Research, pp. 1–34. URL: http://www.bccresearch.com/market-research/chemicals/oleochemical-fatty-acids-markets-chm062a.html (cit. on pp. 2, 98, 124).

Bezerra, Marcos Almeida et al. (2008). "Response surface methodology (RSM) as a tool for optimization in analytical chemistry". In: *Talanta* 76.5, pp. 965–977 (cit. on pp. 15, 17).

Box, G. E. P. and D. W. Behnken (1960). "Some New Three Level Designs for the Study of Quantitative Variables". In: *Technometrics* 2.4, p. 455. ISSN: 00401706. DOI: 10.2307/1266454 (cit. on pp. 15, 18, 76).

Byrne, George D and Lynn A Baird (1985). "Distillation calculations using a locally paramaterized continuation method". In: *Computers & chemical engineering* 9.6, pp. 593–599 (cit. on p. 97).

C. E. Goering et al. (1982). "Fuel properties of eleven vegetable oils". In: *Transactions of the ASAE* 25.6, pp. 1472–1477. ISSN: 2151-0059. DOI: 10.13031/2013.33748 (cit. on p. 71).

Castillo, Jaime and Ignacio E Grossmann (1981). "Computation of phase and chemical equilibria". In: *Computers & Chemical Engineering* 5.2, pp. 99–108 (cit. on p. 37).

Cavalcanti-Oliveira, Elisa d'Avila et al. (2011). "Study of soybean oil hydrolysis catalyzed by Thermomyces lanuginosus lipase and its application to biodiesel production via hydroesterification". In: *Enzyme research* 2011 (cit. on p. 9).

Chenard Diaz, Gisel et al. (2013). "Biodiesel by hydroesterification of oil from the microalgae Scenedesmus dimorphus". In: *Letters in Organic Chemistry* 10.4, pp. 263–268 (cit. on p. 10).

Coleman, Thomas F. and Yuying Li (1993). "An Interior Trust Region Approach for Nonlinear Minimization Subject to Bounds". In: URL: `https://ecommons.cornell.edu/handle/1813/6108` (cit. on p. 83).

Constantinou, Leonidas and Rafiqul Gani (1994). "New group contribution method for estimating properties of pure compounds". In: *AIChE Journal* 40.10, pp. 1697–1710 (cit. on p. 96).

Cunico, Larissa P et al. (2014). "Data, analysis and modeling of physical properties for process design of systems involving lipids". In: *Fluid Phase Equilibria* 362, pp. 318–327 (cit. on p. 97).

Diaz-Tovar, Carlos Axel, Rafiqul Gani, and Bent Sarup (2011). "Computer-Aided Modeling of Lipid Processing Technology". PhD Thesis. Technical University of Denmark, p. 259 (cit. on pp. 48, 76, 96, 97, 134).

Dossat, Valérie, Didier Combes, and Alain Marty (1999). "Continuous enzymatic transesterification of high oleic sunflower oil in a packed bed reactor: influence of the glycerol production". In: *Enzyme and Microbial Technology* 25.3-5, pp. 194–200 (cit. on p. 54).

Dunning, Ted (1993). "Accurate methods for the statistics of surprise and coincidence". In: *Computational linguistics* 19.1, pp. 61–74 (cit. on p. 17).

Ferreira, SL Costa et al. (2007). "Box-Behnken design: an alternative for the optimization of analytical methods". In: *Analytica chimica acta* 597.2, pp. 179–186 (cit. on pp. 14–17).

Foglia, Thomas A. and Kerby C. Jones (1997). "Quantitation of Neutral Lipid Mixtures Using High Performance Liquid Chromatography with Light Scattering Detection†". In: *Journal of Liquid Chromatography & Related Technologies* 20.12, pp. 1829–1838. ISSN: 1082-6076. DOI: `10.1080/10826079708005545` (cit. on p. 78).

Forero-Hernandez, Hector et al. (2017). "A simplified kinetic and mass transfer modelling of the thermal hydrolysis of vegetable oils". In: *Computer Aided*

Chemical Engineering. Vol. 40. Elsevier, pp. 1177–1182 (cit. on pp. 21, 110, 127, 134).

Frutiger, Jerome et al. (2018). "From property uncertainties to process simulation uncertainties–Monte Carlo methods in SimSci PRO/II process simulator". In: *Computer Aided Chemical Engineering*. Vol. 44. Elsevier, pp. 1489–1494 (cit. on p. 95).

Garrett, Donald E (2012). *Chemical engineering economics*. Springer Science & Business Media (cit. on p. 117).

Gautam, Rajeev and Warren D Seider (1979). "Computation of phase and chemical equilibrium: Part I. Local and constrained minima in Gibbs free energy". In: *AIChE Journal* 25.6, pp. 991–999 (cit. on p. 37).

Gmehling, Juergen, Jiding Li, and Martin Schiller (1993). "A modified UNIFAC model. 2. Present parameter matrix and results for different thermodynamic properties". In: *Industrial & Engineering Chemistry Research* 32.1, pp. 178–193. ISSN: 0888-5885. DOI: 10.1021/ie00013a024 (cit. on pp. 38, 47, 75, 145).

Gmehling, Jürgen, Jürgen Lohmann, et al. (1998). "A Modified UNIFAC (Dortmund) Model. 3. Revision and Extension". In: *Industrial & Engineering Chemistry Research* 37.12, pp. 4876–4882. ISSN: 0888-5885. DOI: 10.1021/ie980347z (cit. on pp. 38, 47, 75, 145).

Gmehling, Jürgen, Roland Wittig, et al. (2002). "A Modified UNIFAC (Dortmund) Model. 4. Revision and Extension". In: *Industrial & Engineering Chemistry Research* 41.6, pp. 1678–1688. ISSN: 0888-5885. DOI: 10.1021/ie0108043 (cit. on pp. 38, 47, 75, 145).

Gunstone, Frank D, John L Harwood, and Albert J Dijkstra (2007). *The lipid handbook with CD-ROM*. CRC press (cit. on pp. 8, 49).

Hameed, Bassim H, LF Lai, and LH Chin (2009). "Production of biodiesel from palm oil (Elaeis guineensis) using heterogeneous catalyst: an optimized process". In: *Fuel Processing Technology* 90.4, pp. 606–610 (cit. on p. 117).

Hammond, Earl G et al. (2005). "Soybean oil". In: *Bailey's industrial oil and fat products* (cit. on pp. 97, 98).

Hartman, L. (1951). "Kinetics of the Twitchell Hydrolysis". In: *Nature* 167.4240, pp. 199–199. ISSN: 0028-0836. DOI: 10.1038/167199a0 (cit. on pp. 14, 69).

Hildebrand, Francis Begnaud (1987). *Introduction to numerical analysis*. Courier Corporation (cit. on p. 82).

Hill, Ittner Martin (1949). *Countercurrent hydrolysis of fat*. US Patent 2,480,471 (cit. on p. 6).

Holliday, Russell L, Jerry W King, and Gary R List (1997). "Hydrolysis of vegetable oils in sub-and supercritical water". In: *Industrial & engineering chemistry research* 36.3, pp. 932–935 (cit. on p. 8).

Ilham, Zul and Shiro Saka (2010). "Two-step supercritical dimethyl carbonate method for biodiesel production from Jatropha curcas oil". In: *Bioresource technology* 101.8, pp. 2735–2740 (cit. on p. 50).

Iman, Ronald L. and W. J. Conover (1982). "A distribution-free approach to inducing rank correlation among input variables". In: *Communications in Statistics - Simulation and Computation* 11.3, pp. 311–334. ISSN: 0361-0918. DOI: 10.1080/03610918208812265 (cit. on p. 80).

Istok, Jonathan David (1989). *Groundwater modeling by the finite element method*. Vol. 13. American Geophysical Union Washington, DC (cit. on p. 132).

Jakob, Antje et al. (2006). "Further Development of Modified UNIFAC (Dortmund): Revision and Extension 5". In: *Industrial & Engineering Chemistry Research* 45.23, pp. 7924–7933. ISSN: 0888-5885. DOI: 10.1021/ie060355c (cit. on pp. 75, 145).

Jansen, Michiel JW (1999). "Analysis of variance designs for model output". In: *Computer Physics Communications* 117.1-2, pp. 35–43 (cit. on p. 81).

Jeffreys, G.V. (1961). "Analysis of continuous fat-hydrolysing column". In: *Institution of Chemical Engineers – Transactions* 39.6. URL: http://findit.dtu.dk/en/catalog/2369515048 (cit. on p. 14).

Jogunola, Olatunde et al. (2011). "Rates and equilibria of ester hydrolysis: Combination of slow and rapid reactions". In: *Chemical Engineering and Processing: Process Intensification* 50.7, pp. 665–674 (cit. on p. 54).

Johnson, AI et al. (1975). "Steady state and dynamic studies of a multi product chemical plant". In: *The Canadian Journal of Chemical Engineering* 53.3, pp. 340–346 (cit. on pp. 98, 127).

Kent, James A et al. (2007). *Kent and Riegel's handbook of industrial chemistry and biotechnology*. Vol. 1665. Springer (cit. on p. 7).

Keselman, HJ et al. (1998). "Statistical practices of educational researchers: An analysis of their ANOVA, MANOVA, and ANCOVA analyses". In: *Review of educational research* 68.3, pp. 350–386 (cit. on p. 16).

King, JerryáW, RusselláL Holliday, and GaryáR List (1999). "Hydrolysis of soybean oil. in a subcritical water flow reactor". In: *Green Chemistry* 1.6, pp. 261–264 (cit. on pp. 8, 21, 29, 98).

Klinkert, Julia (2018). "The characterization of uncertainty for steady state multiphase flow models in pipelines". In: (cit. on p. 80).

Kolda, Tamara G, Robert Michael Lewis, and Virginia Torczon (2003). "Optimization by direct search: New perspectives on some classical and modern methods". In: *SIAM review* 45.3, pp. 385–482 (cit. on p. 47).

Kusdiana, Dadan and Shiro Saka (2004). "Two-step preparation for catalyst-free biodiesel fuel production". In: *Proceedings of the Twenty-Fifth Symposium on Biotechnology for Fuels and Chemicals Held May 4–7, 2003, in Breckenridge, CO*. Springer, pp. 781–791 (cit. on p. 50).

Lascaray, Lucio (1949). "Mechanism of Fat Splitting". In: *Industrial & Engineering Chemistry* 41.4, pp. 786–790. ISSN: 0019-7866. DOI: 10.1021/ie50472a025 (cit. on pp. 14, 69).

— (1952). "Industrial fat splitting". In: *Journal of the American Oil Chemist' Society* 29.9, pp. 362–366. ISSN: 0003-021X. DOI: 10.1007/BF02631459 (cit. on pp. 14, 69, 72).

Lee, K-H, M Lombardo, and SI Sandler (1985). "The generalized van der Waals partition function. II. Application to the square-well fluid". In: *Fluid Phase Equilibria* 21.3, pp. 177–196 (cit. on p. 38).

Lemmens, Sanne (2016). "Cost engineering techniques and their applicability for cost estimation of organic Rankine cycle systems". In: *Energies* 9.7, p. 485 (cit. on p. 116).

LL Rocha, Layla et al. (2010). "Production of biodiesel by a two-step niobium oxide catalyzed hydrolysis and esterification". In: *Letters in Organic Chemistry* 7.7, pp. 571–578 (cit. on p. 9).

Lohmann, Jürgen and Jürgen Gmehling (2001). "Modified UNIFAC (Dortmund). Reliable Model for the Development of Thermal Separation Processes." In: *Journal of Chemical Engineering of Japan* 34.1, pp. 43–54. ISSN: 00219592. DOI: 10.1252/jcej.34.43 (cit. on pp. 75, 145).

MacCormack, R and A Paullay (1972). "Computational efficiency achieved by time splitting of finite difference operators". In: *10th Aerospace Sciences Meeting*, p. 154 (cit. on p. 132).

Machado, Sara Aparecida (2013). "Study of the producton of biodiesel by *Acrocomia aculeata*". PhD thesis. Universidade de São Paulo (cit. on p. 9).

Marelli, S. et al. (2019). *UQLab user manual – Sensitivity analysis*. Tech. rep. Report # UQLab-V1.2-106. Chair of Risk, Safety & Uncertainty Quantification, ETH Zürich (cit. on pp. 81–83).

McDonald, Bruce H and Alvin Wexler (1972). "Finite-element solution of unbounded field problems". In: *IEEE Transactions on microwave theory and techniques* 20.12, pp. 841–847 (cit. on p. 132).

McDonald, Conor M and Christodoulos A Floudas (1994). "Decomposition based and branch and bound global optimization approaches for the phase

equilibrium problem". In: *Journal of Global Optimization* 5.3, pp. 205–251 (cit. on p. 37).

Metzger, Jürgen O. and U. Bornscheuer (2006). "Lipids as renewable resources: current state of chemical and biotechnological conversion and diversification". In: *Appl Microbiol Biotechnol* 71, pp. 13–22. DOI: 10.1007/s00253-006-0335-4 (cit. on p. 70).

Michelsen, Michael L (1989). "Calculation of multiphase ideal solution chemical equilibrium". In: *Fluid Phase Equilibria* 53, pp. 73–80 (cit. on p. 47).

Micic, Radoslav D et al. (2015). "Optimization of hydrolysis in subcritical water as a pretreatment step for biodiesel production by esterification in supercritical methanol". In: *The Journal of Supercritical Fluids* 103, pp. 90–100 (cit. on p. 8).

Miller Jr, Rupert G (1997). *Beyond ANOVA: basics of applied statistics*. Chapman and Hall/CRC (cit. on p. 16).

Mills, V and HK McClain (1949). "Fat hydrolysis". In: *Industrial and Engineering chemistry* 41.9, pp. 1982–1985 (cit. on p. 50).

Minami, Eiji and Shiro Saka (2006). "Kinetics of hydrolysis and methyl esterification for biodiesel production in two-step supercritical methanol process". In: *Fuel* 85.17-18, pp. 2479–2483. DOI: 10.1016/j.fuel.2006.04.017 (cit. on pp. 6, 9, 14, 69, 70, 84).

Missen, R.W. and W.R. Smith (1982). *Chemical reaction equilibrium analysis: Theory and algorithms*. eng. John Wiley and Sons, 364 s. ISBN: 0471093475 (cit. on p. 46).

Moquin, Paul HL and Feral Temelli (2008). "Kinetic modeling of hydrolysis of canola oil in supercritical media". In: *The Journal of Supercritical Fluids* 45.1, pp. 94–101 (cit. on p. 6).

Mowla, Omid and Michael Stockenhuber (2019). "Mass transfer and kinetic study on BEA zeolite-catalysed oil hydroesterification". In: *Renewable Energy* 135, pp. 417–425 (cit. on p. 10).

Namdev, P D et al. (1988). "Thermal hydrolysis of vegetable oils and fats. 3. An analysis of design alternatives". In: *Industrial & Engineering Chemistry Research* 27.5, pp. 739–743. ISSN: 0888-5885. DOI: 10.1021/ie00077a003 (cit. on pp. 14, 60, 69, 70).

Noureddini, H., D. W. Harkey, and M. R. Gutsman (2004). "A continuous process for the glycerolysis of soybean oil". In: *Journal of the American Oil Chemists' Society* 81.2, pp. 203–207. ISSN: 0003021X. DOI: 10.1007/s11746-004-0882-y (cit. on p. 71).

O'Connell, J. P. and J. M. Haile (2005). *Thermodynamics: Fundamentals for applications*. Vol. 9780521582. Cambridge: Cambridge University Press,

pp. 1–654. ISBN: 9780511840234. DOI: 10.1017/CBO9780511840234 (cit. on pp. 146, 148).

Patil, T. A., T. S. Raghunathan, and H. S. Shankar (1988a). "Thermal hydrolysis of vegetable oils and fats. 2. Hydrolysis in continuous stirred tank reactor". In: *Industrial and Engineering Chemistry Research* 27.5, pp. 735–739. ISSN: 15205045. DOI: 10.1021/ie00077a002 (cit. on pp. 14, 69, 70, 84).

— (1988b). "Thermal hydrolysis of vegetable oils and fats. 2. Hydrolysis in continuous stirred tank reactor". In: *Industrial and Engineering Chemistry Research* 27.5, pp. 735–739. ISSN: 15205045. DOI: 10.1021/ie00077a002 (cit. on pp. 14, 21, 69–71).

Phuah, Eng-Tong et al. (2012). "Kinetic study on partial hydrolysis of palm oil catalyzed by Rhizomucor miehei lipase". In: *Journal of Molecular Catalysis B: Enzymatic* 78, pp. 91–97 (cit. on p. 5).

Pinto, Jair Sebastião S and Fernando M Lanças (2006). "Hydrolysis of corn oil using subcritical water". In: *Journal of the Brazilian Chemical Society* 17.1, pp. 85–89 (cit. on p. 8).

Poling, Bruce E, John M Prausnitz, John P O'connell, et al. (2001). *The properties of gases and liquids*. Vol. 5. Mcgraw-hill New York (cit. on p. 39).

Prausnitz, John M, Rudiger N Lichtenthaler, and Edmundo Gomes de Azevedo (1998). *Molecular thermodynamics of fluid-phase equilibria*. Pearson Education (cit. on pp. 35, 38).

Price, Jason et al. (2014). "Mechanistic modeling of biodiesel production using a liquid lipase formulation". In: *Biotechnology Progress* 30.6, pp. 1277–1290. ISSN: 87567938. DOI: 10.1002/btpr.1985 (cit. on p. 78).

Rachford, H.H. and J.D. Rice (1952). "Procedure for Use of Electronic Digital Computers in Calculating Flash Vaporization Hydrocarbon Equilibrium". In: *Journal of Petroleum Technology* 4.10, pp. 19–3. ISSN: 0149-2136. DOI: 10.2118/952327-G (cit. on pp. 75, 147).

Rossi, CCRS, L Cardozo-Filho, and R Guirardello (2009). "Gibbs free energy minimization for the calculation of chemical and phase equilibrium using linear programming". In: *Fluid Phase Equilibria* 278.1-2, pp. 117–128 (cit. on p. 37).

Saisana, Michaela, Andrea Saltelli, and Stefano Tarantola (2005). "Uncertainty and sensitivity analysis techniques as tools for the quality assessment of composite indicators". In: *Journal of the Royal Statistical Society: Series A (Statistics in Society)* 168.2, pp. 307–323 (cit. on p. 63).

Saltelli, Andrea et al. (2010). "Variance based sensitivity analysis of model output. Design and estimator for the total sensitivity index". In: *Computer Physics Communications* 181.2, pp. 259–270 (cit. on p. 81).

Sandler, Stanley I (1985). "The generalized van der Waals partition function. I. Basic theory". In: *Fluid Phase Equilibria* 19.3, pp. 238–257 (cit. on p. 38).

— (2017). *Chemical, biochemical, and engineering thermodynamics*. John Wiley & Sons (cit. on pp. 36, 39).

Santana, Harrson S, João L Silva Júnior, and Osvaldir P Taranto (2015). "Numerical simulations of biodiesel synthesis in microchannels with circular obstructions". In: *Chemical Engineering and Processing: Process Intensification* 98, pp. 137–146 (cit. on p. 129).

Santos, Letícia Karen dos et al. (2017). "Experimental factorial design on hydroesterification of waste cooking oil by subcritical conditions for biodiesel production". In: *Renewable energy* 114, pp. 574–580 (cit. on p. 10).

Satyarthi, J. K., D. Srinivas, and P. Ratnasamy (2011). "Hydrolysis of vegetable oils and fats to fatty acids over solid acid catalysts". In: *Applied Catalysis A: General* 391.1-2, pp. 427–435. ISSN: 0926860X. DOI: 10.1016/j.apcata.2010.03.047 (cit. on pp. 14, 70).

Satyarthi, JK, D Srinivas, and P Ratnasamy (2011). "Hydrolysis of vegetable oils and fats to fatty acids over solid acid catalysts". In: *Applied Catalysis A: General* 391.1-2, pp. 427–435 (cit. on p. 5).

Seader, JD, Warren D Seider, and Daniel R Lewin (2004). *Product and process design principles: synthesis, analysis and evaluation*. Wiley (cit. on pp. 113–115, 117, 159).

Shampine, Lawrence F and Mark W Reichelt (n.d.). *The MATLAB ODE Suite*. Tech. rep. URL: https://www.mathworks.com/help/pdf%7B%5C_%7Ddoc/otherdocs/ode%7B%5C_%7Dsuite.pdf (cit. on p. 83).

Shampine, Lawrence F., Mark W. Reichelt, and Jacek A. Kierzenka (1999). "Solving Index-1 DAEs in MATLAB and Simulink". In: *SIAM Review* 41.3, pp. 538–552. ISSN: 0036-1445. DOI: 10.1137/S003614459933425X (cit. on p. 83).

Sharma, Aditi, Satyendra P Chaurasia, and Ajay K Dalai (2013). "Enzymatic hydrolysis of cod liver oil for the fatty acids production". In: *Catalysis today* 207, pp. 93–100 (cit. on p. 6).

Sin, Gürkan and Krist V. Gernaey (2016). "Data Handling and Parameter Estimation". In: *Experimental Methods in Wastewater Treatment*. IWA Publishing, pp. 201–234. ISBN: 9781780404745. DOI: 10.1017/CBO9781107415324.004 (cit. on pp. 83, 84).

Sin, Gürkan, Krist V. Gernaey, and Anna Eliasson Lantz (2009). "Good modeling practice for PAT applications: Propagation of input uncertainty and sensitivity analysis". In: *Biotechnology Progress* 25.4, pp. 1043–1053. ISSN: 87567938. DOI: 10.1002/btpr.166 (cit. on pp. 63, 64, 83).

Sin, Gürkan, Anne S. Meyer, and Krist V. Gernaey (2010). "Assessing reliability of cellulose hydrolysis models to support biofuel process design-Identifiability and uncertainty analysis". In: *Computers and Chemical Engineering* 34.9, pp. 1385–1392. ISSN: 00981354. DOI: 10.1016/j.compchemeng.2010.02.012 (cit. on pp. 63, 79).

Smith, Joseph Mauk (1950). *Introduction to chemical engineering thermodynamics* (cit. on p. 39).

Smith, Ralph C (2013). *Uncertainty quantification: theory, implementation, and applications*. Vol. 12. Siam (cit. on p. 80).

Smith, William and Ronald Missen (1985). "Chemical reaction equilibrium analysis: Theory and algorithms". In: *AIChE Journal* 31.1, pp. 176–176 (cit. on p. 35).

Sobol, Ilya M (1993). "Sensitivity estimates for nonlinear mathematical models". In: *Mathematical modelling and computational experiments* 1.4, pp. 407–414 (cit. on pp. 80, 81).

Sonntag, NOV (1979). "Fat splitting". In: *Journal of the American Oil Chemists' Society* 56.11Part1, 729A–732A (cit. on p. 6).

Sousa, Joab Sampaio de et al. (2010). "Application of lipase from the physic nut (Jatropha curcas L.) to a new hybrid (enzyme/chemical) hydroesterification process for biodiesel production". In: *Journal of Molecular Catalysis B: Enzymatic* 65.1-4, pp. 133–137 (cit. on p. 9).

Sturzenegger, August and Hermann Sturm (1951). "Hydrolysis of Fats at High Temperatures". In: *Industrial & Engineering Chemistry* 43.2, pp. 510–515. ISSN: 0019-7866. DOI: 10.1021/ie50494a054 (cit. on pp. 14, 69).

Talukder, Md. Mahabubur Rahman, Jin Chuan Wu, and Louisa Pei-Lyn Chua (2010). "Conversion of Waste Cooking Oil to Biodiesel via Enzymatic Hydrolysis Followed by Chemical Esterification". eng. In: *Energy and Fuels* 24.3, pp. 2016–2019. ISSN: 15205029, 08870624. DOI: 10.1021/ef9011824, 10.1021/ef9011824 (cit. on p. 9).

Temam, Roger (2001). *Navier-Stokes equations: theory and numerical analysis*. Vol. 343. American Mathematical Soc. (cit. on pp. 129, 130).

The Mathworks Inc. (2016). *MATLAB and Statistics Toolbox, version 2016b*. Natick, Massachusetts, United States (cit. on pp. 47, 83).

Towler, Gavin and Ray Sinnott (2012). *Chemical engineering design: principles, practice and economics of plant and process design*. Elsevier (cit. on pp. 113, 114).

Trambouze, P., H. Van Landeghem, and J. P. Wauquier (1989). "Chemical Reactors: Design, Engineering, Operation". In: *Chemical Engineering Science* 44.7, p. 1599. ISSN: 00092509. DOI: 10.1016/0009-2509(89)80040-5 (cit. on p. 72).

Turton, Richard et al. (2008). *Analysis, synthesis and design of chemical processes*. Pearson Education (cit. on pp. 116, 118).

Voll, Fernando AP et al. (2011). "Thermodynamic analysis of fatty acid esterification for fatty acid alkyl esters production". In: *biomass and bioenergy* 35.2, pp. 781–788 (cit. on pp. 38, 54).

Wang, Wei-cheng Cheng et al. (2013). "Product sampling during transient continuous countercurrent hydrolysis of canola oil and development of a kinetic model". In: *Computers and Chemical Engineering* 58, pp. 144–155. ISSN: 00981354. DOI: 10.1016/j.compchemeng.2013.06.003 (cit. on pp. 84, 133).

West, Alex H, Dusko Posarac, and Naoko Ellis (2008). "Assessment of four biodiesel production processes using HYSYS. Plant". In: *Bioresource technology* 99.14, pp. 6587–6601 (cit. on pp. 96, 111, 112).

White, William B, Selmer Martin Johnson, and George Bernard Dantzig (1958). "Chemical equilibrium in complex mixtures". In: *The Journal of Chemical Physics* 28.5, pp. 751–755 (cit. on p. 37).

Whitman, Walter G. (1962). "The two film theory of gas absorption". In: *International Journal of Heat and Mass Transfer* 5.5, pp. 429–433. ISSN: 00179310. DOI: 10.1016/0017-9310(62)90032-7 (cit. on p. 73).

Willer, Helga et al. (2018). "The world of organic agriculture". In: (cit. on p. 1).

Zhang, Yen et al. (2003). "Biodiesel production from waste cooking oil: 1. Process design and technological assessment". In: *Bioresource technology* 89.1, pp. 1–16 (cit. on p. 97).

Zhu, Yushan, Hao Wen, and Zhihong Xu (2000). "Global stability analysis and phase equilibrium calculations at high pressures using the enhanced simulated annealing algorithm". In: *Chemical Engineering Science* 55.17, pp. 3451–3459 (cit. on p. 37).

Zhu, Yushan and Zhihong Xu (1999). "A reliable prediction of the global phase stability for liquid–liquid equilibrium through the simulated annealing algorithm: Application to NRTL and UNIQUAC equations". In: *Fluid Phase Equilibria* 154.1, pp. 55–69 (cit. on p. 37).

Zubov, Alexandr and Gürkan Sin (2018). “Multiscale modeling of poly (lactic acid) production: From reaction conditions to rheology of polymer melt”. In: *Chemical Engineering Journal* 336, pp. 361–375 (cit. on p. 87).